CHIRAL SYMMETRY BREAKING IN HIGH-TEMPERATURE SUPERCONDUCTORS AND BIREFRINGENT COLD ATOMS, HELICITY MODULUS IN LAYERED BOSONS AND PHASE DIAGRAM OF SUPERCONDUCTOR-INSULATOR TRANSITION

by

Kamran Kaveh

MSc., University of Alberta, 2000

BSc., Sharif University of Technology, 1996

A THESIS SUBMITTED IN PARTIAL FULFILLMENT
OF THE REQUIREMENTS FOR THE DEGREE OF
Doctor of Philosophy

in the
Department of Physics
Faculty of Science

SIMON FRASER UNIVERSITY
Summer 2012

APPROVAL

Name: Kamran Kaveh

Degree: Doctor of Philosophy

Title of Thesis: Chiral Symmetry Breaking in High-Temperature Superconductors and Birefringent Cold Atoms, Helicity Modulus in Layered Bosons and Phase Diagram of Superconductor-Insulator Transition

Examining Committee:

Dr. J. Steven Dodge, Associate Professor
Chair

Dr. Igor Herbut, Professor
Senior Supervisor

Dr. Michael Plischke, Professor
Supervisor

Dr. Malcolm Kennett, Associate Professor
Supervisor

Dr. Mohammad Amin, Adjunct Professor
Internal Examiner

Dr. Marcel Franz, Professor, Department of Physics, UBC
External Examiner

Date Approved: June 26th, 2012

Partial Copyright Licence

Abstract

This work is a compilation of several research projects with them main theme being high-temperature superconductivity.

We construct the field theory of underdoped cuprates beginning with a well-defined d-wave superconductor and adding the vortex degree of freedom using a singular gauge transformation. The symmetries of the theory both in the presence and absence of a quasi-particle mass are studied. Nodal quasi-particles are known to obey a relativistic Lorentz symmetry while their massless nature represent another symmetry which we will identify as a chiral SU(2) symmetry. It is shown that 2+1 quantum electrodynamics is the effective theory that describes underdoped cuprates in the zero-temperature pseudogap regime.

We focus on the mechanism of dynamical mass generation in three dimensional quantum electrodynamics and theories with four-fermion interactions. This is a field that has been subject of extensive research in last two decades. However, our momentum-shell renormalization group approach is new to the field and through that we are able to estimate the conditions for the mass generation mechanism and also work out the phase diagram of the theory for charge and interaction strength. We discuss the applications of momentum-shell renormalization group to other four-fermionic theories in the absence of a gauge field. The justification for this is the fact that in the superconducting regime the system can be described by a massive gauge field theory coupled to relativistic quasi-particles which effectively represent a four-fermionic theory.

Inspired by the field theory constructed for underdoped cuprates we discuss the superfluid response of the underdoped materials using an anisotropic bosonic model and compare it to experiment. The idea is to see how c-axis superfluid density measurements can help one set the parameters in our field theory for underdoped cuprates. The behaviours of the superfluid responses in both out-of-plane and in-plane measurements has been detailed as a function of temperature and density (doping) and it is shown that there is disagreement with the measured c-axis response using the

conjectured bosonic Hamiltonian. Discussions of the limitations of the layered bosonic model to explain the superfluid response of a underdoped cuprate is detailed at the end of Chapter 4.

Chapters 5 and 6 digress from the subject of high-temperature superconductivity. Chapter 5 discusses broken chiral symmetry in context of fermions in optical lattices. A particular model is constructed in which there is broken chiral symmetry for relativistic quasi-particles. However, the mechanism of symmetry breaking is different from dynamical mass generation. The effects of different staggered potentials and interactions in this model are briefly discussed.

The final topic is the superconductor-insulator transition (SI) in the context of low-dimensional disordered systems. We construct a bosonic theory for a conventional BCS superconductor in the presence of quenched disorder and show that in the phase diagram of the theory the phase-disordered Bose Glass phase, survives for arbitrary weak-disorder and interaction strengths. The general features of such SI transitions are very similar to high temperature superconductors in the pseudogap regime. The main difference is the absence of nodal quasi-particles and relativistic invariance that follows from their gapless nature.

Acknowledgments

First and foremost I should thank my supervisor Dr. Igor Herbut for introducing me to the exotic field of quantum condensed matter and in particular, quantum phase transition. It has been a long journey for both of us and at many times frustrating but looking back I can see how blessed I have been to be able to work in so many variety of problems in our field. I am indebted forever for the knowledge I learnt from him and also the methodology for scientific research which is invaluable.

I need to particularly thanks Dr. Steve Dodge, for his critical help on every step of the thesis to assure this project will finish. I do not think without his help and support and organizatitonal skills I would ever be able to finish this doctoral project.

I have to thank my best friends and colleagues Drs. Matthew Case, Babak Seradjeh and Bitan Roy whom during the years taught me many things on the problems we worked together and have been great friends at the same time as being professional colleagues. I am specially indebted to Dr. Case with whom we worked on some parts of Chapter four of this thesis and also Dr. Roy for collaboration on the Sec 2.10.1. I would also like to thank my committee members Drs. Michael Plischke and Malcolm Kennett for their help and support during my long Ph.D time and also invaluable feedback on the manuscript. I need to particularly thank Malcolm for letting me into his research group and giving me the opportunity to collaborate with him and his group. I also should thank Dr. David Broun for his support during the years and also discussion on the superfluid density.

A warm thanks also to my friends and colleagues: Mohammad Amin, Mohammad Iazdi, Rasoul Nariman, Mohsen Havaej, Kamyar Saeidi, Mehran Shaghaghi, Peter Smith, Mehrdad Rastan, Daniel Vernon, Gerlad Lim, Suckjoon Jun, Helen Fan and Junco Kumon.

Finally, but most importantly, I would like to recognize my mother and my brother, my closest friends in life and for their years of support and encouragement.

I am here with the help of every one of you!.

Contents

List of Figures

Chapter 1

Effective Field Theory of Phase Fluctuating High Temperature Superconductors

The discovery of high temperature superconductivity in cuprates [1] and the rapid raising of the transition temperature to well above the boiling point of nitrogen has attracted the attention of many experimental and theoretical physicists. While there are are hundreds of high-T_c compounds, they all share the layered structure and up of one or more copper-oxide planes (up to seven layers in mercury-based materials). With an anisotropic crystal structure, it is expected that anisotropic behaviour should be observed in the measurements of different quantities. In fact measurements such as electron transport, penetration depth and superfluid density all indicate that high-T_c superconductivity is quite two-dimensional, occurring primarily in the cuprate planes.

The parent compounds of the cuprate materials are known to be insulators. In stark contrast with conventional superconductors where the BCS mechanism works best for metallic type of materials, this type of insulator is known as a Mott insulator. The concept of a Mott insulator corresponds to the situation that according to band theory the material should be metallic but is an insulator due to strong electronic repulsion. Initially different features of the Mott insulators were worked out in the pioneering works of Mott and Anderson using the electronic Hubbard model. In the cuprate materials it also follows that the Mott insulator should be an anti-ferromagnet (AF).

The anti-ferromagnetic ground state of these Mott insulator is sensitive to introducing extra electrons or holes to the system, a mechanism known as doping. One can introduce extra electrons

to the Cu-O planes, or substitute the intra-layer atoms with different type of atoms with different valence bands. For the case of $\mathrm{YBa_2Cu_3O_7}$ doping is indicated with change in the percentage of oxygen atoms, $\mathrm{YBa_2Cu_3O_{6-x}}$.

The other well-established fact about the cuprate superconductors is their pairing symmetry of their superconducting phase. It has been shown by many different experiments [2] - including microwave measurements of penetration depth [2]- that Cooper pairs in such materials have a d-wave symmetry, particularly, a $d_{x^2-y^2}$ one which is the possibility imposed by the symmetry of the lattice. This symmetry of the pairing potential imply that at some point of the Fermi surface the gap function can go to zero and the quasi-particle system is basically gapless in low energies. The power law behaviour of specific heat and the linear behaviour of the normal density/penetration depth at very low temperatures can be explained by the above assumption.

The phase diagram of the cuprate materials has been the subject of an extensive research and has a very rich form. The phase diagram of a typical high-T_c material for temperature vs. doping is shown in Fig.(1.1). It is well established that at $x = 0$ the phase is a well-defined AF. Upon doping holes the AF order parameter rapidly suppresses and eventually reaches a superconducting state. The region of phase diagram with doping x less than that of the maximum T_c is called underdoped region. The not-very-well-defined phase in between AF and d-wave superconductor is known as pseudogap phase. Angel-resolved photoemission spectroscopy (ARPES) experiments show that while the superconducting long-range order is gone in this phase as one passes a pseudogap temperature, T^*, the pairing amplitude is still finite indicating that although the Cooper pairs persist the long-range superfluid order is lost through a phase disordering mechanism. This part of the phase diagram is the subject of focus of this Chapter.

The doping corresponding to maximum T_c is known as optimal doping and after that the system is called overdoped. In the overdoped region cuprates are known to have metallic behaviour (finite conductivity). The anomalous region above optimal doping is sometimes referred to as the "strange metal" region. A popular notion is that the strange metal is characterized by a quantum critical point lying under the superconducting dome.

The emergence of superconductivity from an anti-ferro-magnetically ordered Mott insulating state seems paradoxical. In conventional materials, the superconducting state arises due to an instability of the weak interacting Fermi liquid to phonon mediated pairing between electrons (Cooper instability). It is difficult to imagine the same mechanism in high-T_c cuprates because of the strong electron repulsion. Beginning from Hubbard model of highly interacting electrons- which describes as AF state well - another mechanism for the pairing is suggested using an approximation to the

original Hubbard Hamiltonian known as the $t-J$ model. Mean-field solutions of the $t-J$ model show d-wave pairing for the electron pairs. In the $t-J$ model the bosonic degrees of freedom that mediated electrons interactions in conventional superconductors are replaced by a different bosonic degree of freedom known as *slave bosons*.

ARPES experiments (see Ref.[3]) show that the superconducting order parameter - pairing amplitude - does not go to zero at non-zero temperatures when a cuprate system gradually enters the underdoped regime from the optimal doping. Thus, it is believed that in the pseudogap regime the superconductivity is destroyed by phase fluctuation of the quasi particles. The strength of these phase fluctuations, however, is also mediated by a bosonic field. The destruction of superconducting order parameters has been seen in disordered two-dimensional materials before and is known to have the same mechanism as the Kousterlitz-Thouless transition [4]. Bosonic fields in high-T_c materials represent the magnetic vortex degrees of freedom of the system as cuprates are very strong type-II superconductors and the coupling between the fermionic (quasi-particle) and bosonic (vortices) excitations is strong.

In this chapter we closely follow a new field theoretical framework for this phase disordering beginning from the d-wave state as our starting point. The mechanism of disordering through a new type of gauge-field was recently suggested by M. Franz and Z. Tesanovic. I.F. Herbut very soon after showed a d-wave superconductor is unstable with respect to the fluctuations of the gauge field which results in mass generation for the originally massless excitations, and the mass generated is the antiferromagnetic order parameter. The two key aspect of this new field theory are (i) the gauge transformation which transforms the singular/vortex phase of the d-wave order parameter into a gauge-field minimally coupled to the nodal quasi-particles (ii) the mechanism of mass generation for nodal quasi-particles coupled to such a singular gauge field. In relevant limits, the mass generation is shown to be the same as *dynamical mass generation* in three dimensional quantum electrodynamics. Remarkably, the mass generation can only happen in low-dimensional systems ($d<3$). This is in the same line as the common belief that the quantum phase transition in high temperature superconductors is mainly due to the layered, quasi two-dimensional nature of the cuprates.

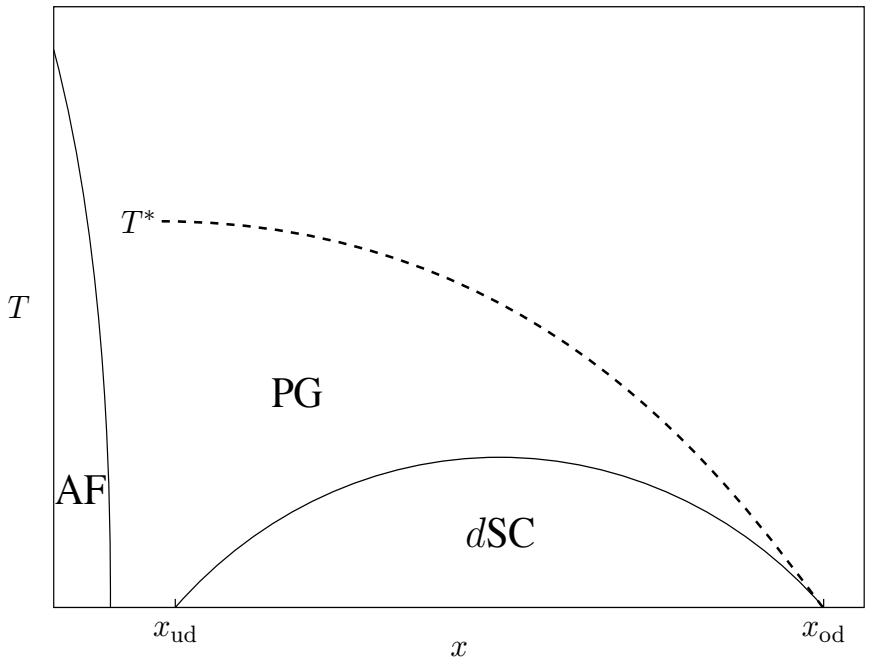

Figure 1.1: The typical phase diagram of a cuprate superconductor. T^* represents the pseudogap (PG) temperature below which the d-wave state is phase-disordered. Our focus is on the zero-temperature part of the phase diagram and possible quantum critical point between the anti-ferromagnetic state (AF) and d-wave superconducting phase (dSc).

1.1 Nodal quasi-particle action

The conventional approach to superconducting phase transitions is to consider the superconducting state as an instability of the *normal* phase to some small perturbation - normally weak attractive interactions. To explain the pseudogap regime and quantum phase transition from a d-wave state to an anti-ferromagnetic one, we take an opposite approach. We assume the d-wave state which experimentally and theoretically is known to have sharp d-wave excitations as the starting point and then proceed to study how under-doping the system from optimal doping can introduce phase fluctuations and disorder the d-wave state. In this section, however, we proceed beginning with a review of the BCS d-wave action limit of the electronic Hubbard model and focus on low-energy, low-temperature behaviours where the nodal excitations dominate.

Consider the BCS action given by

$$S_{\mathrm{q-p}} = \mathrm{T} \sum_{i\omega_n,\sigma,\mathbf{p}} (-i\omega_n + \varepsilon(\mathbf{p}))c^\dagger_\sigma(\omega,\mathbf{p})c_\sigma(\omega,\mathbf{p}) - \frac{\sigma}{2}\Delta(\mathbf{p})c^\dagger_\sigma(\omega,\mathbf{p})c^\dagger_{-\sigma}(-\omega,-\mathbf{p}) + h.c., \quad (1.1)$$

where $c_\sigma(\omega,\mathbf{p})$ and $c^\dagger_\sigma(\omega,\mathbf{p})$ are electronic operators with momentum $\mathbf{p}$, spin σ, and Matsubara frequency ω. Here a lattice tight-binding model with free particle dispersion $\varepsilon_{\mathbf{p}} = -4t\cdot(\cos(p_x a) + \cos(p_y b)) - \mu$ is assumed where t is the hopping amplitude, μ is the chemical potential and, a,b are lattice spacings on the x-y plane. The gap function, $\Delta_{\mathbf{p}} = (\Delta_0/2)(\cos(p_x) - \cos(p_y))$, is assumed to have $d_{x^2-y^2}$ symmetry. This is dictated by the layered tetragonal crystal structure of most of the HTS's. In the action (1.1) we have ignored any quartic interaction between electrons, and concentrated on the well-defined BCS quasi-particle ground state and the phase fluctuations around mean-field solutions.

A novel feature of the $d_{x^2-y^2}$ pairing symmetry is that the gap function, $\Delta_{\mathbf{p}}$, vanishes along lines $p_x = \pm p_y$. These lines intersect the two-dimensional fermi surface at four points in momentum space. Near these four *nodal* points, there are electronic excitations with arbitrary low energy. These low energy excitations dominate well below the transition temperature and lead to power law corrections in quantities such as the electronic specific heat and penetration depth.

To obtain the low-energy behaviour of the theory, we concentrate on the four nodes of the gap which appear on the $\pm\pi/4, \pm 3\pi/4$ angles around the Fermi surface. Each node is distinguished by vectors $\pm\mathbf{K_I}$ and $\pm\mathbf{K_{II}}$, where $\mathbf{K_I} = (\pi/2,\pi/2), \mathbf{K_{II}} = (-\pi/2,\pi/2)$ (Fig.(1.2)). Rewrite the momentum $\mathbf{p}$ in a $\pi/4$-rotated new coordinates around one node (say $\mathbf{K_I}$):

$$\mathbf{p} = p_F \begin{pmatrix} 1 \\ 1 \end{pmatrix} + q_x \begin{pmatrix} 1 \\ 1 \end{pmatrix} + q_y \begin{pmatrix} 1 \\ -1 \end{pmatrix} \quad (1.2)$$

where q_x and q_y are the rotated momenta measured from the Fermi surface. The Fermi momentum, p_F, is the amplitude of the wave-vectors $\mathbf{K}_i$. The chemical potential, μ, can be determined from the fact that the zero energy level lies on the Fermi surface $\varepsilon(\mathbf{K}_i) = 0$. Now the free particle dispersion and gap function can be written in terms of q_x and q_y as follows:

$$\varepsilon(\mathbf{p}) \simeq 2\sqrt{2}t\sin(K_{\mathbf{I},x})q_x \quad (1.3)$$

$$\Delta_{\mathbf{p}} \simeq \sqrt{2}\Delta_0\sin(K_{\mathbf{I},x})q_y. \quad (1.4)$$

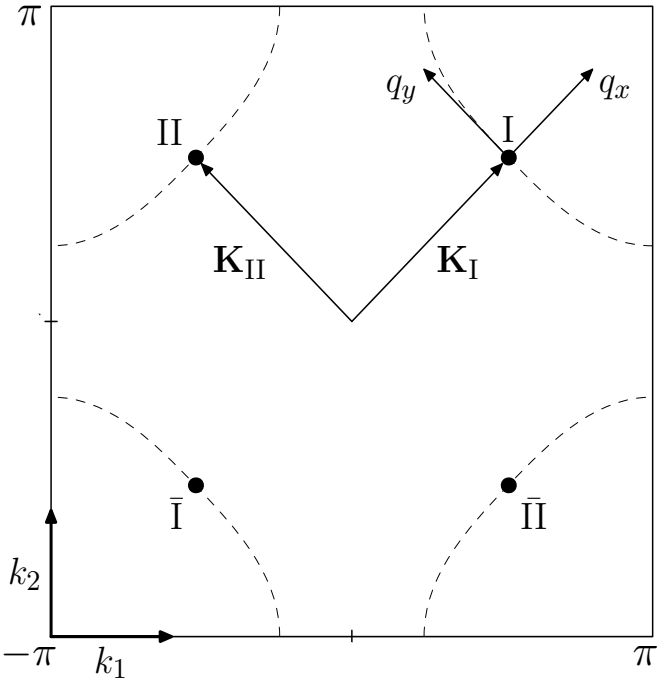

Figure 1.2: d-wave gap function of a typical d-wave superconductor and the nodal vectors $K_{\mathbf{I},\mathbf{II}}$.

Adopting a two-component Nambu spinor representation for electronic operators,

$$\Psi'^{(2)} = \begin{pmatrix} c_\uparrow(\omega, \mathbf{p}) \\ c_\downarrow^\dagger(-\omega, -\mathbf{p}) \end{pmatrix} \tag{1.5}$$

using the above linearized forms of the energy and gap function, the action is subsequently written in a linearized form,

$$S_{\mathrm{q-p}} = \sum_{i\omega,\mathbf{p}} \Psi_{\mathbf{I}}'^{(2)\dagger}\{i\omega\mathbf{1} + iv_F\sigma_3 q_x + iv_\Delta\sigma_1 q_y\}\Psi_{\mathbf{I}}'^{(2)} + (\mathbf{I} \to \mathbf{II}, x \to y), \tag{1.6}$$

where σ's are Pauli matrices. This can be made into a Lorentz invariant form by introducing the matrix $\gamma_0 = \sigma_2$ and defining spinor $\bar{\Psi}^{(2)}$ as $\gamma_0\Psi^{(2)}$. The other two gamma matrices γ_1 and γ_2 are σ_3 and σ_1 respectively. In the real space representation the action would be

$$S_{\mathrm{q-p}} = \int_0^\beta \mathrm{d}\tau \int \mathrm{d}^2\mathbf{x}\bar{\Psi}_{\mathbf{I}}'^{(2)}\{\gamma_0\partial_\tau + v_F\gamma_1\partial_x + v_\Delta\gamma_2\partial_2\}\Psi_{\mathbf{I}}'^{(2)} + (\mathbf{I} \to \mathbf{II}, x \to y). \tag{1.7}$$

Correspondingly, the *relativistic* energy spectrum of the quasi-particles reads as

$$E_{\mathbf{q}} = \sqrt{v_{\mathbf{F}}^2 q_x^2 + v_{\Delta}^2 q_y^2}. \tag{1.8}$$

It is well-known that in three-dimensions the fundamental representation of the Euclidean Clifford algebra[1] is the set of 2×2 Pauli-matrices. This limits the number of the elements of the Clifford algebra from 16 in 3+1-dimensions to 4 elements in 2+1-dimensions.

In 3+1 dimensions, there is an extra element of the Clifford algebra that anti-commutes with all the set of γ-matrices appearing in Dirac action, $\gamma_5 = i\gamma_0\gamma_1\gamma_2\gamma_3$. The Dirac action is invariant under the "chiral"-rotations generated by γ_5 unless there is an scalar mass term in the action. The distinction of massive and massless theories from a point of view of symmetry breaking is an important feature that is missing from our construction above.

Now we proceed by choosing a *four-component* representation for the spinors around each node (each node stands for a "flavour" in the spinor representation). Two flavours of the spinors- each belonging to one node of the gap function will be defined as

$$\Psi_{\mathbf{I}} = \begin{pmatrix} c_\uparrow(\omega, \mathbf{p}) \\ c_\downarrow^\dagger(-\omega, -\mathbf{p}) \\ c_\uparrow(\omega, \mathbf{p} + \mathbf{K_I}) \\ c_\downarrow^\dagger(-\omega, \mathbf{K_I} - \mathbf{p}) \end{pmatrix}, \qquad \Psi_{\mathbf{II}} = \begin{pmatrix} c_\uparrow(\omega, \mathbf{p}) \\ c_\downarrow^\dagger(-\omega, -\mathbf{p}) \\ c_\uparrow(\omega, \mathbf{p} + \mathbf{K_{II}}) \\ c_\downarrow^\dagger(-\omega, \mathbf{K_{II}} - \mathbf{p}) \end{pmatrix}. \tag{1.9}$$

The construction implemented above clearly is not unique. In our definition Eq.(1.9), each field is composed of two Nambu spinors, one for each of the nodes in diagonally opposed pairs. One could also combine the spin-reversed states in a similar manner. The choice one makes with regards the construction of the spinors is dictated by the particular symmetry of the problem. The spin-reversed combination would recover the full spin-rotation symmetry of the problem, while our choice yields a hidden chiral SU(2) symmetry. We will elaborate this matter as we proceed.

Using the spinors defined above and the linearized quasi particle dispersion will give rise to the action

$$S = T \sum_{i\omega, \mathbf{p}} \Psi_{\mathbf{I}}^\dagger(-i\omega + v_F q_x M_1 + v_\Delta q_y M_2)\Psi_{\mathbf{I}} + \Psi_{\mathbf{II}}^\dagger(-i\omega + v_F q_x M_2 + v_\Delta q_y M_1)\Psi_{\mathbf{II}}, \tag{1.10}$$

[1] A Euclidean Clifford algebra is defined by its generators, γ_μ, satisfying the anti-commutation relations: $\gamma_\mu, \gamma_\nu = 2\delta_{\mu\nu}$.

where $v_F \equiv 2\sqrt{2}t\sin(K_{\mathbf{I},x}), v_\Delta \equiv \sqrt{2}\Delta_0\sin(K_{\mathbf{I},x})$ and the matrices M_1 and M_2 are

$$M_1 = i\begin{pmatrix} \sigma_3 & 0 \\ 0 & -\sigma_3 \end{pmatrix} \tag{1.11}$$

$$M_2 = -i\begin{pmatrix} \sigma_1 & 0 \\ 0 & -\sigma_1 \end{pmatrix}. \tag{1.12}$$

The reader should notice the asymmetric role of spinors $\Psi_{\mathbf{I}}$ and $\Psi_{\mathbf{II}}$ under the exchange x and y axes ($x \leftrightarrow y$). The reader might notice that M_1 and M_2 belong to the SU(2) generators of spin rotation in a four-component representation. Correspondingly they anti-commute with each other. This form can also be written in a Dirac form for fermions by introducing an appropriate matrix γ_0 which anti-commutes with both M_1 and M_2. Assuming a general form for γ_0 and bearing in mind that γ_0 is Hermitian, the Dirac action now looks like:

$$S = \int \frac{\mathrm{d}^3q}{(2\pi)^3}\overline{\Psi}_{\mathrm{I}}(iq_0\gamma_0 + v_F q_x\gamma_1 + v_\Delta q_y\gamma_2)\Psi_{\mathrm{I}} + \overline{\Psi}_{\mathrm{II}}(iq_0\gamma_0 + v_\Delta q_y\gamma_1 + v_F q_x\gamma_2)\Psi_{\mathrm{II}}, \tag{1.13}$$

where $\overline{\Psi}$ is defined as $\overline{\Psi} \equiv \Psi^\dagger\gamma_0$. The isotropic form of the theory ($v_F = v_\Delta$) would now look like:

$$S = \int \frac{\mathrm{d}^3q}{(2\pi)^3}\left\{\overline{\Psi}_{\mathrm{I}}(iq_\mu\gamma_\mu)\Psi_{\mathrm{I}} + \overline{\Psi}_{\mathrm{II}}(iq_\mu\gamma_\mu)\Psi_{\mathrm{II}}\right\}. \tag{1.14}$$

This action represents the spectrum of nodal quasi-particles at low energies. The fact that quasi-particles are massless is the signature of the chiral symmetry in our theory. Each of the two nodes now represent a "flavour" for our Dirac field Ψ and the gapless nature of quasi-particles is hidden in both the linear form of action and the γ-matrices algebra. We proceed by deriving all possibilities for the proposed γ_0 matrix. Writing γ_0 in terms of four 2×2 matrices A, B, C and D,

$$\gamma_0 = \begin{pmatrix} A & C \\ C^\dagger & B \end{pmatrix}. \tag{1.15}$$

A, B, C, and D can be expanded in the basis of $\mathbf{1}, \sigma_1, \sigma_2, \sigma_2$. For the sake of simplicity we choose them to be one of the basis members. The conditions that γ_0 anti-commute with both M_1 and M_2 and also squares to unity determines the unknown components A, B, C, and D.

$$\begin{aligned} \gamma_0 M_1 = -M_1\gamma_0 &\Longrightarrow \{A,\sigma_3\} = 0, \{B,\sigma_3\} = 0, [C,\sigma_3] = 0. \\ \gamma_0 M_2 = -M_2\gamma_0 &\Longrightarrow \{A,\sigma_1\} = 0, \{B,\sigma_1\} = 0, [C,\sigma_1] = 0. \end{aligned} \tag{1.16}$$

$$\Longrightarrow A = a\,\sigma_2, B = b\,\sigma_2, C = c\,\mathbf{1}. \tag{1.17}$$

and finally requiring $\gamma_0^2 = \mathbf{1}$ gives rise to

$$a^2 + |c|^2 = 1, \;\; b^2 + |c|^2 = 1 \tag{1.18}$$

$$ac + cb = 0, \;\; ac^* + bc^* = 0 \tag{1.19}$$

Independent solutions of the above equations ($a = \pm 1, b = \pm 1, c = 0$ or $a = b = 0, c = 1, i$) give rise to four candidates for γ_0 as

$$\begin{aligned} \gamma_0^{(1)} &= \sigma_1 \otimes \mathbf{1} \\ \gamma_0^{(2)} &= \sigma_3 \otimes \sigma_2 \\ \gamma_0^{(3)} &= \sigma_2 \otimes \mathbf{1} \\ \gamma_0^{(4)} &= \mathbf{1} \otimes \sigma_2 \end{aligned} \tag{1.20}$$

This arbitrariness in the definition of γ_0 can be interpreted in terms of a symmetry of the action. The same feature persists in a four dimensional massless relativistic model. However, in four dimensions γ_0 is arbitrary up a to a "chiral" rotation by γ_5. The lower dimensionality, $d = 3$, enriches the symmetry structure of the model as will be discussed in more detail in later sections.

1.2 Phase fluctuations

1.2.1 Singular gauge transformation

In the pseudo-gap regime the phase fluctuations of the order parameter determine the critical behaviour of the system. Thus in this Section we turn our focus to the phase fluctuations of the order parameter. We assume that the fluctuations of the amplitude for the order parameter are ignorable, and approximate it by a constant. The phase of the order parameter is be divided to its regular and singular parts as

$$\phi(\mathbf{x}) = \phi_{\mathrm{r}}(\mathbf{x}) + \phi_{\mathrm{s}}(\mathbf{x}). \tag{1.21}$$

ϕ_{r} and ϕ_{s} are regular and singular parts and can be distinguished as one circles around a singularity of the order parameter. To avoid more discussions regarding mathematical definitions of singular phase on a lattice, we do the following discussion in a continuum limit. However both limits share the concept of singular phases for the order parameter and later on I come back to a lattice model to describe such singularities.

$$\oint \nabla\phi_{\rm r}(\mathbf{x}).{\rm d}\mathbf{s} = 0,$$
$$\oint \nabla\phi_{\rm s}(\mathbf{x}).{\rm d}\mathbf{s} = 2\pi m, \tag{1.22}$$

where m is an integer that determines the *vorticity* of the singularity. The superfluid current can be written as the gradient of the phases

$$\mathbf{j}(\mathbf{x}) \sim \nabla\phi_{\rm r}(\mathbf{x}) + \nabla\phi_s(\mathbf{x}). \tag{1.23}$$

The current can also be decomposed into an irrotational piece (regular) and incompressible piece (vortices) too. By introducing the vorticity $\vec{w}(\mathbf{x})$ the current can be written

$$= \nabla\phi_r(\mathbf{x}) + \nabla \times \vec{w}(\mathbf{x}), \tag{1.24}$$

where $\nabla \times \vec{w}(\mathbf{x}) = \nabla\phi_s(\mathbf{x})$ and $\vec{w}(\mathbf{x})$ satisfies

$$\nabla^2 w_{\mathbf{x}} = \sum_i m_i \delta(\mathbf{x} - \mathbf{x}_i), \tag{1.25}$$

where m_i's are the vorticity of individual indices positioned at $\mathbf{x} = {\rm x}_i$. It is desirable to include the explicit phase degree of freedom into the quasi-particle action by introducing a gauge transformation which absorbs the phase of the order parameter into the fermionic operators. The simplest way of doing this is divide total phase equally between each spin-up/down electron. i.e.,

$$c_\uparrow(\mathbf{x}) \rightarrow e^{-i\phi(\mathbf{x})/2} c_\uparrow(\mathbf{x})$$
$$c_\downarrow(\mathbf{x}) \rightarrow e^{-i\phi(\mathbf{x})/2} c_\downarrow(\mathbf{x})$$
$$\Delta(\mathbf{x}) = \langle c_\uparrow(\mathbf{x}) c_\downarrow(\mathbf{x})\rangle \rightarrow |\Delta|. \tag{1.26}$$

However, the above transform is not well-defined in the presence of the vortices: $c_{\uparrow,\downarrow} \rightarrow \exp(i\pi)\cdot c_{\uparrow,\downarrow}$. This will introduce branch cuts associated with each vortex which makes things more complicated than it is already. The symmetric dividing of the phase, however, would be well-defined if we only consider double-vorticity vortices. This will lead to the Z_2 gauge theory representation of the problem. We will not pursue this approach since the single-vorticity vortices are the ones to become relevant at a Kosterlitz-Thouless transition. To avoid this we adopt Franz-Tesanovic gauge

transformaion [10][9] that allows for a symmetric split of the regular-phase of the order parameter between the electrons but assigns only the phase of vortices in a group (group A or B) to each fermion with spin up/down. i.e.,

$$\begin{aligned} c_\uparrow(\mathbf{x}) &\rightarrow e^{-i\phi_A(\mathbf{x})}c_\uparrow(\mathbf{x}), \\ c_\downarrow(\mathbf{x}) &\rightarrow e^{-i\phi_B(\mathbf{x})}c_\downarrow(\mathbf{x}), \end{aligned} \tag{1.27}$$

while

$$\begin{aligned} \phi(\mathbf{x}) &= \phi_A(\mathbf{x}) + \phi_B(\mathbf{x}), \\ \phi_A &\equiv \frac{\phi_r}{2} + \phi_{s,A}, \\ \phi_B &\equiv \frac{\phi_r}{2} + \phi_{s,B} \end{aligned} \tag{1.28}$$

It is important to emphasize that each fermion acquires a singular phase solely from one set of vortices - arbitrarily chosen. We will return to this point while constructing the vortex dynamics through duality transform in the Sec. 1.3. Since the dividing of the vortices (loops) into two groups A and B is arbitrary, we assume an average over all possible configuration of the A and B groups in the partition function. Every fixed group in our case will act as a fixed singular-gauge, and by summing over all possible configuration we restore the gauge invariance.

1.2.2 Minimal coupling

In the previous Section we did not consider the phase fluctuations of the order parameter and the corresponding topological excitations of the system corresponding to that. This issue will be illuminated in this section [9][5][11]. However, we have to modify our construction of the Dirac quasi-article action to include the fluctuations of the order parameter

$$\Delta(\mathbf{x},\tau) = (\Delta_0 + \delta\Delta(\mathbf{x},\tau))e^{i\phi(\mathbf{x},\tau)}, \tag{1.29}$$

Where $\delta\Delta(\mathbf{x},\tau)$ indicates the amplitude fluctuations and $\phi(\mathbf{x},\tau)$ is the total phase of of order parameter. If we rewrite the off-diagonal contributions in the original BCS Hamiltonian in spatial coordinates - back to a tight binding lattice model and allow time and spatial dependence of the phase:

$$S_\Delta = \frac{1}{2}\sum_{\mu=x,y}\int \mathrm{d}\tau \mathrm{d}^2\mathbf{x}\cdot\Delta_\mu e^{i\phi(\mathbf{x},\tau)}\{c^\dagger_\uparrow(\mathbf{x},\tau)c^\dagger_\downarrow(\mathbf{x}+\hat{\mu},\tau) - c^\dagger_\downarrow(\mathbf{x},\tau)c^\dagger_\uparrow(\mathbf{x}+\hat{\mu},\tau)\} + \mathrm{h.c.}, \quad (1.30)$$

where

$$\Delta_\mu = \begin{cases} +\Delta_0 & \hat{\mu}=\hat{x}, \\ -\Delta_0 & \hat{\mu}=\hat{y}, \end{cases} \quad (1.31)$$

expanding $c(\mathbf{x}+\hat{\mu},\tau)$ and $c^\dagger(\mathbf{x}+\hat{\mu},\tau)$ in the continuum

$$\begin{aligned} S_\Delta = \frac{1}{2}\int \mathrm{d}\tau \mathrm{d}^2\mathbf{x}\cdot e^{i\phi(\mathbf{x},\tau)}\{&(c^\dagger_\uparrow(\mathbf{x},\tau)\partial_x c^\dagger_\downarrow(\mathbf{x},\tau) - c^\dagger_\downarrow(\mathbf{x},\tau)\partial_x c^\dagger_\uparrow(\mathbf{x},\tau)) \\ &-(c^\dagger_\uparrow(\mathbf{x},\tau)\partial_y c^\dagger_\downarrow(\mathbf{x},\tau) - c^\dagger_\downarrow(\mathbf{x},\tau)\partial_y c^\dagger_\uparrow(\mathbf{x},\tau))\} + \mathrm{h.c.}\ . \end{aligned} \quad (1.32)$$

Upon $\pi/4$ rotation of the x-y frame: $\partial_x - \partial_y \to \partial_y$ we have

$$\begin{aligned} S_\Delta = \frac{1}{2}\int \mathrm{d}\tau \mathrm{d}^2\mathbf{x}\cdot e^{i\phi(\mathbf{x},\tau)}&(c^\dagger_\uparrow(\mathbf{x},\tau)\partial_y c^\dagger_\downarrow(\mathbf{x},\tau) - c^\dagger_\downarrow(\mathbf{x},\tau)\partial_y c^\dagger_\uparrow(\mathbf{x},\tau) \\ &+e^{-i\phi(\mathbf{x},\tau)}(c_\downarrow(\mathbf{x},\tau)\partial_y c_\uparrow(\mathbf{x},\tau) - c_\uparrow(\mathbf{x},\tau)\partial_y c_\downarrow(\mathbf{x},\tau), \end{aligned} \quad (1.33)$$

integrating by parts for second and fourth terms gives rise to

$$S_\Delta = \int_{\mathbf{x},\tau} c^\dagger_\uparrow\cdot\frac{1}{2}\{e^{i\phi},\partial_y\}\cdot c^\dagger_\downarrow + c_\downarrow\cdot\frac{1}{2}\{e^{-i\phi},\partial_y\}\cdot c_\uparrow, \quad (1.34)$$

so the previous quasi particle action can be modified by replacing ∂_y with $\frac{1}{2}\{e^{i\phi},\partial_y\}$ in $c^\dagger c^\dagger$ terms and ∂_y with $\frac{1}{2}\{e^{-i\phi},\partial_y\}$ in cc terms. Thus, the quasi-particle action can be written as

$$S_{\mathrm{q-p}} = \int \mathrm{d}\tau \mathrm{d}^2\mathbf{x}\Psi^{\dagger\prime}_{\mathbf{I}}(\partial_\tau + v_F\cdot\tilde{M}_1\partial_x + |v_\Delta|\cdot\tilde{M}_2\partial_y)\Psi_{\mathbf{I}} + (\mathbf{I}\to\mathbf{II}, x\to y). \quad (1.35)$$

where the matrix $\tilde{M}_2$ is

$$\tilde{M}_2 = -i\frac{1}{2}\begin{pmatrix} & \{e^{i\phi},\partial_y\} & & \\ \{e^{-i\phi},\partial_y\} & & & \\ & & & -\{e^{i\phi},\partial_y\} \\ & & -\{e^{-i\phi},\partial_y\} & \end{pmatrix}, \quad (1.36)$$

Now we apply our singular gauge transform

$$\begin{aligned} c_\uparrow(\mathbf{x},\tau) &\longrightarrow e^{i\phi_A(\mathbf{x},\tau)}\cdot c_\uparrow(\mathbf{x},\tau), \\ c_\downarrow(\mathbf{x},\tau) &\longrightarrow e^{i\phi_B(\mathbf{x},\tau)}\cdot c_\downarrow(\mathbf{x},\tau), \end{aligned} \tag{1.37}$$

where $\phi_A(\mathbf{x},\tau)+\phi_B(\mathbf{x},\tau)=\phi(\mathbf{x},\tau)$. Correspondingly the spinor Ψ' can be transformed using the unitary transform $U\Psi=\Psi'$.

$$U=\begin{pmatrix} e^{i\phi_A} & & & \\ & e^{-i\phi_B} & & \\ & & e^{i\phi_A} & \\ & & & e^{-i\phi_B} \end{pmatrix}. \tag{1.38}$$

Introducing the gauge fields $\mathbf{a}(\mathbf{x},\tau)$ and $\mathbf{v}(\mathbf{x},\tau)$ as

$$\begin{aligned} \vec{a}(\mathbf{x},\tau) &= \nabla(\phi_A(\mathbf{x},\tau)-\phi_B(\mathbf{x},\tau)), \\ \vec{v}(\mathbf{x},\tau) &= \nabla(\phi_A(\mathbf{x},\tau)+\phi_B(\mathbf{x},\tau)), \end{aligned} \tag{1.39}$$

using the commutation relations $[U,M_1]=0$ and $[U,M_2]=\exp(i\phi)$ the action can be rewritten with the gauge field $\mathbf{a}(\mathbf{x},\tau)$ minimally coupled to the gradient term while the gauge field $\mathbf{v}(\mathbf{x},\tau)$ *only* couples to the current term in the action

$$\begin{aligned} S_{q-p}=\int \mathrm{d}\tau\mathrm{d}^2\mathbf{x}\Psi^\dagger_{\mathbf{I}}(\mathbf{x},\tau)\{(\partial_\tau+ia_\tau)+M_1(\partial_x+ia_x)+M_2(\partial_y+ia_y)\}\Psi_{\mathbf{I}}(\mathbf{x},\tau) \\ +(\mathbf{I}\to\mathbf{II},x\to y)+J_\mu v_\mu, \quad \mu=0,1,2 \end{aligned} \tag{1.40}$$

where the with the current coupled to the field v_μ is

$$J_\mu=\left(\sum_{i=\mathbf{I},\mathbf{II}}\Psi^\dagger_i(\mathbf{1}\otimes\sigma_3)\Psi_i, iv_F\Psi^\dagger_{\mathbf{I}}(\sigma_3\otimes\mathbf{1})\Psi_{\mathbf{I}}, iv_F\Psi^\dagger_{\mathbf{II}}(\sigma_3\otimes\mathbf{1})\Psi_{\mathbf{II}}\right). \tag{1.41}$$

If we write the imaginary-time component J_0 in terms of the electronic operators, it will appear to be proportional to the electron density operator.

$$J_0=i(c^\dagger_\uparrow(\mathbf{x},\tau)c_\uparrow(\mathbf{x},\tau)+c^\dagger_\downarrow(\mathbf{x},\tau)c_\downarrow(\mathbf{x},\tau)), \tag{1.42}$$

while the x and y components of the current represent the electronic current

$$J_{1,2} = i(c_{\uparrow}^{\dagger}(\mathbf{x},\tau)c_{\uparrow}(\mathbf{x},\tau) - c_{\downarrow}^{\dagger}(\mathbf{x},\tau)c_{\downarrow}(\mathbf{x},\tau)). \tag{1.43}$$

To obtain the above I have taken advantage of the form of the Ψ spinors around both nodes in the spatial coordinates

$$\Psi_{\mathbf{I}}(\mathbf{x},\tau) = \begin{pmatrix} e^{-iK_{\mathbf{I}}x}c_{\uparrow} \\ e^{-iK_{\mathbf{I}}x}c_{\downarrow}^{\dagger} \\ e^{iK_{\mathbf{I}}x}c_{\uparrow} \\ e^{iK_{\mathbf{I}}x}c_{\downarrow}^{\dagger} \end{pmatrix}, \quad \Psi_{\mathbf{II}}(\mathbf{x},\tau) = \begin{pmatrix} e^{-iK_{\mathbf{II}}x}c_{\uparrow} \\ e^{-iK_{\mathbf{II}}x}c_{\downarrow}^{\dagger} \\ e^{iK_{\mathbf{II}}x}c_{\uparrow} \\ e^{iK_{\mathbf{II}}x}c_{\downarrow}^{\dagger} \end{pmatrix}. \tag{1.44}$$

To conclude this section we look at the gauge symmetry property of the new representation of the theory above.

1.3 Dynamics of the gauge fields

Now we can more carefully illuminate the meaning of the singular gauge transformations by investigating the coupling of the vortex action and the quasi-particle action including the vortex fluctuation into the theory.

For the phase fluctuating part of the theory we take the 3D XY-model on a cubic lattice as the simplest theory that resembles all the expected behaviours:

$$Z_{\mathrm{3D-XY}} = \int_0^{2\pi} [\Pi \mathrm{d}\phi_i] \exp\left(\frac{K}{2}\sum_{i,\hat{\mu}} \cos(\Delta_\mu \phi_i)\right), \tag{1.45}$$

where ϕ_i is the field variable on the lattice site $\vec{i}$ and $\hat{\mu}$ is the vector connecting to the nearest-neighbour sites.

To begin we look at the Villain approximation to the XY-model [19]

$$Z_{\mathrm{XY}} = \int_0^{2\pi} [\Pi \mathrm{d}\phi_i] \sum_{m_{i,\mu}} \exp\left(-\frac{K}{2}\sum_{i,\hat{\mu}} (\Delta_\mu \phi_i - 2\pi m_{i,\mu})^2\right). \tag{1.46}$$

The above theory is invariant under the gauge transformation

$$\phi_i \rightarrow \phi_i + 2\pi N_i,$$
$$m_{i,\mu} \rightarrow m_{i,\mu} - 2\pi\Delta_\mu N_i. \tag{1.47}$$

This will let us to extend the integral between $\{0, 2\pi\}$ to $\{-\infty, +\infty\}$. Decoupling the quadratic term by introducing the real fields $b_{i,\mu}$

$$Z_{\mathrm{XY}} = \int [\Pi \mathrm{d}\phi_i][\Pi \mathrm{d}b_{i,\mu}] \sum_{m_{i,\mu}} \exp\left(\sum_{i,\hat{\mu}} -b_{i,\mu}^2 + ib_{i,\mu}(\Delta_\mu\phi_i - 2\pi m_{i,\mu})\right) \tag{1.48}$$

Recalling the Poisson summation formula

$$\sum_n e^{2\pi n x} = \sum_m \delta(x - m), \tag{1.49}$$

and integrating over the angular variable forces the auxiliary field to be divergence free

$$Z = \int [\Pi \mathrm{d}b_{i,\mu}] \sum_{m_{i,\mu}} \delta[\Delta_\mu b_{i,\mu}] \exp\left(\sum_{i,\hat{\mu}} -b_{i,\mu}^2 + 2\pi m_{i,\mu} b_{i,\mu}\right), \tag{1.50}$$

the $b_{i,\mu}$ thus can be rewritten as the curl of another real vector field

$$Z = \int [\Pi \mathrm{d}s_{i,\mu}] \sum_{n_{i,\mu}} \exp\left(\sum_{i,\hat{\mu}} -(\epsilon_{\nu\mu\rho}\partial_\nu s_{i,\mu})^2 + 2\pi n_{i,\mu} s_{i,\mu}\right), \tag{1.51}$$

where $\vec{n} \equiv \nabla \times \vec{m}$ is the integer vortex field that forces $s_{i,\mu}$ to take integer values. This is the current representation of the XY-model. Before we proceed let us stop to understand the meaning of the vortices in this model. Consider the line integral of the original field variable ϕ_i around a lattice point i on the adjacent bonds.

$$\sum_{\mathrm{loop}} \Delta_\mu \phi_i = 2\pi n_{i,\mu}, \tag{1.52}$$

where the integer valued vector field $n_{i,\mu}$ represents the quantized flux/vortex variables. In the Villain representation with the angular variable divided into $\phi_i \rightarrow \phi_i + 2\pi N_i$ with $0 \leq \phi_i \leq 2\pi$, this will lead to

$$\sum_{\mu} \Delta_{\mu}\phi_i = 2\pi \sum_{\mu} m_{i,\mu} = n_{\mu,i}$$
$$\Longrightarrow \vec{n}_i = \nabla \times \vec{m}_i. \tag{1.53}$$

The condition that $n_{i,\mu}$ is also divergence free makes it a vortex loop.

Back to the Eq.(1.51), we decouple the vortex field terms by introducing two gauge-fields, $\vec{a}_i$ and $\vec{v}_i$.

$$\begin{aligned} Z_{\rm XY} &= \int \mathrm{d}[\vec{a},\vec{v}] \sum_{m_A,m_B}{}' \delta[\nabla \times (\mathbf{m}_{A,i} - \mathbf{m}_{B,i})] \cdot \exp(-2K \cdot \sum_i \vec{v}_i^2 \\ &+ 2\pi i \vec{v}_i \cdot (\nabla \times (\mathbf{m}_{A,i} + \mathbf{m}_{B,i}))), \\ Z_{\rm XY} &= \int \mathrm{d}[\vec{a},\vec{v}] \sum_{m_A,m_B}{}' \cdot \exp(-2K \cdot \sum_i \vec{v}_i^2 \\ &+ 2\pi i \vec{v}_i \cdot (\nabla \times (\mathbf{m}_{A,i} + \mathbf{m}_{B,i})) + 2\pi i \vec{a}_i \cdot (\nabla \times (\mathbf{m}_{A,i} - \mathbf{m}_{B,i}))), \end{aligned} \tag{1.54}$$

where index ($'$), on the summation indicates that the sum is over divergence-less fields. Integrating over the gauge field $\mathbf{v}_i$ and introducing real fields $\Phi_{A,i}$ and $\Phi_{B,i}$ give rise to

$$\begin{aligned} Z = \int \mathrm{d}[\vec{a}_i, \mathbf{\Phi}_+, \mathbf{\Phi}_-] \sum_{l_A,l_B}{}' \exp[\frac{1}{8K}(\nabla \times \mathbf{\Phi}_{+,i})^2 + i\vec{a}_i \cdot (\nabla \times \mathbf{\Phi}_{-,i}) \\ +2\pi i \cdot (\mathbf{l}_A \cdot \mathbf{\Phi}_{A,i} + \mathbf{l}_B \cdot \mathbf{\Phi}_{B,i})]. \end{aligned} \tag{1.55}$$

where $\mathbf{\Phi} \equiv \mathbf{\Phi}_A \pm \mathbf{\Phi}_B$ and $\mathbf{l}_A$ and $\mathbf{l}_B$ force $\mathbf{\Phi}_{\pm}$ fields to take integer values.

Now we introduce chemical potential term,

$$x \cdot \sum_i \left(\mathbf{l}_{A,i}^2 + \mathbf{l}_{B,i}^2\right), \tag{1.56}$$

while assuming the limit of $x \to 0$. To keep the gauge invariance for fields Φ_+ and Φ_-

$$\begin{aligned} \Phi_{+,i\mu} &\to \Phi_{+,i\mu} + \Delta_{\mu}\chi_i, \\ \Phi_{-,i\mu} &\to \Phi_{-,i\mu} + \Delta_{\mu}\phi_i, \end{aligned} \tag{1.57}$$

we should impose the conditions that both fields l_A and $\mathbf{l}_B$ are divergence free,

$$\begin{aligned} \nabla \cdot \mathbf{l}_{A,i} &= 0, \\ \nabla \cdot \mathbf{l}_{B,i} &= 0. \end{aligned} \tag{1.58}$$

There are other ways that chemical potential could be introduced, such as,

$$x \cdot \sum_i (\mathbf{l}_{A,i} + \mathbf{l}_{B,i})^2 + (\mathbf{l}_{A,i} - \mathbf{l}_{B,i})^2. \tag{1.59}$$

This would directly take us to the one-flavour representation of the Frozen Superconductor representation of the XY model [13]. However if I assume that the vortex fields m_A and m_B (similarly l_A and l_B) belong to different groups, i.e., no overlap between the two fields, the form Eq(1.56) is justified.

Finally, we arrive at the Frozen Lattice Superconductor (FLS) representation of the XY model by forcing the zero-divergence condition on the vortex fields $\mathbf{l}_A$ and $\mathbf{l}_B$ [13][15]:

$$\begin{aligned} Z = \lim_{x\to 0} \sum_{l_A, l_B} \int \Pi[\mathrm{d}\theta_{A,i}]\Pi[\mathrm{d}\theta_{B,i}]\Pi[\mathrm{d}a_{i,\mu}] \exp(\sum_i \frac{1}{8K}(\nabla \times \mathbf{\Phi}_{+,i})^2 + i\mathbf{a}\cdot(\nabla\times\mathbf{\Phi}_i) + \\ 2\pi i(\mathbf{l}_A \cdot \mathbf{\Phi}_{A,i} + \mathbf{l}_B \cdot \mathbf{\Phi}_{B,i}) - \frac{x}{2}(\mathbf{l}_{A,i} + \mathbf{l}_{B,i})^2 + 2\pi i(\nabla\cdot\mathbf{l}_{A,i})\cdot\theta_{A,i} + 2\pi i(\nabla\cdot\mathbf{l}_{B,i})\cdot\theta_{B,i}). \end{aligned} \tag{1.60}$$

Poisson-resumming over $\mathbf{l}_A$ and $\mathbf{l}_B$ and using the reverse form of Villain approximation, we obtain:

$$\begin{aligned} Z_{XY} = \lim_{x\to 0} \int_{-\infty}^{\infty} \mathrm{d}[\vec{a}_i, \mathbf{\Phi}_A, \mathbf{\Phi}_B] \int_0^{2\pi} \mathrm{d}[\theta_A, \theta_B] \exp(-\sum_{i,\mu} \frac{1}{8K}(\nabla\times\mathbf{\Phi}_{+,i})^2 + \\ i\mathbf{a}\cdot(\nabla\times\mathbf{\Phi}_{-,i}) - \frac{1}{2x}\cos(\Delta_\mu\theta_{A,i} - 2\pi\mathbf{\Phi}_{A,i\mu}) - \frac{1}{2x}\cos(\Delta_\mu\theta_{A,i} - 2\pi\mathbf{\Phi}_{A,i\mu})), \end{aligned} \tag{1.61}$$

where the angles $\theta_{A,B}$ represents two-flavoured "dual" fields with respect to original angular field ϕ_i.

The usefulness of this representation is seen when we try to calculate the correlation function for $\vec{a}$:

$$\langle(\nabla\times\vec{a})_{i,\gamma}(\nabla\times\vec{a}_{j,\mu})\rangle = \delta_{ij}\delta_{\mu\nu}\frac{\pi^2}{x}\langle\cos(\Delta_\mu\theta_i + 2\pi\Phi_{i\mu})\rangle_{\mathrm{FLS}}. \tag{1.62}$$

It is well established that the lattice superconductor at a small but finite *temperature* x has a phase transition, as stiffness K is varied in the same universality class as in the frozen limit [14]. We can therefore relax the constraint $x \to 0$ and assume x to be finite. The average on the righthand side of Eq. (1.62) can be calculated to be:

$$\frac{1}{x}\langle \cos(\Delta_\mu \theta_i + 2\pi \Phi_{i\mu})\rangle_{\rm FLS} \propto |\langle \exp(i\theta_i)\rangle|^2. \tag{1.63}$$

This is simply a restatement of the fact that in the ordered phase the dual angles are correlated while through the Anderson-Higgs mechanism the gauge field $\vec{a}$ becomes massive. The expression for the correlation function for $\vec{a}$ at low momenta is therefore:

$$\langle (\nabla \times \vec{a})_\gamma (\nabla \times \vec{a})_\mu \rangle \propto (|\langle \Phi \rangle| + O(q^2))(\delta_{\mu\nu} - \hat{a}_\mu \hat{q}_\nu). \tag{1.64}$$

While the stiffness is inversely proportional to the expectation value of the dual loop condensate $\langle \Phi \rangle \sim \langle e^{i\theta} \rangle$ the fugacity of the vortex-loop corresponds to the charge for the gauge field $\vec{a}$. This will lead us to the effective theory at low temperature for quasi-particles as:

$$\begin{aligned} S[\Phi] &= \int d^2\mathbf{x} d\tau (\Psi_I(\gamma_0(\partial_\tau + i a_0) + \gamma_1 v_F(\partial_x + i a_x) + \gamma_2 |v_\Delta|(\partial_y + i a_y)) \\ &+ (\mathrm{I} \to \mathrm{II}, x \leftrightarrow y) + \frac{1}{2|\langle \Phi \rangle|^2}(\nabla \times \vec{a})^2), \end{aligned} \tag{1.65}$$

where the effect of vortices is simplified into a Maxwell's term for dynmaics of $\vec{a}$-field. This is a central result and starting point for the dynamical mass generation in this theory which we will discuss in the next sections.

Back to the vortex part of the action, notices that another duality transform on Eq. (1.61) using the identity:

$$\begin{aligned} &\int (\prod_i d\theta_i d\Phi_i) \exp\{\sum \frac{1}{T}\cos(\Delta\theta + \Phi) - \frac{i}{2\pi}\vec{a}\cdot(\nabla \times \vec{A})\} = \\ &\lim_{x\to 0} \int (\prod_i d\Psi_i) \exp\{\frac{1}{x}\cos(\Delta\Psi + \vec{a}) - \frac{T}{8\pi^2}(\nabla \times \vec{a})^2, \end{aligned} \tag{1.66}$$

will lead to the action

$$S_b = \lim_{x\to 0}\left(-2K\sum_i v_i^2 + \frac{1}{2x}\sum_{i,\mu}\cos(\Delta_\mu \Psi_{A,i} + v_i + a_i) + \frac{1}{2x}\cos(\Delta_\mu \Psi_i + v_i - a_i)\right). \tag{1.67}$$

Notice that we have recovered the $\vec{a}$ and $\vec{v}$ gauge field in the dual-dual transformed action. From symmetry considerations, it is straightforward to determine the continuous version of S_b by

introducing bosonic fields $b_i^{(n)}$

$$\begin{aligned} S_b[b_i^{(n)}] &= \int_0^\beta d\tau \int d^2r (2Kv_\mu^2 + \frac{1}{2}\sum_{n=1}^{2} |(\partial_\mu - i(v_\mu + (-1)^n a_\mu))b_i^{(n)}|^2 \\ &+ \alpha \sum_{n=1}^{2} |b_n|^2 + \frac{\beta_1}{2}(\sum_{n=1}^{2} |b_i^{(n)}|^2)^2 + \frac{\beta_2}{2}(\sum_{n=1}^{2} |b_i^{(n)}|^4)). \end{aligned} \tag{1.68}$$

Minimizing the action with respect to the b_i's, gives:

$$|\langle b_1 \rangle|^2 = |\langle b_2 \rangle|^2 = \frac{\alpha}{2\beta_1 + \beta_2}, \tag{1.69}$$

and leads to S_b as

$$S_b \to \int_0^\beta \int d^2r (K(v_\mu + A_\mu) + \frac{|\alpha|}{2\beta_1 + \beta_2}(v_\mu^2 + a_\mu^2)). \tag{1.70}$$

Notice that now a_μ and v_μ fields are coupled and thus we can write down the total action decomposed into quasi-particle and spin and charge sectors, i.e.

$$S[\Psi, b_n, \vec{a}, \vec{v}] = S_{\text{spin}}[\Psi, \vec{a}, \vec{v}] + S_{\text{charge}}[b_n, \vec{a}, \vec{v}], \tag{1.71}$$

where S_{spin} and S_{charge} are defined as

$$S_{\text{spin}} = S_{q-p} - i(v_\mu + A_\mu)J_\mu + \frac{|\alpha|}{2\beta_1 + \beta_2} a_\mu^2, \tag{1.72}$$

$$S_{\text{charge}} = i(v_\mu + A_\mu)J_\mu + 2K(v_\mu + A_\mu)^2 + \frac{|\alpha|}{2\beta_1 + \beta_2} v_\mu^2. \tag{1.73}$$

We will use the S_{charge} later on in this thesis to derive a general superfluid form for response in this theory.

The theory, so far, is represented by two sectors, each indicating one degree of freedom of the system. The fermionic excitations are represented by a Dirac action which is coupled through a singular gauge field to a two-component Frozen Lattice superconductor version of bosonic vortex loops. The lattice bosons can be simplified - as we just did - into a two component Landau-Ginzburg action in the presence of the two gauge-fields. Two new features which makes it difficult to analyze are the fact that the vortex loops are represented by two fields, not one, and the coupling of the two singular gauge fields $\vec{a}$ and $\vec{v}$ to the vortex loops is very non-trivial. One main feature of the theory, however, is that the spin-sector of the theory, i.e., the quasi-particle coupled to the field $\vec{a}$, can generate a mass for fermions if the dynamics of the field $\vec{a}$ is strong enough. This is allowed

as soon as the vortex loops are condensed, which creates an effective charge for our gauge field and thus a dynamics. In the following, we briefly discuss the mechanism of mass generation following the original work of Appelquist *et al* for three dimensional quantum electrodynamics [25]. A more detailed discussion on the subject dynamical mass generation is postponed until the Chapter two.

1.4 Dynamical mass generation in Dirac theory

As discussed before, the effect of the vortex degree of freedom in the nodal excitation sector of the theory is to introduce an effective charge for the quasi-particles. The charge is directly proportional to the vortices' fugacity. Ignoring anisotropies in the theory in the three dimensional electrodynamics, QED_3 (Eq.(1.65)) there is a mechanism known as dynamical mass generation, which leads to non-zero expectation values of $\bar{\Psi}\Psi$ and creates a mass for fermionic excitations. This is due to the fluctuations of the gauge-field $\mathbf{a}$ [17][16][24]. This is the signature of the chiral symmetry breaking, which we will discuss in the next section. Dynamical mass generation can also lead to other kinds of mass/order-parameter such as $\langle\Psi^{\dagger}\Gamma\Psi\rangle$, for which Γ does not commute with chiral symmetry generators.

Dynamical mass generation can be better formulated under a large-N approximation, where N is flavour of fermionic degrees of freedom ($N = 2$ in the original theory, i.e., the number of nodes). Writing down the Schwinger-Dyson equation for fermion self-energy $\Sigma(q)$ and gauge-field polarization function $\Pi_{\mu\nu}(q)$, the self-energy will look like,

$$\Sigma(q) = e^2\gamma_\nu \int \frac{\mathrm{d}^3p}{(2\pi)^3} \frac{D_{\mu\nu}(p-q)\Sigma(p)}{p^2+\Sigma^2(p)} \tag{1.74}$$

with the gauge-field propagator $D_{\mu\nu}$ (in transverse gauge) as,

$$D_{\mu\nu}(p) = \frac{1}{p^2+\Pi(p)}\left(\delta_{\mu\nu} - \hat{p}_\mu\hat{p}_\nu\right). \tag{1.75}$$

We are interested to see if a self-energy with $\Sigma(0) = m$ can satisfy in Eqs.(1.74) and (1.75) self-consistently. Polarization function can be straightforwardly calculated,

$$\begin{aligned}\Pi(p) &= \frac{Ne^2}{2\pi m}\left[2 + \frac{p^2-4}{p}\sin^{-1}\left(\frac{p}{\sqrt{4+p^2}}\right)\right] \\ &= \frac{Ne^2}{2\pi m} f(p),\end{aligned} \tag{1.76}$$

to the leading order in N.

Re-scaling the momentum $p/m \to p$, self-energy $\Sigma(p)/m \to m$ and polarization $\Pi(p)/m^2 \to \Pi(p)$, in the limit $q \to 0$ we have,

$$1 = \frac{e^2}{\pi^2 m} \int_0^{\Lambda/m} \frac{p^2 \Sigma(p)}{[p^2 + \Sigma^2(p)]\,[p^2 + \Pi(p)]}, \tag{1.77}$$

The right-hand side of Eq.(2.17) is a decreasing function of m, so for solution with $m \neq 0$ to exist we just need the right-hand side greater than 1 for $m = 0$. This introduces a critical flavour number N_c, as

$$N_c = \frac{4}{\pi} \int_0^{\infty} \mathrm{d}p \frac{p^2 \Sigma(p)}{(p^2 + \Sigma^2)\, f(p)} \tag{1.78}$$

Evaluation of the above integral needs $\Sigma(p)$ to be self-consistently calculated. The full solution yields $N_c = 32/\pi$ to the leading order in N[16]. Solution for the self-energy then determines the mass m,

$$m \propto \exp\left[-\frac{2\pi}{\sqrt{\frac{N_c}{N} - 1}} \right] \tag{1.79}$$

The higher order calculations in large-N approximation still give a critical flavour number close to the above result [20]. Since the value of $N_c \simeq 3.2$ is bigger than the number of actual fermion flavours, $N = 2$, this indicates that dynamical mass generation mechanism can happen in the phase-fluctuating HTS and the chiral symmetry will be broken.

The three phases of the system now can be distinguished by the effective charge in the above QED_3, by the generated mass of the Dirac fermions, and by the possible mass of the gauge field $\vec{a}$. At zero-temperature for higher doping the vortices are bound in the superconducting phase. This leads to an effective charge for gauge fields. Also the condensation of the dual-vortex loop fields $b(\mathbf{x}, \tau)$, results in an effective mass for $\vec{a}$ in Eq.(1.72). Notice that we have assumed the coefficient α in Eq.(1.72), to be related to relative doping $x - x_c$, and the gauge field becomes massless as soon as one passes the critical doping x_c. Right on the critical point the gauge field is massless and the dynamical mass generation mechanism has not created a mass yet, thus the parent state phase is not present yet. In higher temperatures, the quantum critical region where the quantum fluctuations still dominate the thermal ones determine the pseudogap phase. In the pseudogap phase the gauge field is massless and the mass for the quasi-particles is not created yet. Upon lowering the doping to less than x_c- at zero temperature - the dynamical mass generation mechanism begins to work

and some parent insulating phase appears. In the next Section we discuss different possibilities for these insulators and show that the anti-ferromagnetic order parameter in fact is one of the candidate insulators which comes out of the chiral symmetry breaking in QED_3.

1.5 Symmetries of Dirac action in 2+1 dimensions

Lorentz symmetry: Lorentz invariance of the action represents the d-wave nature of the Cooper pairing of electrons at low energies. In a sense this stands for lattice symmetry of the different cuprate materials such as YBCO. In terms of the Clifford algebra elements, the symmetry generators are $\gamma_0\gamma_1$, $\gamma_0\gamma_2$ and $\gamma_1\gamma_2$. The first two are *boosts* while the third is the rotation around the c-axis.
Chiral symmetry: The notion of chiral symmetry in general comes from the fact that there exists at least one extra element in the Clifford algebra that anti-commutes with the rest of the γ's.

In 3+1 dimensions it is easy to show that the only matrix with such property is $\gamma_5 \equiv i\gamma_0\gamma_1\gamma_2\gamma_3$. This presents itself as a freedom in choosing γ_0, since the $\mathrm{U}(1)$ group generated by γ_5 introduces a new γ_0

$$\tilde{\gamma}_0 = e^{-i\theta\gamma_5}\gamma_0 e^{i\theta\gamma_5}, \tag{1.80}$$

which is also an eligible γ_0, i.e., anti-commutes with the rest of the γ-matrices. As discussed in the previous sections, in three dimensions the minimal representation of the Clifford algebra is 2×2 and there exists no other fourth matrix that anti-commutes with γ_0, γ_1 and γ_2.

The chiral symmetry breaking is a signature of mass generation in Dirac theory. This creates finite fugacity/charge for vortices which lead to a complex mechanism of dynamical mass generation for quasi-particles.

We will choose to work with four-component representation of the algebra to reveal a chiral symmetry. In this case there are four independent γ_0's to chose among (Eq. (1.20)). Different candidate $\tilde{\gamma}_0$'s in Eq.(1.20) can be written in terms of the generators of the chiral group:

$$\begin{aligned}
\tilde{\gamma}_0^{(1)} &= \gamma_0 \\
\tilde{\gamma}_0^{(2)} &= i\gamma_0\gamma_3 \\
\tilde{\gamma}_0^{(3)} &= i\gamma_0\gamma_5 \\
\tilde{\gamma}_0^{(4)} &= i\gamma_1\gamma_2 \\
&= i\gamma_0\gamma_{35}
\end{aligned} \tag{1.81}$$

The elements of the chiral group will rotate these candidate γ_0's among each other. Unlike the

four-dimensional case, now there exists three independent elements of the Clifford algebra that anti-commute with γ_0, γ_1 and γ_2, and the chiral group is a $\mathrm{SU}(2)$. The generators of this $\mathrm{SU}(2)$ will be denoted by γ_3, γ_5 and γ_{35} ($\equiv i\gamma_3\gamma_5$). Notice that $\tilde{\gamma_0^4}$ is a scalar under the chiral group and does not mix with other $\tilde{\gamma}_0$'s under a chiral rotation

The effect of each of the individual generators on γ_0 would be:

$$\begin{aligned}\tilde{\gamma}_0 &= e^{-i\theta\gamma_3}\gamma_0 e^{i\theta\gamma_3}, \\ &= \cos(2\theta)\tilde{\gamma}_0^{(1)} + \sin(2\theta)\tilde{\gamma}_0^{(3)},\end{aligned} \tag{1.82}$$

where the $\tilde{\gamma}_0^{(i)}$'s are candidates γ_0's from Eq.(1.20). For $\theta = \pi/4$, the rotated $\tilde{\gamma}_0$ would be:

$$\begin{aligned}\tilde{\gamma}_0^{(3)} &= e^{-i\frac{\pi}{4}\gamma_5}\tilde{\gamma}_0^{(1)}e^{i\frac{\pi}{4}\gamma_5} \\ \tilde{\gamma}_0^{(2)} &= e^{-i\frac{\pi}{4}\gamma_3}\tilde{\gamma}_0^{(1)}e^{i\frac{\pi}{4}\gamma_3} \\ \tilde{\gamma}_0^{(2)} &= e^{-i\frac{\pi}{4}\gamma_{35}}\tilde{\gamma}_0^{(3)}e^{i\frac{\pi}{4}\gamma_{35}},\end{aligned} \tag{1.83}$$

For a fixed γ_0 in a given representation. The last $\tilde{\gamma}_0^{(4)}$ does not transform under the chiral group and in fact is a singlet under chiral transformations. As one can see from the Eq.(1.81) that beginning from a fixed γ_0 the rest of the γ_0's can be constructed using the elements of the chiral group. Now the question that naturally arises is that how given the form of the quasi-particle pairing near the Fermi surface, which shows itself in the form matrices M_1 and M_2, can limit the possible forms of γ_0's or the symmetry generators. Put in a different language, we are basically investigating the connection between the generators of Lorentz group which purely come from γ_1, γ_2 and γ_0 - which are given through the matrices $M_{1,2}$ and chiral group generators $\gamma_3, \gamma_5, \gamma_{35}$ with the freedom of γ_0 choice as the bridge between the two. Given the matrices $M_{1,2}$ assume the symmetry generators of two SU(2) groups,

$$\begin{aligned}\{M_1, M_2, M_1M_2\} &= \mathrm{SU}(2)\ \text{ generators}, \\ \{\gamma_3, \gamma_5, \gamma_{35}\} &= \mathrm{SU}_c(2)\ \text{ generators},.\end{aligned} \tag{1.84}$$

In fact the existence of four candidates for γ_0's is not accidental. It can be shown that there exists the following set of bilinear forms,

$$\Gamma = (\Psi^\dagger\gamma_0\Psi, \Psi^\dagger i\gamma_0\gamma_3\Psi, \Psi^\dagger i\gamma_0\gamma_5\Psi), \tag{1.85}$$

vector under chiral $\mathrm{SU}_c(2)$ and scalar under the Lorenz group. This means we can interpret them as mass, while a chiral generator can rotate them among each other. Any linear combination of the above masses where $\Gamma^2 = 1$ is also a candidate chiral mass. The fourth choice for γ_0 corresponds however, to a parity breaking mass and not chiral breaking and is also a scalar under $\mathrm{SU}_c(2)$.

The physical significance of these chiral symmetry generators is clear when we write the masses generated in terms of the electronic operators. Using $\gamma_0 = \tilde{\gamma}_0^{(1)}$ which we used in our representation leads to,

$$\begin{aligned} m\Psi^\dagger\gamma_0\Psi &= m\left\{c_\uparrow^\dagger(\mathbf{K}_i+\mathbf{q})c_\uparrow(-\mathbf{K}_i+\mathbf{q}) - c_\downarrow^\dagger(\mathbf{K}_i-\mathbf{q})c_\downarrow(-\mathbf{K}_i-\mathbf{q})\right\} \\ &\to 2m\sum_{\sigma=pm}\sigma\cos(2\mathbf{K}_i\cdot\mathbf{r})c_\sigma^\dagger(\mathbf{r})c_\sigma(\mathbf{r}), \end{aligned} \tag{1.86}$$

which can be recognized as staggered spin density wave (SDW) order, the periodicity of which is given by the node-spanning wave vector, $2\mathbf{K}_i$. As discussed before this is particularly intriguing since the antiferromagnetic order is the natural parent phase to the superconducting state. Thus the SDW is a natural candidate for the doping-evolved state. Repeating the same exercise for the next candidate, $\gamma_0 \to \tilde{\gamma}_0^{(2)} = \gamma_0\gamma_3$, one gets sine-SDW rather than cosine-SDW,

$$m\Psi^\dagger\gamma_0\Psi \to 2m\sum_{\sigma=pm}\sigma\sin(2\mathbf{K}_i\cdot\mathbf{r})c_\sigma^\dagger(\mathbf{r})c_\sigma(\mathbf{r}). \tag{1.87}$$

For $\tilde{\gamma}_0^{(3)}$ the situation is slightly different; in this case, the mass acts like a particle-particle potential encouraging the opening of a pairing gap in addition to the already established d-wave gap. The sign of the potential is reversed for opposing nodes, and so we interpret this as p-wave pairing. The resultant state, then, is a $d + ip$ insulator.

The mass term associated with $\tilde{\gamma}_0^4$ is quite different from the other three. As we previously noted, the fourth does not allow a representation of the chiral $\mathrm{SU}_c(2)$, and so the mass term does not break this symmetry. The mass term does, however, break parity (e.g., $x \to -x$) and time-reversal symmetry ($t \to -t$), both of which are expected to be preserved in QED_3. For this reason, the term $m\Psi_i^\dagger\tilde{\gamma}_0^4\Psi_i$ is not expected to become dynamically generated. We discuss this issue in detail in the next chapter.

Thus the main result of this construction of the peudogap field theory is the fact that the antiferromagnetic phase is naturally derived from phase-disordering a d-wave superconductor. However, the chiral symmetry mechanism does not distinguish between any of the above masses/order parameters and one might as well expect a $d + ip$ mass instead of sin- or cos- SDWs. It has been argued

using energy considerations [35], that the SDW has the lowest minimum energy of the system with respect to any other chiral symmetry breaking mass.

To conclude this chapter, we mention two important factors that have to be included in the QED_3 theory constructed above. First is the effect of anisotropy $v_\Delta \neq v_\mathrm{F}$ for the nodal quasi-particles. Although the value of anisotropy is significant, $v_\mathrm{F}/v_\Delta \sim 10$, it can be shown that the mechanism of dynamical mass generation remains intact. O. Vafek *et al* and D. Lee and I.F. Herbut have investigated the effect of small anisotropy in the above model and shown that a weak anisotropy can be ignored as it turns out to be marginal under renormalization [21][22]. There is recent work on the effect of the very strong anisotropy which we refer the reader in Ref.[23].

Chapter 2

Renormalization Group Approach to QED and Four-Fermion Models in Three Dimensions

2.1 Introduction

In the previous chapter we established the field theoretical framework for cuprate superconductors in the pseudogap regime and proposed that the quantum critical point corresponding to the pseudogap region of the d-wave superconductors is derived from a well-known mechanism for low-dimensional quantum field theories known as dynamical mass generation. Dynamical mass is commonly created in fermionic field theories with strong interactions either with other fermionic fields or gauge fields with dynamics. It is sensitive to the number of the degrees of freedom - flavours - and the mechanism of mass generation can only happen if the flavour number, N, is less than a certain critical number N_c. Since the whole notion of dynamical mass generation comes from the a large-N expansion formalism - the estimates of N_c should be carefully executed. Continuing from the previous chapter, our emphasis is on quantum electrodynamics in three dimensions which represents the spin sector of the underdoped cuprates in the pseudogap phase. Upon increasing the doping towards optimal doping, the gauge field $\vec{a}$ gains a mass and the system becomes a superconductor. the massive gauge field theory is shown to be equivalent to a Dirac action with quartic interaction which preserves the chiral symmetry of the theory. The effective theory is known as the *Thirring* model and will be the subject of our subsequent discussion.

In QED_3, current estimates of N_{c0} strongly disagree. Early studies of Schwinger-Dyson equations in the large-N approximation - as discussed in previous chapter - gave $N_{c0} = 32/\pi^2 \approx 3.24$ [16]. Vertex corrections [28], or the next-to-leading-order terms in the $1/N$ expansion [20] did not change N_{c0} significantly, and if anything, only increased its value. On the other hand, Appelquist *et al* have argued that $N_{c0} < 3/2$ [29]. Adding to the controversy, recent lattice calculations have found no decisive signal for chiral symmetry breaking for $N = 2$, but did detect a significant fermion mass for $N = 1$ [30]. It has been argued, however, that although greatly increased compared to early studies, the sizes of the systems considered in the lattice calculations may still not be close enough to the thermodynamic limit [31]. In fact, due to the essential singularity at $N = N_c$ the value of the mass at $N = 2$, if finite, should be rather small, and the results of numerical simulations are not necessarily in conflict with the values obtained from the Schwinger-Dyson equations [30], [32].

We apply the momentum-shell renormalization group (RG) to QED_3 theory with N fermion flavours with four-fermion interactions which break the $\mathrm{U}(2)$ symmetry per flavour and later on to Thirring model. The gauge-invariant β-functions for the charge and the four-fermion couplings are computed to the leading order in $1/N$. The value of N_c may be obtained from the RG flow simply by inverting the dependence of the critical coupling(s) g on N. In case of symmetry breaking interaction we show that N_c obtained this way is necessarily a monotonic function of the interaction coupling, i.e. that an infinitesimal interaction, although irrelevant, alters the value of N_c. In particular, this suggests that even if $N_{c0} < 2$ in pure QED_3, the low-energy theory of underdoped cuprates with repulsive interactions included [**?**] is likely to lie below the (shifted) critical point for dynamical mass generation. The flow of the chirally-symmetric interactions, on the other hand, suggests that the chirally symmetric mass cannot get spontaneously generated in pure QED_3.

Our method relies on identification of the RG runaway flow of the chiral-symmetry-breaking interaction coupling constant with the dynamical mass generation. This conjecture is supported by the exact solution in the limit $N = \infty$ and of zero charge. The idea is rather general, however, and similar to the standard way of determining a spontaneously broken symmetry in statistical physics: first allow a weak explicit symmetry breaking perturbation, take the thermodynamic limit, and only then take the perturbation to zero. The thermodynamic limit would in the RG language correspond to letting the momentum cutoff go to zero.

2.2 Large-N expansion

The large-N expansion is applied in theories for which weak-coupling perturbative expansions are not justified by dimensional arguments . The idea is too look at the limit of the same theory in which it is assumed that the field degrees of freedom have N copies where N is a large number. Physical quantities can now be expanded in terms of a new small parameter: $1/N$. In this section we will discuss some of the general features of the ideas behind large-N expansion before we proceed to implement it in our renormalization approach to the three-dimensional quantum electrodynamics in the presence of four-fermionic interactions in later sections.

The basic mechanism of the $1/N$-expansion is the summation of infinite number of Feynman diagrams. This can go beyond perturbative power counting. Consider the subset of diagrams formed by the chain of bubbles in the geometric series in Fig(2.1). If the inverse coupling is tuned to cancel the leading divergence in the bubble diagram, then the geometric sum can become finite as the cutoff $\Lambda \to \infty$. This is indeed what happens in the $d = 2 + 1$ dimensions. Interestingly, the fine-tuning requirement here is exactly the same as the Hartree-Fock approximation. In a diagrammatic notation Hartree-Fock corresponds to the self-consistent sum of the cactus graphs in Fig2.2.

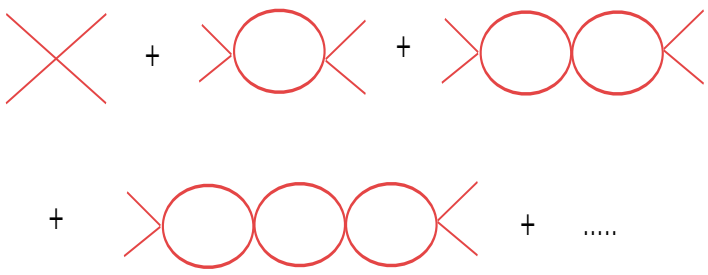

Figure 2.1: Infinite re-summation of the bubble diagrams in the leading order of $1/N$ for a four-fermion vertex.

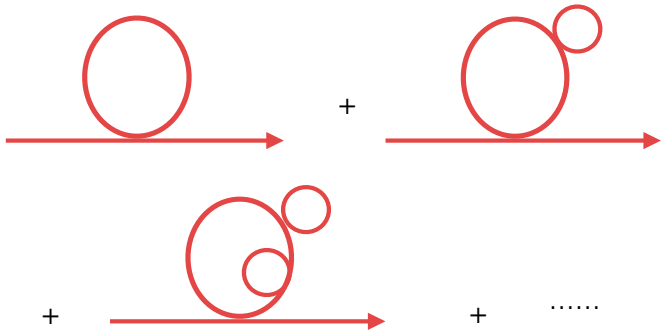

Figure 2.2: Infinite re-summation of cactus mass-loop diagrams to leading order in $1/N$

In a $1/N$ resummation method the leading order contribution for any connected Green's function is defined by the infinite set of diagrams for which the powers of N coming from the flavour contractions (P), is equal to the number of the loops (L). For self-energy terms this is just the cactus graphs as in Fig.(2.2), and the sum can be performed provided we take the coupling to be of the order of unity in units of N. In general, the n-th order of the resummation has $P = L - n$. The resummation can be codified in a convenient way using an auxiliary field to decouple the interaction terms.

Here we proceed with simplest four-fermionic model with interaction of the form

$$\mathcal{L}_{\text{int}} = \frac{g}{N}(\bar{\Psi}\Psi)^2, \tag{2.1}$$

using an auxiliary field σ, the Lagrangian is rewritten as,

$$\mathcal{L} = \sum_i i\Psi_i\gamma_\mu\partial_\mu\Psi_i + \sigma\bar{\Psi}_i\Psi_i - \frac{N\sigma^2}{2g}, \tag{2.2}$$

where i indicates the flavour index. Integrating out the fermionic degrees of freedom is straight forward and one gets the effective action for auxiliary field σ,

$$S_{\text{eff}} = N \cdot \int \mathrm{d}^d x \left\{ \frac{\sigma^2}{2g} - \mathrm{Tr}\ln\left(i\partial_\mu + \sigma\right) \right\}. \tag{2.3}$$

The explicit N-dependence will let us to look at the saddle-point solutions for large-N which leads to exactly the same equation as the Hartee-Fock eqaution. Notice that the infinite resummation is automatically done upon the integration over the fermionic degrees of freedom.

The large-N limit now corresponds to a saddle-point solution for the auxiliary field σ whose its average value is the the fermionic two-point Green's function. In weak-coupling perturbative expansions the fluctuations of the auxiliary field are suppressed by the coupling (or the system size) this is now replaced by new tuning parameter $1/N$. In the limit of the $N \to \infty$, σ is static and saddle point solutions of the above action represent a dynamical mass. This is equivalent to calculating the $\sigma(p)$ propagator, $D_\sigma(p)$ from the geometric sum in Fig.(2.3).

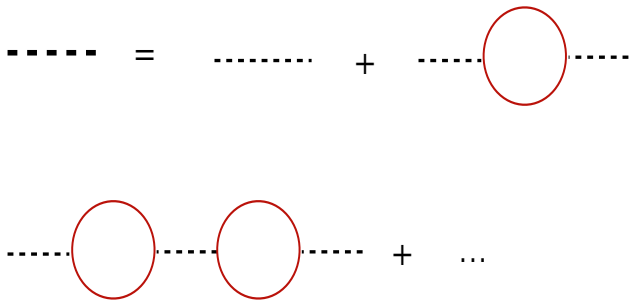

Figure 2.3: The chain of diagrams giving a contribution to the $D_\sigma(p)$ in the zeroth order of the 1/N expansion. The thick dashed lines indicate the full-propagator D_σ.

In theories for which the form of interaction terms preserves the symmetries of the original non-interacting theory, such as gauge-field coupling in QED_3 and the current-current interaction in the Thirring model, the mechanism of mass generation is more sophisticated. In QED the gauge field to the first order in $1/N$ is obtained from a infinite sum of polarization bubbles, Fig.(2.4). As discussed in Chapter 1 this leads to a $1/p$ behaviour for the gauge propagator at low-momenta. Including this result in the wave-function renormalization diagram Fig.(2.5), one can derive self-consistent solution with a dynamical mass $\Sigma(p \to 0) \neq 0$, where Σ is the self-energy.

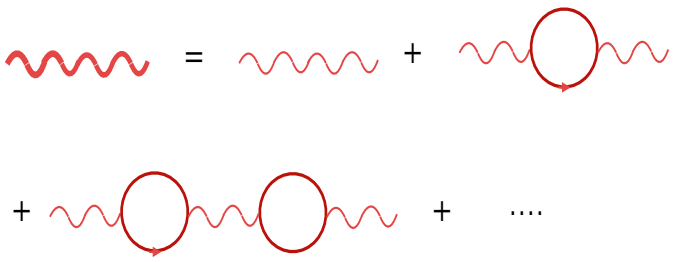

Figure 2.4: The leading order bubble corrections to the gauge-field propagator $D_{\mu\nu}(p)$.

Interestingly the wave-function renormalization diagram with all the bubbles included in the gauge field propagator play the role of mass generating bubbles. This can naively be seen as the result of the fact that for the screened propagator, one can imagine the wave-function renormalization/self-energy diagram have the legs cut off into a mass generating Hartree-Fock term.

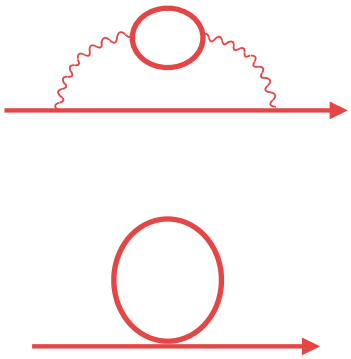

Figure 2.5: The mass generation diagrams in QED_3 (a) vs Hartree mass term diagram (b). Both bubbles are calculated with the full fermionic propagator.

2.3 QED$_3$ and quartic interactions

We begin by recalling that the spin sector of the low-energy theory of the phase-disordered d-wave superconductor described by the action $S = \int \mathrm{d}^3x\, \mathcal{L}$, with the Lagrangian

$$\mathcal{L}_{\mathrm{QED}_3} = \bar{\Psi}_i \gamma_\mu (\partial_\mu + i a_\mu) \Psi_i + \frac{1}{2e^2} (\nabla \times \vec{a})^2. \tag{2.4}$$

Ψ_i, $i = 1, 2$ represent the electrically neutral spin-1/2 fermions (spinons), $\bar{\Psi} = \Psi^\dagger \gamma_0$, γ_μ's are the usual Dirac gamma matrices ($\mu = 0, 1, 2$), and we define $\gamma_5 = \gamma_0\gamma_1\gamma_2\gamma_3$, and $\gamma_{35} = i\gamma_3\gamma_5$ for later use [**?**]. The charge $e^2 \sim |\langle \Phi \rangle|^2$, where Φ is the vortex loop condensate [7][5], [37]. As discussed in the previous chapter, the complementary charge sector of the theory may be shown to be describing an insulator [38]. Later on in this chapter we will get back to discuss the insulating/phase disordered section of the lagrangian when we are discussing the Thirring model.

Let us first consider the case of single fermion species, and then generalize to $N > 1$. To construct the quartic interaction that breaks the $\mathrm{SU}_c(2)$ symmetry down to $\mathrm{U}_c(1)$ we notice that the three-component objects,

$$\begin{aligned} \mathbf{A} &= (\bar{\Psi}\Psi,\ \ \bar{\Psi} i\gamma_3 \Psi,\ \ \bar{\Psi} i\gamma_5 \Psi), \\ \mathbf{B}_\mu &= (\bar{\Psi}\gamma_\mu\gamma_{35}\Psi,\ \ \bar{\Psi} i\gamma_\mu\gamma_3 \Psi,\ \ \bar{\Psi} i\gamma_\mu\gamma_5 \Psi), \end{aligned} \tag{2.5}$$

are the only triplets under the chiral group. Upon breaking the symmetry to $\mathrm{U}_c(1)$, we look at the projection of $\mathbf{A}$ and $\mathbf{B}_\mu$ along the direction corresponding to the remaining generator of the $\mathrm{SU}_c(2)$. In this case, these are $\bar{\Psi}\Psi$ and $\bar{\Psi}\gamma_\mu\gamma_{35}\Psi$ which remain invariant under the action of γ_{35}. Thus, the required quartic chiral-symmetry-breaking (CSB) interaction will have the form

$$\mathcal{L}_{\mathrm{CSB}} = \frac{g}{N} (\bar{\Psi}\Psi)^2 + \frac{g'}{N} (\bar{\Psi}\gamma_\mu\gamma_{35}\Psi)^2. \tag{2.6}$$

On the other hand, the two $\mathrm{SU}_c(2)$ singlets

$$C_\mu = \bar{\Psi}\gamma_\mu\Psi, \qquad C_{35} = \bar{\Psi}\gamma_{35}\Psi, \tag{2.7}$$

may be used to construct chiral-symmetry-preserving (CSP) quartic interactions, as

$$\mathcal{L}_{\mathrm{CSP}} = \frac{\lambda}{N} (\bar{\Psi}\gamma_{35}\Psi)^2 + \frac{\lambda'}{N} (\bar{\Psi}\gamma_\mu\Psi)^2. \tag{2.8}$$

For a general N we will therefore define the following $\mathrm{U}(N) \otimes \mathrm{U}(N)$ symmetric theory

$$\begin{aligned}
\mathcal{L} &= \mathcal{L}_{\mathrm{QED}_3} + \mathcal{L}_{\mathrm{CSB}} + \mathcal{L}_{\mathrm{CSP}}, \\
&= \{\bar{\Psi}_i \gamma_\mu (\partial_\mu + i a_\mu) \Psi_i + \frac{1}{2e^2} (\nabla \times \vec{a})^2 + \frac{g}{N} (\bar{\Psi}_i \Psi_i)^2 \\
&+ \frac{g'}{N} (\bar{\Psi}_i \gamma_\mu \gamma_{35} \Psi_i)^2 + \frac{\lambda}{N} (\bar{\Psi}_i \gamma_{35} \Psi_i)^2 + \frac{\lambda'}{N} (\bar{\Psi}_i \gamma_\mu \Psi_i)^2\}, \\
i &= 1 \cdots N. \qquad (2.9)
\end{aligned}$$

In principle, one could imagine other interaction terms satisfying the required symmetry. However, it can be shown that these would have to be a linear combination of the already introduced quartic terms. For example, the interaction $g_1|\mathbf{A}|^2 + g_2|\mathbf{B}_\mu|^2$ can be written as a linear combination of C_μ^2 and C_{35}^2. This follows from Fierz identities which imply that there are only two linearly independent quartic terms invariant under the $\mathrm{U}(2N)$. For $\mathrm{U}(N) \otimes \mathrm{U}(N)$ theory, the number of independent couplings doubles to four, which are precisely the introduced $g,\ g',\ \lambda$ and λ'. For a more detailed discussion we refer the reader to Appendix B.

Notice the particular way we have treated the large-N flavours in the theory. A four-component Dirac spinon can be rotated with the chiral generators and the lagrangian can manifest chiral symmetry. At the same time, the rotations in a larger space of large-N flavours, trivially leave both bare and interaction Lagrangian intact. This to us means that the symmetry broken model always preserve a $\mathrm{U}(N)$ symmetry. In general, we could repeat the above construction of quartic terms for all $\mathrm{U}(2N)$ generators and categorize them based on the behaviour under the symmetry transform. This could be done by carefully gong through the Cartan construction of the $\mathrm{U}(N)$ generators. However, we are merely interested on the mass generation mechanism for each node -the flavour in our theory - and not the rotations of spinon/quasi-particles in the larger space of two nodes. So we keep the interaction terms to the above form in Eq.(2.9). There has been suggestions in the literature that inclusion of the inter-node generators into the symmetry group can represent some exotic phases such as charge-stripes [35].

Special cases of the above interaction Lagrangian can cover many of the commonly discussed four-fermionic models in the context of low-dimensional field theories and/or dynamical mass generation. The simplest model is Gross-Neveu model which corresponds to $g' = \lambda = \lambda' = 0$, without a gauge-field present $e = 0$.

$$\mathcal{L}_{\mathrm{Gross-Neveu}} = \bar{\Psi}_i (\gamma_\mu \partial_\mu) \Psi_i + \frac{g}{N} (\bar{\Psi}_i \Psi_i)^2. \qquad (2.10)$$

The Thirring model is a similar model with current-current interaction term and can represent the chiral symmetry preserving sector of the Lagranigian and defined as $g = g' = \lambda = 0$,

$$\mathcal{L}_{\text{Thirring}} = \bar{\Psi}_i(\gamma_\mu \partial_\mu)\Psi_i + \frac{g}{N}(\bar{\Psi}_i \gamma_\mu \Psi_i)^2, \tag{2.11}$$

where a sum over γ_μ in the interaction term is implied. We, however, restricted ourselves to one of the three generators of the chiral symmetry group to construct the chiral symmetry breaking section of the Lagrangian. Including all chiral generators it is possible to construct a different chiral symmetric theory known as the Nambu-Joana-Lasisnio (NJL) model,

$$\mathcal{L}_{\text{NJL}} = \bar{\Psi}_i(\gamma_\mu \partial_\mu)\Psi_i + \frac{g}{N}\{(\bar{\Psi}_i \Psi_i)^2 + (\bar{\Psi}_i i\gamma_3 \Psi_i)^2 + (\bar{\Psi}_i i\gamma_5 \Psi_i)^2\}, \tag{2.12}$$

which is basically the $\mathbf{A}^2$ and invariant under chiral rotations. Before we proceed further, in the next chapter, I will spend some time to introduce the concept of large-N expansion in such field theoretical models and devote some discussion to the non-perturbative nature of this approach.

2.4 Dynamical mass generation in the RG language

In this section I explain our methodology by simplifying the interaction Lagrangian in Eq.(2.9) to a simple Gross-Neveu model in the presence of the gauge-field

For the $N \to \infty$, mean-field, limit of the Gross-Neveu model, the dynamically generated mass, $m \sim \langle \bar{\Psi}\Psi \rangle$, is determined by the gap equation

$$-\frac{1}{g} = 8 \int \frac{d^3p}{(2\pi)^3} \frac{1}{p^2 + m^2}, \tag{2.13}$$

which after the integration gives

$$1 = \frac{4g\Lambda}{\pi^2}\left(\frac{m}{\Lambda}\tan^{-1}\frac{\Lambda}{m} - 1\right), \tag{2.14}$$

with $\Lambda \gg m$ being the assumed ultraviolet (UV) cutoff. Demanding m to be invariant under the change of cutoff $\Lambda \to \Lambda/b$, the β-function at $N = \infty$ is readily obtained to be exactly

$$\beta_g = \frac{dg}{d\ln b} = -g - g^2, \tag{2.15}$$

where g has been rescaled as $4g\Lambda/\pi^2 \to g$. We see that at weak coupling g is irrelevant, but that the flow for $g < g_* = -1$, which represents the infrared (IR) unstable fixed point, is towards negative infinity. Since the same values of g yield a finite mass from the gap equation, it is natural

to identify the runaway flow of g with dynamical mass generation. Note that the same Eq.(2.15) can alternatively be obtained in the standard Wilson's momentum-shell one-loop RG.

The second solvable limit of the theory is pure QED_3 without any four-fermion interactions, again in the limit $N \to \infty$. The flow of the charge is then

$$\beta_e = \frac{de^2}{d\ln b} = e^2 - Ne^4, \tag{2.16}$$

where the dimensionless charge is defined as $(4/3)(e^2/(2\pi^2\Lambda)) \to e^2$. While the theory is free in the UV region, there is a non-trivial IR stable fixed point at $e_*^2 = 1/N$. (Notice that the quartic interactions, even when present, can not appear in β_e to the leading order in large N as a consequence of the Ward-Takahashi identity.)

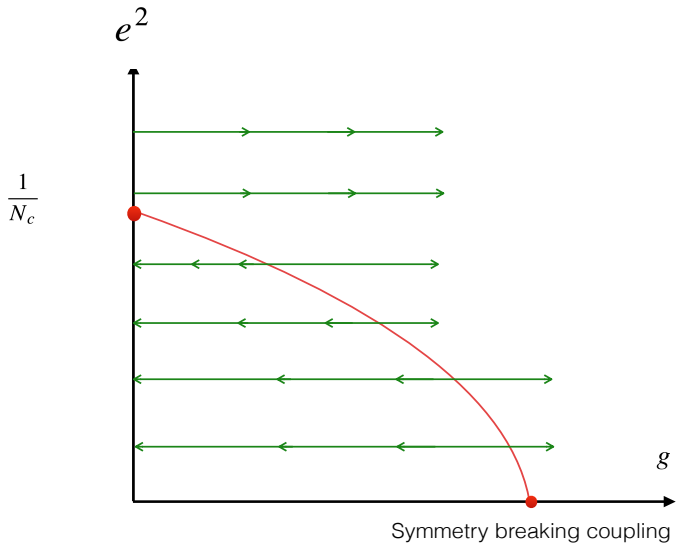

Figure 2.6: Flow diagram in the charge-coupling plane. Near the critical charge e_c^2 fixed point the runaway flows change from attractive to repulsive.

Next, we want to consider the interplay of the charge e and the quartic coupling g, and in particular to examine the influence of a weak charge on the value of g_*. One expects the effect of the gauge field on β_g to be

$$\frac{dg}{d\ln b} = -g - g^2 + (\text{const.})\, e^2 g,$$

to the leading order in e^2 and $1/N$. In particular, $\beta_g(g=0)=0$ even when $e \neq 0$, since otherwise it would be possible to *generate* the CSB interaction in the chirally symmetric theory. So $g=0$ is *always* a fixed point. Since at the fixed point $e_*^2 = 1/N$, decreasing N is the same as increasing the charge in Eq. (13). Since the factor in front of the last term is expected to be positive (as it indeed turns out to be the case), decreasing N will reduce the absolute value of the non-trivial critical coupling g_*, until it eventually merges with the trivial fixed point, permanently located at $g=0$. There will therefore exist a critical charge $e_c^2 = 1/N_{c0}$, above which an *infinitesimal* symmetry breaking interaction suffices to cause the runaway flow of g. We identify this point with the *spontaneous* chiral symmetry breaking in pure QED_3. The flow diagram with this structure has been depicted in Fig.(2.7).

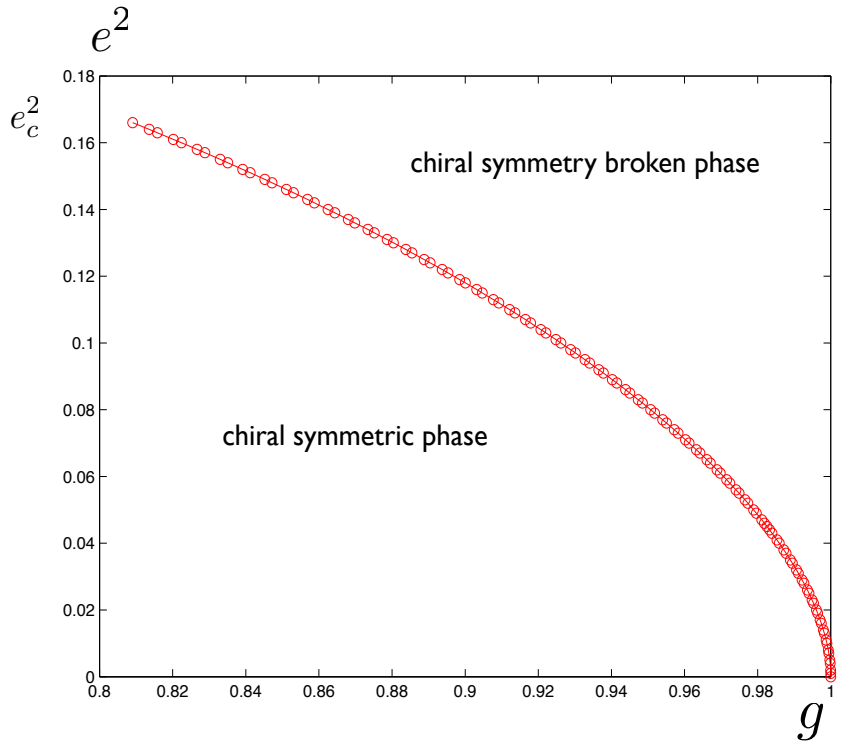

Figure 2.7: The phase-diagram in the interaction-charge plane, for the chiral symmetry breaking interaction. The value of the charge is $e^2 = 1/N$. N_c is a continuous function of the symmetry breaking interaction, as a consequence of the existence of the fixed point at $g=0$ at any charge.

When $N < \infty$ the terms with an explicit N-dependence in β_g, such as g^3/N, should also be included. These terms may be understood as contributing $1/N$ corrections to N_{c0} in the following way: one can expand the critical charge (corresponding to the double-root of β_g at $g = 0$) in powers of $1/N$ as

$$e_c^2 = a_0 + \frac{a_1}{N_{c0}} + \frac{a_2}{N_{c0}^2} + \cdots . \tag{2.17}$$

Since $e_c^2 = 1/N_{c0} + O(1/N_{c0}^2)$ from β_e, this effectively generates then the $1/N$-expansion for N_{c0}.

One may analogously consider the CSP interaction $(\lambda/N)(\bar{\Psi}\gamma_{35}\Psi)^2$, which when alone leads to the dynamically generated mass $m \sim \langle\bar{\Psi}\gamma_{35}\Psi\rangle$ for $\lambda < -1$, in the $N \to \infty$ limit. In the presence of the charge, however, there is a crucial difference between the β_λ and β_g. Since the CSP interaction term has the same full chiral symmetry as pure QED_3, finite charge may, and in fact does, *generate* the coupling λ. This manifests itself as the e^4 contribution in β_λ, which will now take the form

$$\frac{d\lambda}{d\ln b} = -\lambda - \lambda^2 + (\text{const.})\, e^2\lambda + (\text{const.})\, e^4. \tag{2.18}$$

With the last term, however, $\lambda = 0$ *is not* a fixed point any longer. Furthermore, the sign of the e^4-term turns out to be *positive*, so that the critical coupling actually *increases* with charge. We interpret the latter feature as that the spontaneous dynamical generation of the chiral symmetry preserving mass in pure QED_3 is not possible. This would be in agreement with conclusions of earlier studies [39], [40].

Before we proceed further with deriving the β-functions of the coupled theory, it is worth mentioning that the derivation of the charge fixed point was based on a dimensional regularization and unlike the Schwinger-Dyson bubble-resummation for the gauge field propagator which inherently scereens the propagator dynamics into a $1/p$ in low-momenta, the Wilson RG does keep the $1/p^2$ form of the propagator. Under the framework that we have been discussing this is completely consistent - as long as theory shows proper sensitivity to the external symmetry breaking perturbations. This will be troublesome when we consider a true 2+1 dimensional model at $T = 0$, where there is no cutoff over imaginary time and there is an intrinsic anisotropy in the system. The β-function of charge, then, cannot be properly calculated using the Wilson RG scheme as dimensional regularization does not work in the anisotropic quasi $3 - \epsilon$ models. We have included discussion on such model at the end of the chapter with suggested RG equations and some more discussions on the matter.

2.5 RG for chiral symmetry breaking interactions and the value of N_{c0}

In general, the β-functions for all four quartic interactions will be coupled and the flow is non-trivial. To the leading order in $1/N$, however, the calculation simplifies considerably. In the following two theorems we show that the β-functions for the CSB and CSP interactions are completely decoupled in this limit.

Theorem I: To the leading order in $1/N$ and for $e = 0$, different β-functions decouple.

Proof: Only particle-hole diagrams, as in Fig.(2.8) contribute to leading order in large-N. Such diagrams are proportional to:

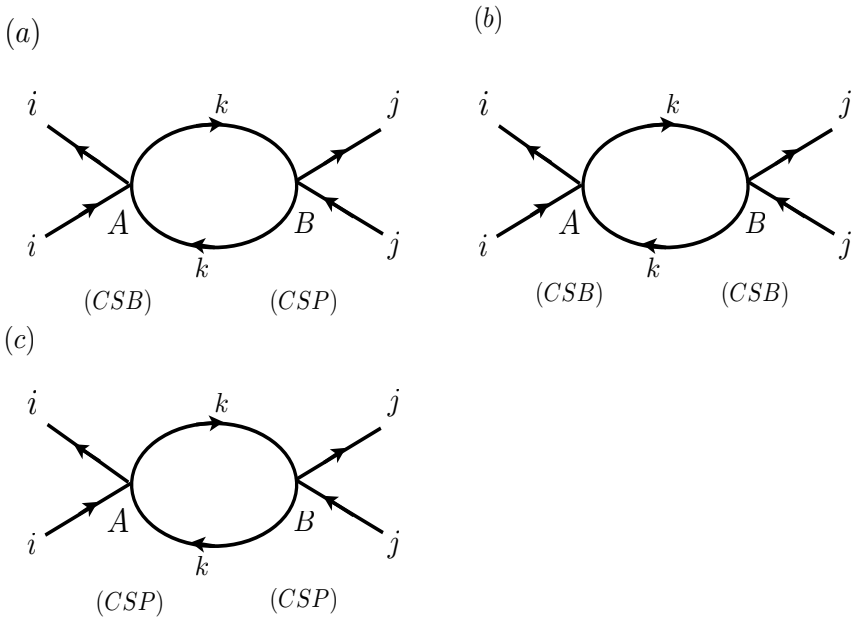

Figure 2.8: Particle-hole diagrams to the leading order in $1/N$.

$$\propto g_A g_B \cdot \int d^3q \, \mathrm{Tr}(\Gamma_A G(q) \Gamma_B G(q)) \propto \mathrm{Tr}(\Gamma_A \Gamma_B). \tag{2.19}$$

Here, Γ_A and Γ_B's are the matrices in the kernel of the quadratic form accompanying either g_A or

g_B,

$$\Gamma_A, \Gamma_B \in \{\mathbf{1}, \gamma_\mu, \gamma_{35}\gamma_\mu, \gamma_{35}\} \tag{2.20}$$

It is easy to see that these diagrams are zero unless $g_A = g_B$. For diagrams that mix CSB and CSP interactions in Fig.(2.8a), Eq.(2.19) contains the trace of an odd number of γ-matrices and thus yields zero. For the CSB-CSB or CSP-CSP diagrams in Figs.(2.8b) and 2.8c, the identities $\mathrm{Tr}(\gamma_\mu\gamma_\nu) = 4\delta_{\mu\nu}$ and $\mathrm{Tr}(\gamma_\mu\gamma_{35}) = 0$, imply that all the mixing terms are zero unless $\mu = \nu$, i. e. $g_A = g_B$.

So, to the leading order, the coupling between different quartic interactions in the β-functions can only be mediated through charge. One may easily see, however, that the symmetry requires that the β-functions for the CSB and CSP couplings still remain decoupled. We will state it in the form of the following theorem:

Theorem II: There are no $\sim \lambda e^2$ or $\sim \lambda' e^2$ terms in β_g or $\beta_{g'}$, nor $\sim g e^2$ and $\sim g' e^2$ terms in β_λ and $\beta_{\lambda'}$, to the leading order in $1/N$.

Proof: λe^2 and $\lambda' e^2$ terms obey the full chiral symmetry, and thus cannot generate a CSB interaction. To prove the equivalent statement for the CSB couplings, we notice that to the leading order in $1/N$ the ge^2 and $g'e^2$ terms differ from the λe^2 and $\lambda' e^2$ terms by a single γ_{35} matrix, and thus necessarily break the chiral symmetry. They therefore cannot generate a CSP coupling.

The above theorems allow us to significantly reduce the number of relevant Feynman diagrams. The straightforward calculation of the diagrams in Figs.2.8 and 2.9 leads to the following β-functions for the symmetry breaking interactions:

$$\begin{aligned}
\frac{de^2}{d\ln b} &= e^2 - Ne^4, \\
\frac{dg}{d\ln b} &= -g - g^2 + 4e^2 g + 18 e^2 g', \\
\frac{dg'}{d\ln b} &= -g' + g'^2 + \frac{2}{3} e^2 g,
\end{aligned} \tag{2.21}$$

with conveniently rescaled parameters

$$4g\Lambda/\pi^2 \to g, 4g'\Lambda/(3\pi^2) \to g', 2e^2/(3\pi^2\Lambda) \to e^2.$$

Note that the coupling g' becomes generated by g and e even if absent initially, so in principle it must be included into the analysis. A notable feature of the above β-functions is also their independence from the gauge-fixing parameter ξ. This derives from the exact cancellation between the gauge-dependent part of the diagrams in Fig.(2.8) and the wave-function renormalization factor Z

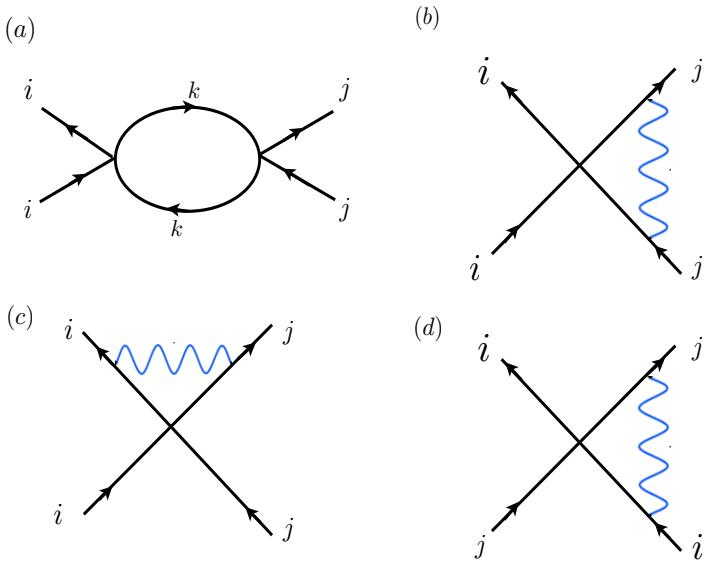

Figure 2.9: Diagrams contributing to the renormalized couplings to the leading order in $1/N$.

(Fig.(2.10)):

$$Z = 1 + (\xi - \frac{2}{3})e^2 \ln b. \tag{2.22}$$

The flow diagram on the $g - g'$ plane for $N = \infty$ ($e^2 = 0$) is given in Fig.(2.10). For $N < \infty$, the fixed point value of the charge becomes $e^2 = 1/N$, and the locations of all the fixed points, except the trivial one at the origin, shift in the directions as indicated. The point at which the RG trajectory that starts at the purely repulsive fixed point (initially at $(-1, 1)$) and terminates at the 'Gross-Neveu' fixed point (initially at $(-1, 0)$) intersects the g-axis determines the location of the phase boundary in the $g - e^2$ ($g' = 0$) plane. At small charge we obtain such a phase boundary at

$$g = -1 + 4e^2 + O(e^4), \tag{2.23}$$

whereas at low g

$$g = -\frac{144}{13}\left(\frac{1}{6} - e^2\right) + O\left(\left(\frac{1}{6} - e^2\right)^2\right). \tag{2.24}$$

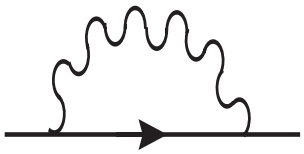

Figure 2.10: Diagram contributing to the wavefunction renormalization.

A numerical solution at a general coupling is given in Fig.(2.7). The critical point in pure QED_3, N_{c0}, is determined by the value of N for which the 'Gross-Neveu' fixed point reaches the origin. For $N > N_{c0}$, the flow beginning at an infinitesimal negative g and $g' = 0$ then runs away to infinity. To the leading order in $1/N$, this criterion yields $N_{c0} = 6$. At $N = N_{c0}$ the other two non-trivial fixed points are still at finite values. The role of g' is therefore only to modify the phase boundary in the $g - e^2$ plane and the value of N_{c0} quantitatively, but not qualitatively. Neglecting the flow of g' entirely would lead, for example, to $N_{c0} = 4$. This would correspond to the value at which the dimension of the coupling g at the charged fixed point changes sign.

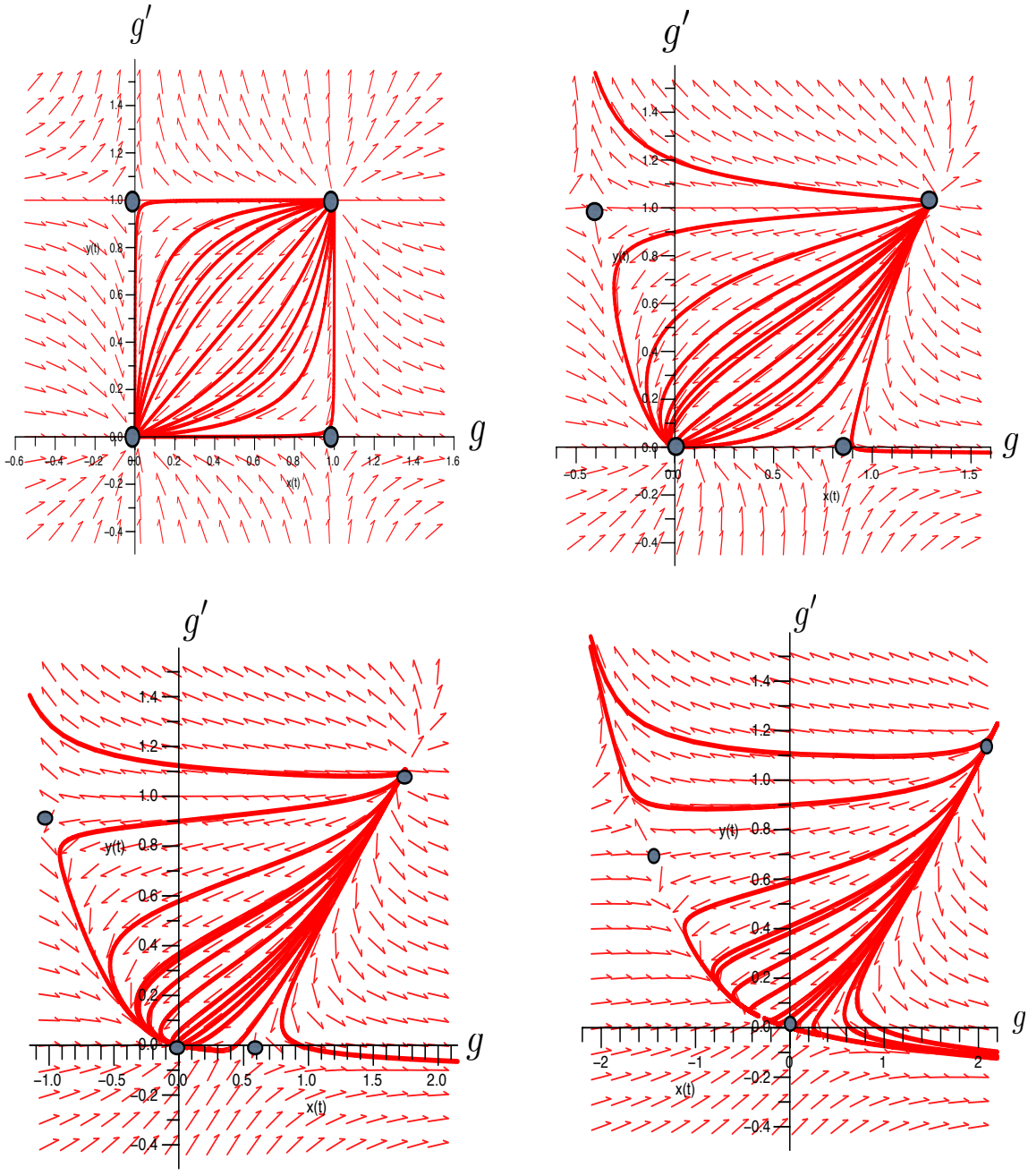

Figure 2.11: Renormalization group flow diagrams for the chiral symmetry breaking strengths, g and g' at (a) $e^2 = 0.0$, (b) $e^2 = 0.03$, (c) $e^2 = 0.1$ and (d) $e^2 = 0.2 > e_c^2$

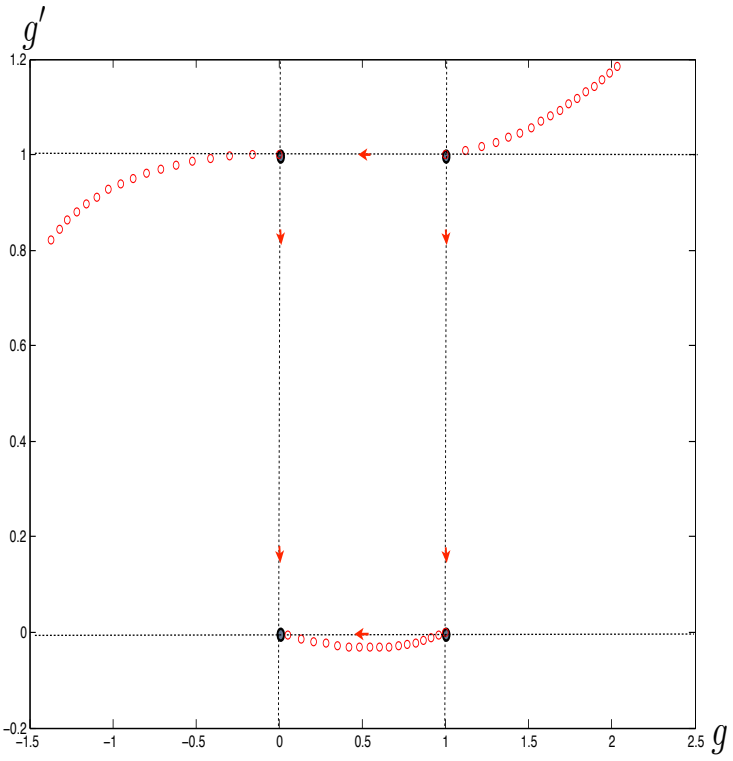

Figure 2.12: The RG flow (dashed lines) in the plane of the two symmetry-breaking interactions g and g' for $N = \infty$. circles mark the evolution of the four fixed points with decrease of N.

2.6 RG for chiral symmetry preserving interactions

We now turn to the analysis of the theory in Eq.(2.9) with $g = g' = 0$, i. e. when the quartic terms respect the full chiral symmetry. This exercise underlines the important role of symmetry in the phase diagram. The diagrams are still the same as in the CSB case, with the addition of the two diagrams in Fig.(2.14). These new terms *generate* the coupling λ, and thus change the evolution of the flow diagram with N in an important way, as mentioned in the introduction and depicted in Fig.(2.19). We obtain the following β-functions for the couplings λ, λ' and e^2:

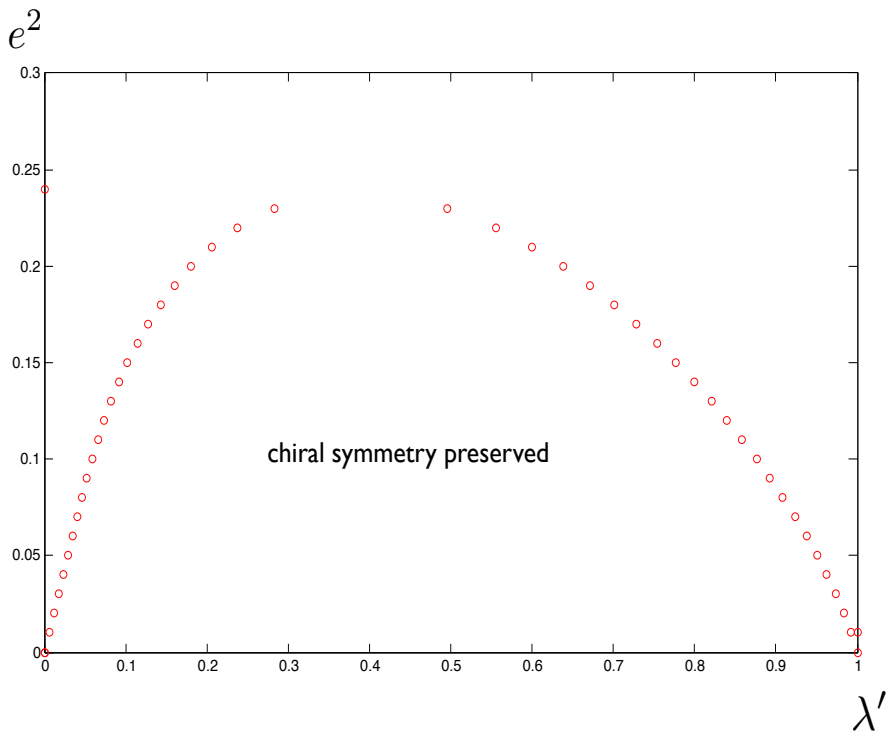

Figure 2.13: The phase-diagram in the interaction-charge plane, for the chiral symmetry breaking interaction. The value of the charge is $e^2 = 1/N$. N_c is a continuous function of the symmetry breaking interaction, as a consequence of the existence of the fixed point at $g = 0$ at any charge.

$$\begin{aligned}
\frac{de^2}{d\ln b} &= e^2 - Ne^4, \\
\frac{d\lambda}{d\ln b} &= -\lambda - \lambda^2 + 4e^2\lambda + 18e^2\lambda' + 9Ne^4, \\
\frac{d\lambda'}{d\ln b} &= -\lambda' + \lambda'^2 + \frac{2}{3}e^2\lambda.
\end{aligned} \tag{2.25}$$

Notice that the flow equations for the CSB and CSP cases are identical, apart from the positive e^4 term. This term, however, prevents the fixed point that was located at $(-1, 0)$ for $N = \infty$ from ever merging with the Gaussian fixed point, and consequently, no spontaneous generation of the chiral-symmetry-preserving mass should be allowed in pure QED_3.

To conclude our achievement so far, we reformulated the problem of dynamical mass generation

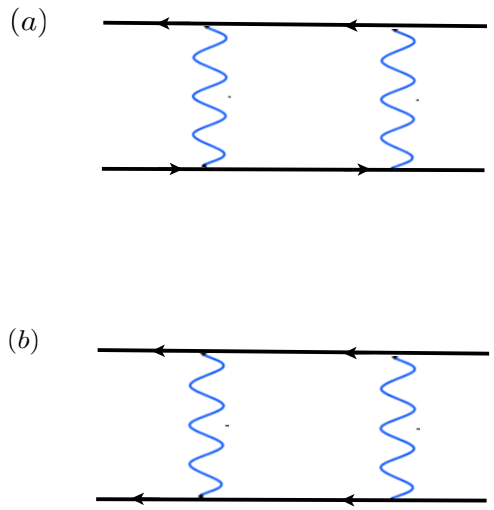

Figure 2.14: The diagrams that give e^4 term in β_λ.

in QED_3 with four-fermion interactions in terms of the renormalization group flows, and we found that the critical number of fermions N_c is a continuous function of the chiral-symmetry-breaking interaction strength. By taking the limit of vanishing interactions we estimated that $N_{c0} = 6$ in pure QED_3. Our analysis of the chiral-symmetry-preserving interactions suggests that the chiral-symmetry-preserving mass cannot become dynamically generated in pure QED_3.

The result that N_c may depend on an infinitesimal symmetry breaking interaction should be contrasted with the previous studies of Schwinger-Dyson equations in QED_3 with symmetry preserving interactions (the 'gauged Nambu-Jona-Lasinio model'). There, the N_c was found to depend on the quartic interaction only if the latter is larger than a certain value [41]. In the RG language this would correspond to the merger of the two fixed points, like the Gaussian and the 'Gross-Neveu' fixed points in our case, at a *finite* value of the coupling. In fact, we find that occurring in the Eqs.(2.21) for CSP interactions: the 'Gaussian' fixed point (initially at $(0, 0)$) and the 'Thirring' fixed point (initially at $(0, 1)$) meet at $(1.78, 0.43)$ for $N = 4.83$. For $N > 4.83$ both couplings become complex, and the flow that begins at the line $\lambda = 0$ is always towards infinite λ'. It is tempting to identify this runaway flow with the phase with broken chiral symmetry and the dynamically generated mass, as proposed in [42]. We refrain from doing so, however, since the runaway flow for $\lambda' > 1$ at

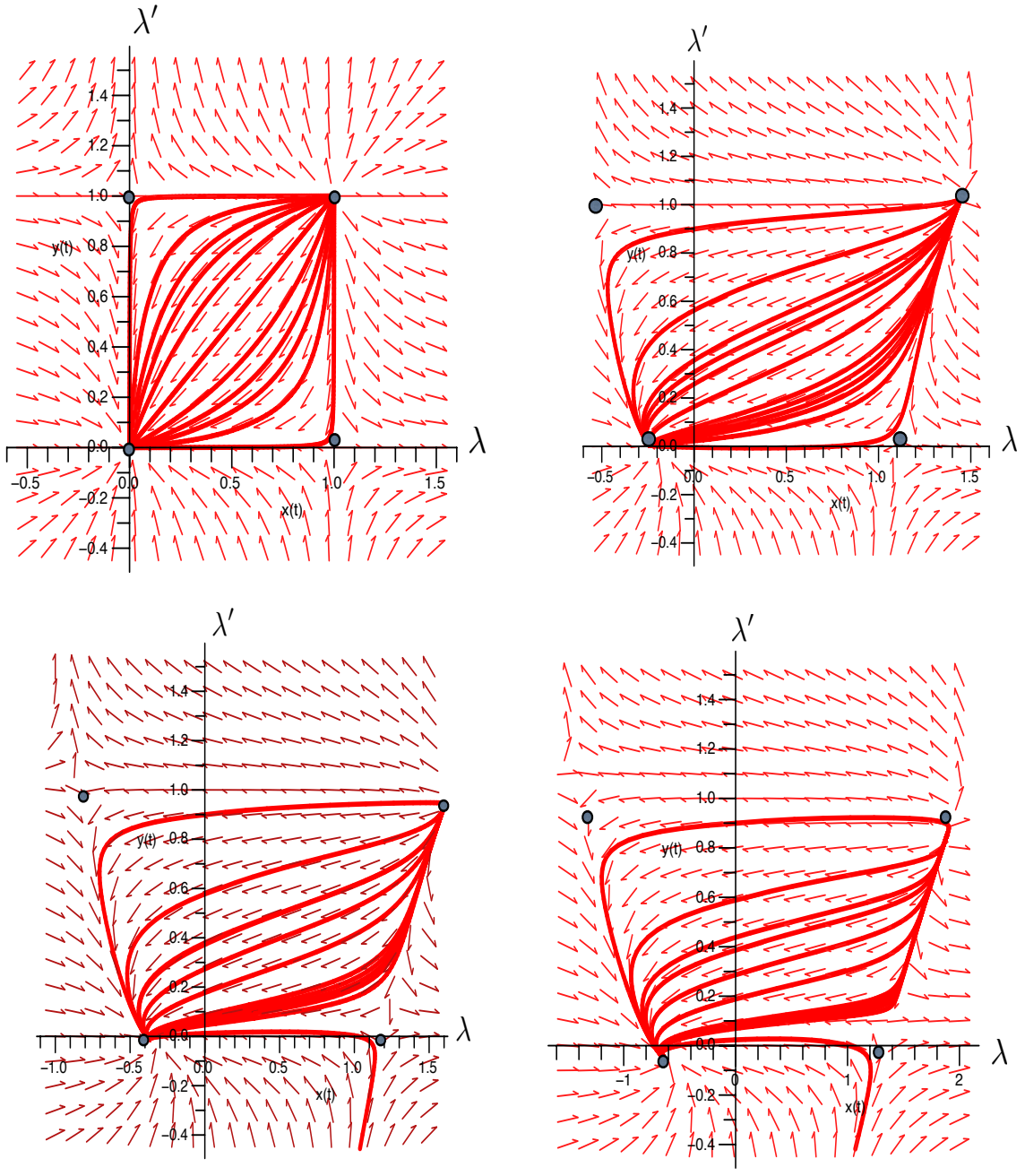

Figure 2.15: Renormalization group flow diagrams for the chiral symmetry breaking strengths, g and g' at (a) $e^2 = 0.0$, (b) $e^2 = 0.03$, (c) $e^2 = 0.1$ and (d) $e^2 = 0.2 > e_c^2$

.

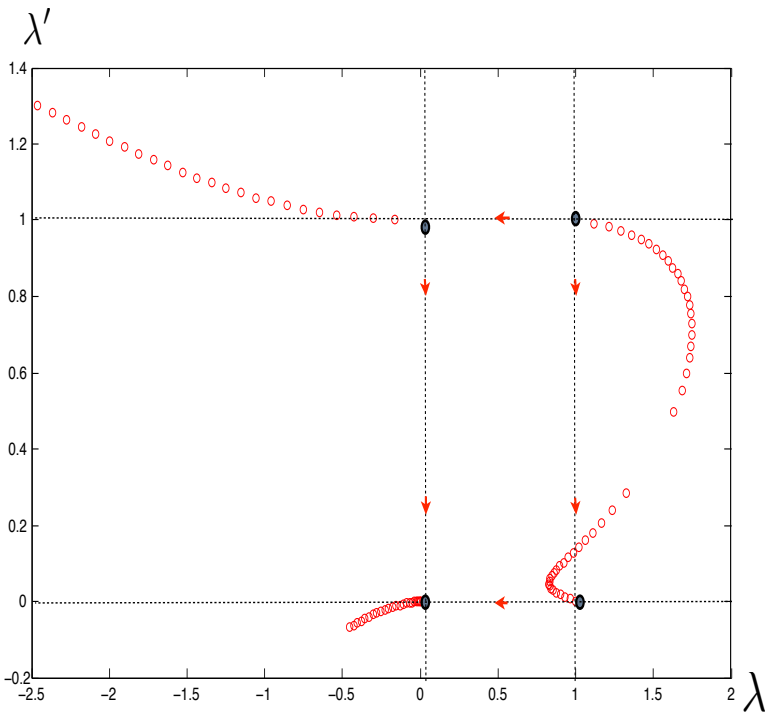

Figure 2.16: The evolution of the chiral symmetry preserving fixed points in the $\lambda - \lambda'$ plane with the increase of charge.

$e = \lambda = 0$ (the 'Thirring model'), actually *does not* correspond to broken symmetry phase, as one can easily check by directly solving the gap equation in this case at $N = \infty$. The transition in the Thirring model occurs only at the order of $1/N$ [43], and so we suspect that the above runaway flow of λ' may be an artifact of the $N = \infty$ limit. This issue is the subject of the following section.

Finally, although our scheme provides a systematic way of computing N_{c0}, for example, it becomes rapidly complicated. To the next order in $1/N$ chiral symmetry breaking and chiral symmetry preserving coupling constants mix in the β-functions. Since the couplings λ and λ' get generated by the charge, and then mix into β_g, one necessarily has to track the flow of all four couplings. The next-to-the leading order calculations are in fact necessary if one wants to calculate the critical value of N_c for QED_3 with a massive gauge field. This is shown to be equivalent to the Thirring model and is the subject of discussion in Sec.2.7 and 2.8.

2.7 Dynamical mass generation in the next order of large-N

If one wants to generalize the above arguments to the next order in $1/N$-expansion some tedious calculation from further diagrams arises. At the same time, the two theorems we proved about the form of the renormalization group equations and the chiral symmetry breaking and the chiral symmetry preserving coupling terms do not hold anymore. On the other hand, some of the current-current interaction terms that did not generated mass through the gap equation Eq.(2.13), now in the finite-but-large N limit give rise to small dynamically generated masses. To analyze this mass generation mechanism we begin with the most general four-fermion theory which include previous models such as Thirring and Gross-Neveu in addition to NJL. To simplify things we discuss things in the absence of the gauge-field. The action for most general theory will look like,

$$\begin{aligned} S = \int \mathrm{d}x^3 \sum_i \bar{\Psi}\gamma_\mu\partial_\mu\Psi_i + \frac{g}{N}(\bar{\Psi}_i\Psi_i)^2 + \frac{g'}{N}(\bar{\Psi}_i\gamma_\mu\gamma_{35}\Psi_i)^2 \\ + \frac{g_3}{N}(\bar{\Psi}_i\gamma_3\Psi_i)^2 + \frac{g_3'}{N}(\bar{\Psi}_i\gamma_5\gamma_\mu\Psi_i)^2 \\ + \frac{g_5}{N}(\bar{\Psi}_i\gamma_5\Psi_i)^2 + \frac{g_5'}{N}(\bar{\Psi}_i\gamma_\mu\gamma_3\Psi_i)^2 \\ + \frac{\lambda}{N}(\bar{\Psi}_i\gamma_{35}\Psi_i)^2 + \frac{\lambda'}{N}(\bar{\Psi}_i\gamma_\mu\Psi_i)^2, \end{aligned} \tag{2.26}$$

which is basically the same as the form of Eq.(2.5), $g_i\mathbf{A}_i^2 + g_i'\mathbf{B}_{\mu,i}^2 + \lambda\mathbf{C}_0^2 + \lambda'\mathbf{C}_\mu^2$. If the couplings g_i are all the same ($g_i = g, g_i' = g'$) and the chiral preserving interaction couplings λ and λ' are zero, one recovers the NJL model, which is also a chiral symmetry preserving theory. For the case of only $\lambda' \neq 0$ it is the Thirring model. Dynamical mass generation in both of these theories is well-known and extensively studied. For the case of NJL, the RG equations for the couplings g, g_3 and g_5 will be identical to and decoupled in the same way as the RG equations obtained in Eq.(2.21). In the presence of a gauge field there exists no N_c for the dynamical mass generation as new chiral preserving coupling terms are generated in e^4 diagrams. This indicates that the identical form of the chiral symmetry breaking and chiral symmetry preserving β-functions is not accidental and is a reflection of the fact that the chiral symmetry breaking β-function can also represent the NJL-model at the same time as the couplings corresponding to a different generator of the chiral group are decoupled in the leading order limit.

However, the fact that RG equations are de-coupled might not be the case for the next order calculations, thus one has to go through a somewhat tedious calculation of different one-loop diagrams

to find the full-form of the RG equations. If we put the NJL model aside for a moment and look at the chiral symmetry breaking and chiral symmetry preserving actions introduced earlier the results are interesting. We will proceed with the analysis of finding N_c for different four-fermion theories- Eq.(2.26) in general - in few steps: first we analyze how there will be mass generation to the next order of the $1/N$ in the mean-field limit gap equation. Next, we focus on the chiral preserving limit, i.e., the Thirring model, as the new diagrams to be calculated are bound to obey chiral symmetry and thus there will be no couplings between chiral symmetry preserving and breaking couplings (λ's and g's). Finally we approach the four-fermionic chiral symmetry breaking action in the limit of zero charge and calculate the general form of the RG equations. We will argue that the value of the N_c calculated from the merging of the Gross-Neveu fixed point to the Gaussian fixed point can be interpreted as the Thirring model's N_c. The value of the N_c for the NJL model can similarly be calculated but we will not address it in this Chapter. Finally we repeat the same procedure for both of the chiral symmetry breaking + chiral symmetry preserving model in the presence of the gauge field and calculated the modifications to the critical flavour number N_c.

Consider the chiral symmetry preserving interaction action,

$$S = \int \mathrm{d}x^3 \sum_i \bar{\Psi}\gamma_\mu \partial_\mu \Psi_i + \frac{\lambda}{N}(\bar{\Psi}_i \gamma_{35}\Psi_i)^2 + \frac{\lambda'}{N}(\bar{\Psi}_i\gamma_\mu\Psi_i)^2, \tag{2.27}$$

The gap equation for λ was calculated before in equation Eq.(2.13). However the gap equation for the term $\lambda'(\bar{\Psi}\gamma_\mu\Psi)^2$ can be calculated using the Fierz identity Eqs.(B.13) (see Appendix B),

$$\begin{aligned} -(\bar{\Psi}^a\gamma_\mu\Psi^a)^2 = (\bar{\Psi}^a\Psi^b)(\bar{\Psi}^b\Psi^a) + (\bar{\Psi}^a i\gamma_3\Psi^b)(\bar{\Psi}^b i\gamma_3\Psi^a) \\ +(\bar{\Psi}^a i\gamma_5\Psi^b)(\bar{\Psi}^b i\gamma_5\Psi^a) + (\bar{\Psi}^a\gamma_{35}\Psi^b)(\bar{\Psi}^b\gamma_{35}\Psi^a) + (\bar{\Psi}^a\gamma_{35}\Psi^a)^2). \end{aligned} \tag{2.28}$$

It is interesting to notice that both terms $(\bar{\Psi}^a\gamma_{35}\Psi^b)(\bar{\Psi}^b\gamma_{35}\Psi^a)$ and $(\bar{\Psi}^a\gamma_{35}\Psi^a)^2$ appear in this new form of the Thirring interaction. Both of these terms, however, will lead to a parity breaking mass term. Decoupling all the first four terms in Eq.(2.28) in Fock-channel using the auxiliary field matrix $\hat{M}_{ab}$ gives

$$\exp\left\{\frac{\lambda'}{N}(\bar{\Psi}^a\Gamma\Psi^b)(\bar{\Psi}^b\Gamma\Psi^a)\right\} = \int [D\hat{M}] \exp\left\{-\frac{N\cdot \mathrm{Tr}(\hat{M}_{ab}\hat{M}_{ba})}{4\lambda'} + \mathrm{Tr}\ln\left(\gamma_\mu\partial_\mu + \hat{M}\Gamma\right)\right\}. \tag{2.29}$$

Using a de-coupling in the Hartree-channel for the $(\bar{\Psi}\gamma_{35}\Psi)^2$ term using the scalar auxiliary field m_{35}, and writing $\hat{M}$ in terms of the chiral generators:

$$\hat{M} = M_0 + iM_3\gamma_3 + iM_5\gamma_5 + M_{35}\gamma_{35}, \tag{2.30}$$

we end up the following effective form for the action:

$$S_{\text{eff}}[M_0, M_3, M_5, M_{35}, m_{35}] = \frac{N}{4\lambda'}\left(M_0^2 + M_3^2 + M_5^2 + M_{35}^2 + Nm_{35}^2\right) + \\ \text{Tr}\ln\left(\gamma_\mu\partial_\mu + M_0 + iM_3\gamma_3 + iM_5\gamma_5 + M_{35}\gamma_{35}\right). \tag{2.31}$$

One can notice that since γ_{35} commutes with the rest of the γ_μ and chiral generators, in the limit of $N \to \infty$ where we need to square the action Eq.(2.31), the mass term M_{35} does not let us have a gap equation in the form of Eq.(2.13). This means that in the $N \to \infty$ limit the gap equation can either give us a parity breaking mass OR a chiral symmetry breaking mass and not both together from one interaction term. The above two gap equations are based on the fact that the chiral symmetry and parity symmetry breaking does not happen at the same time.

Since we are interested in chiral symmetry breaking masses, we drop both parity violating masses m_{35} and M_{35} and the gap equations can simply be written as,

$$\begin{aligned} \frac{1}{\lambda} &= \sum_k \frac{1}{k^2 + m_{35}^2}, \\ \frac{1}{\lambda'} &= \frac{1}{N}\sum_k \frac{1}{k^2 + M_0^2 + M_3^2 + M_5^2}. \end{aligned} \tag{2.32}$$

The new mass $M^2 = M_0^2 + M_3^2 + M_5^2$ is however chiral symmetric and the gap equation above is exactly the saddle-point limit of the NJL model. The Thirring fixed point on the $\lambda = 0$ axis will represent chiral symmetry breaking through the above mechanism. The above mean-field approach is somewhat crude and will not show how different coupling strengths might compete with each other for the chiral (or parity) symmetry breaking. One important feature of the above analysis is to show that the mass generated through the Fock channel decomposition will be of order of $1/N$ and can be ignored in the limit of $N \to \infty$. Thus the above discussion shows that we do expect that a mass gets created for the Thirring model in the same manner as we have it for NJL, and also we expect the mass be small in the limit of large-N that we are considering. In the next Section we try to approach the same question beginning from a chiral symmetry preserving model including the next order corrections. The next oder corrections should probably tell us if there is any mass generation mechanism like the gap equation obtained above can be seen in the renormalization group approach and wether the critical flavour number N_c for the Thirring model can be obtained from it.

2.8 Next-order chiral symmetry preserving RG equations

In this Section we will restrict ourself to a chiral symmetry preserving Lagrangian and calculate the $1/N$-corrections to the β-functions derived in Eq.(2.25). To simplify calculations we consider the limit of $e = 0$ only and look at the evolution of the fixed-points as N changes. Notice that now N appears directly in the RG equations and *not* through the charge-renormalization as in the QED_3 case.

For the next order calculations we have to look at diagrams in which the number of vertices - which carry $1/N$ - with respect the number of loops - which give rise to a factor of N - differ by only 1. In principle many cactus diagrams such as the one in Fig.(2.17a) qualify for the next order calculations. However, symmetry considerations prohibit any mass-loop terms for our chiral symmetric model and thus we can ignore such diagrams. On the other hand internal loops such as the diagrams in Fig.(2.17b) and Fig.(2.17c) are of higher order in $1/N$ by a simple power counting: $(\lambda/N)^4 \cdot N^2 \sim (1/N)^2$. The only possibility at this order of expansion is to consider the one-loop diagrams which incorporate particle-particle and hole-hole terms. All such diagrams are listed in Fig.(2.18).

The above argument would become substantially more difficult if we had non-zero charge. Higher-order radiative-corrections had to be included in the $\mathcal{O}(1/N)$ diagrams. We are going to leave this issue for future studies and will not address a full next-to-the leading order RG analysis for QED_3 problem in this thesis.

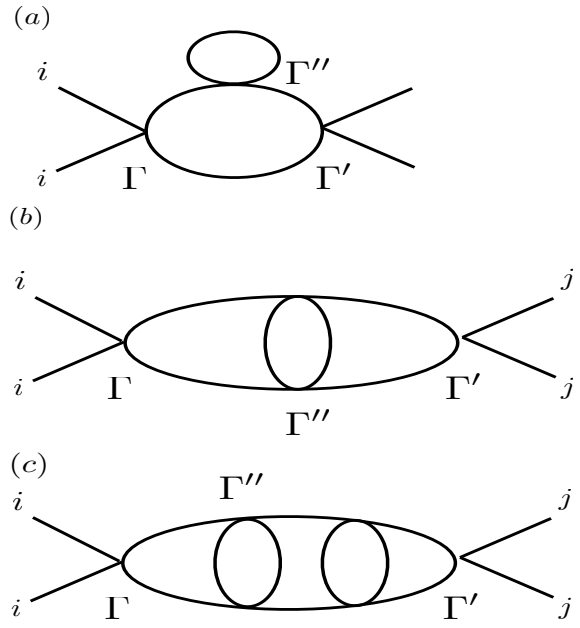

Figure 2.17: Some of the possible diagrams in higher orders of $1/N$.

The number of diagrams to account for is still high. The diagrammatic calculations can be simplified if we notice that the interaction terms of the form $\lambda_{\Gamma}(\bar{\Psi}\Gamma\Psi)^2$ and $\lambda_{\Gamma'}(\bar{\Psi}\Gamma'\Psi)^2$ leads to

$$\frac{\lambda_{\Gamma'}\lambda_{\Gamma}}{N^2}\left(\bar{\Psi}\left(\Gamma G\Gamma' - \Gamma' G\Gamma\right)\Psi\right)^2, \tag{2.33}$$

There are two other forms appearing in the one-loop diagrams, corresponding to the figures Fig.(2.18 a), Fig.(2.18 b),Fig.(2.18 c) and Fig.(2.18 d),

$$\frac{\lambda_{\Gamma'}\lambda_{\Gamma}}{N^2}\left(\left(\bar{\Psi}\Gamma G\Gamma' G\Gamma\Psi\right)\cdot\left(\bar{\Psi}\Gamma'\Psi\right)\right) \quad + \quad \Gamma \longleftrightarrow \Gamma', \tag{2.34}$$

and the contribution from the diagrams Eq.(2.18 e) and (2.18 f) in the figure is,

$$\frac{\lambda_{\Gamma'}g\lambda_{\Gamma}}{N^2}\left(\left(\bar{\Psi}\Gamma G\Gamma G\Gamma'\Psi\right)\cdot\left(\bar{\Psi}\Gamma'\Psi\right)\right) \quad + \quad \Gamma \longleftrightarrow \Gamma', \tag{2.35}$$

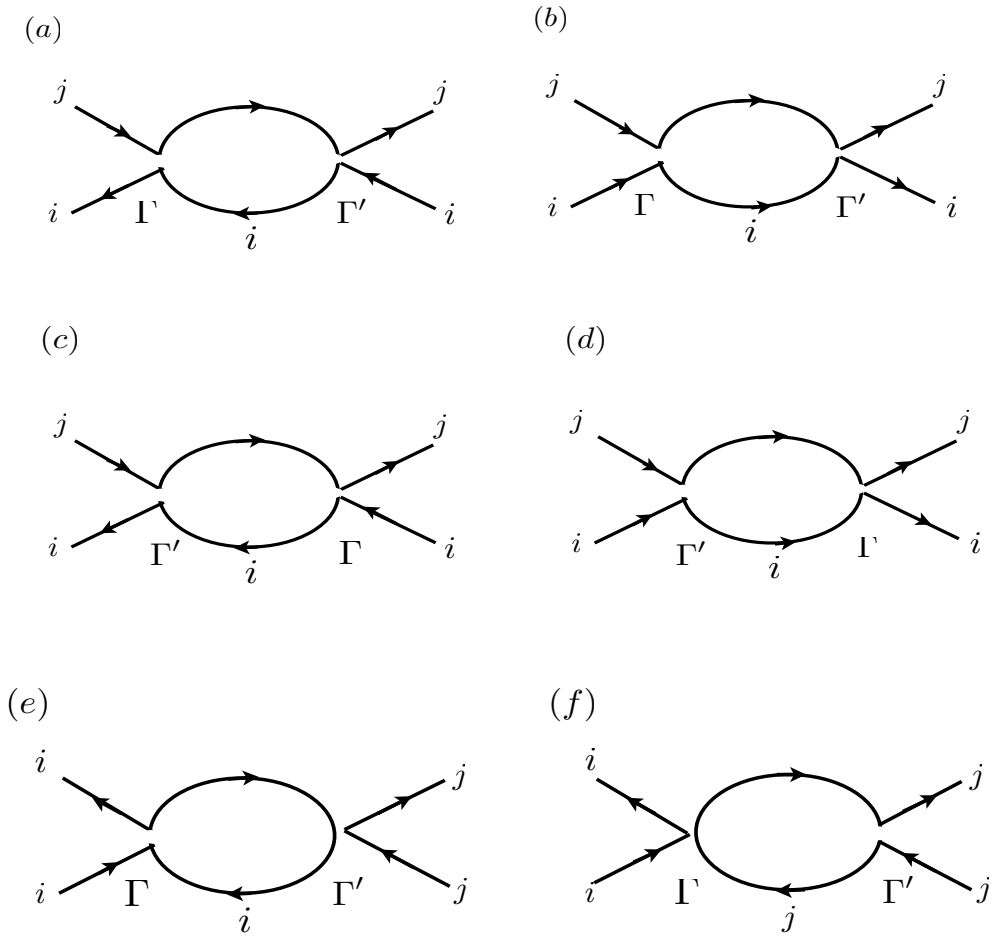

Figure 2.18: Particle-particle and hole-hole diagrams to the leading order in $1/N$.

upon summing up the particle-particle and particle-hole terms. Here, G represents the fermionic Green's function. Performing the calculations for the chiral symmetry preserving coupling strengths g and g' leads to,

$$\begin{aligned}\frac{\mathrm{d}\lambda}{\mathrm{d}\ln b} &= -\lambda - \left(1 - \frac{1}{2N}\right)\lambda^2 + \frac{9}{2N}\lambda'^2 + \frac{9}{2N}\lambda\lambda', \\ \frac{\mathrm{d}\lambda'}{\mathrm{d}\ln b} &= -\lambda' + \left(1 + \frac{1}{2N}\right)\lambda'^2 + \frac{1}{2N}\lambda\lambda'. \end{aligned} \tag{2.36}$$

This is the same as the RG equations derived in Ref.[46]. In the absence of the gauge field the flavour number dependence has a totally different form from the RG equations obtained for QED_3 in presence of the symmetry preserving interactions. The e^4 term in the β-function of the parity-breaking mass $\bar{\Psi}\gamma_{35}\Psi$ is absent and all the linear couplings between the charge e^2, i.e., $\frac{1}{N}$, and chiral symmetry preserving coupling strengths that came from the radiative corrections diagrams now are missing too. The N-dependence is of higher order in coupling strength now and comes from λ^2, λ'^2 and $\lambda\lambda'$ terms. This leads to a less sensitive behaviour for the fixed points and critical points to the change of the flavour number N. The solutions to the RG equations in Eq.(2.36) are plotted below in Fig.(2.19) for different values of large-N. As can be seen the fixed- points of neither the parity breaking not the Thirring interaction terms merge towards the Gaussian fixed-point for $N > 1$. In fact there is nothing to prevent spontaneous symmetry breaking for this theory at some smaller value of large-N parameter as the e^4 term in the β-function of coupling λ is missing. For values of $N \approx 0.1$ the Thirring fixed-point seems to approach the Gaussian one. However, since this corresponds to very small N and is out of the range of the large-N limit, we do not consider it as a physically acceptable result.

A more detailed analysis of the above RG equations can be found in the Ref.[46]. The authors analyzed the domains of broken chiral symmetry and parity in the theory and derived the phase diagram of the Thirring model. Remarkably, the fixed-point corresponding to the chiral symmetry broken phase however, turns out to be $\lambda = 1, \lambda' = 1$. Similarly to our findings, Ref.[46] has reported that the value of N_c cannot be obtained from the above RG equations.

To calculate the value of N_c for the Thirring model we will proceed by including the chiral symmetry breaking interaction into the theory, i.e., considering the most general theory. This is the subject of the discussion in the next section.

Figure 2.19: (a) Evolution of the Thirring coupling, λ', with respect to change of the flavour number N. Thirring critical point merges with the gaussian one at $N_c \sim 0.3$. (b) The evolution of the parity breaking interaction coupling strength, λ, as N increases. Upon change of N the critical point moves further away from zero. (c) The motion of the fixed point in the $\lambda - \lambda'$ space. Two of the fixed points (out of four) do not move significantly.

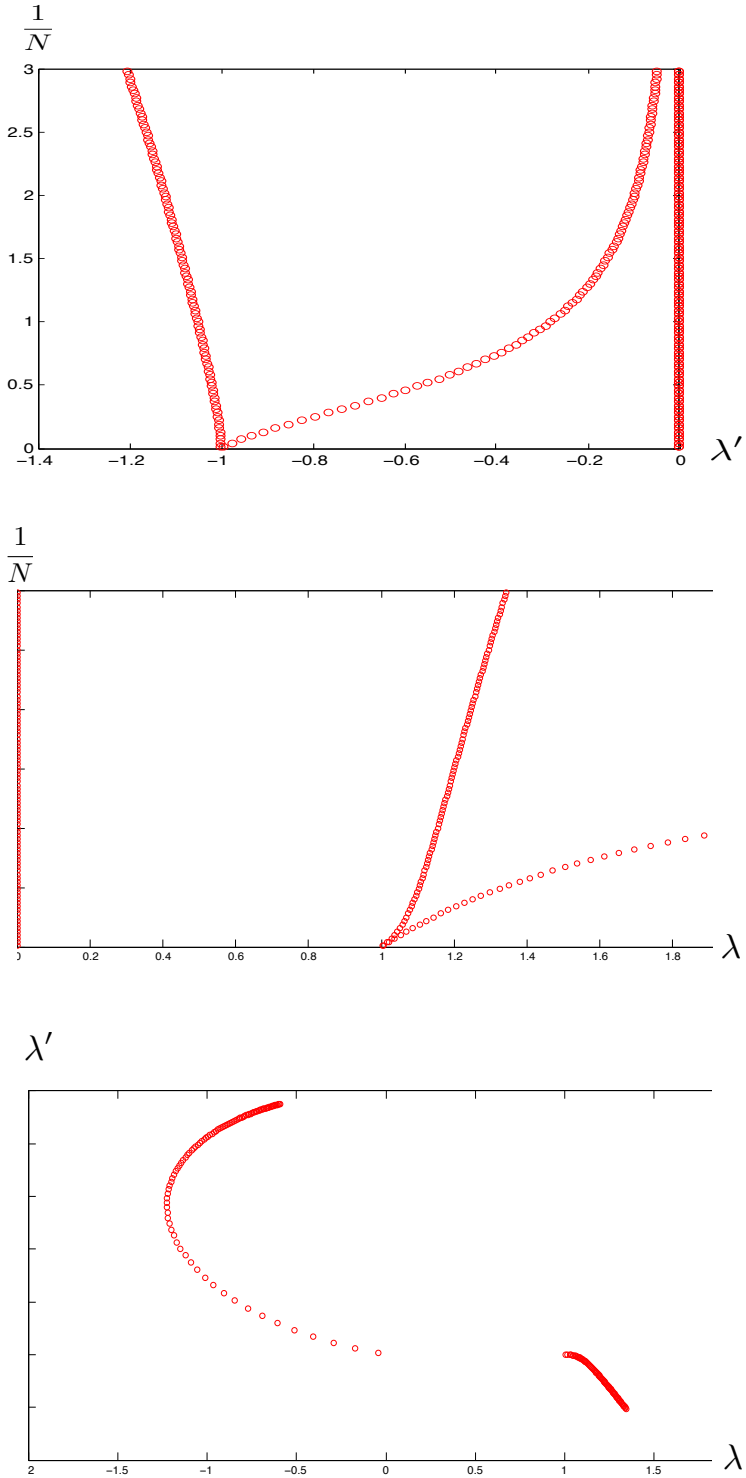

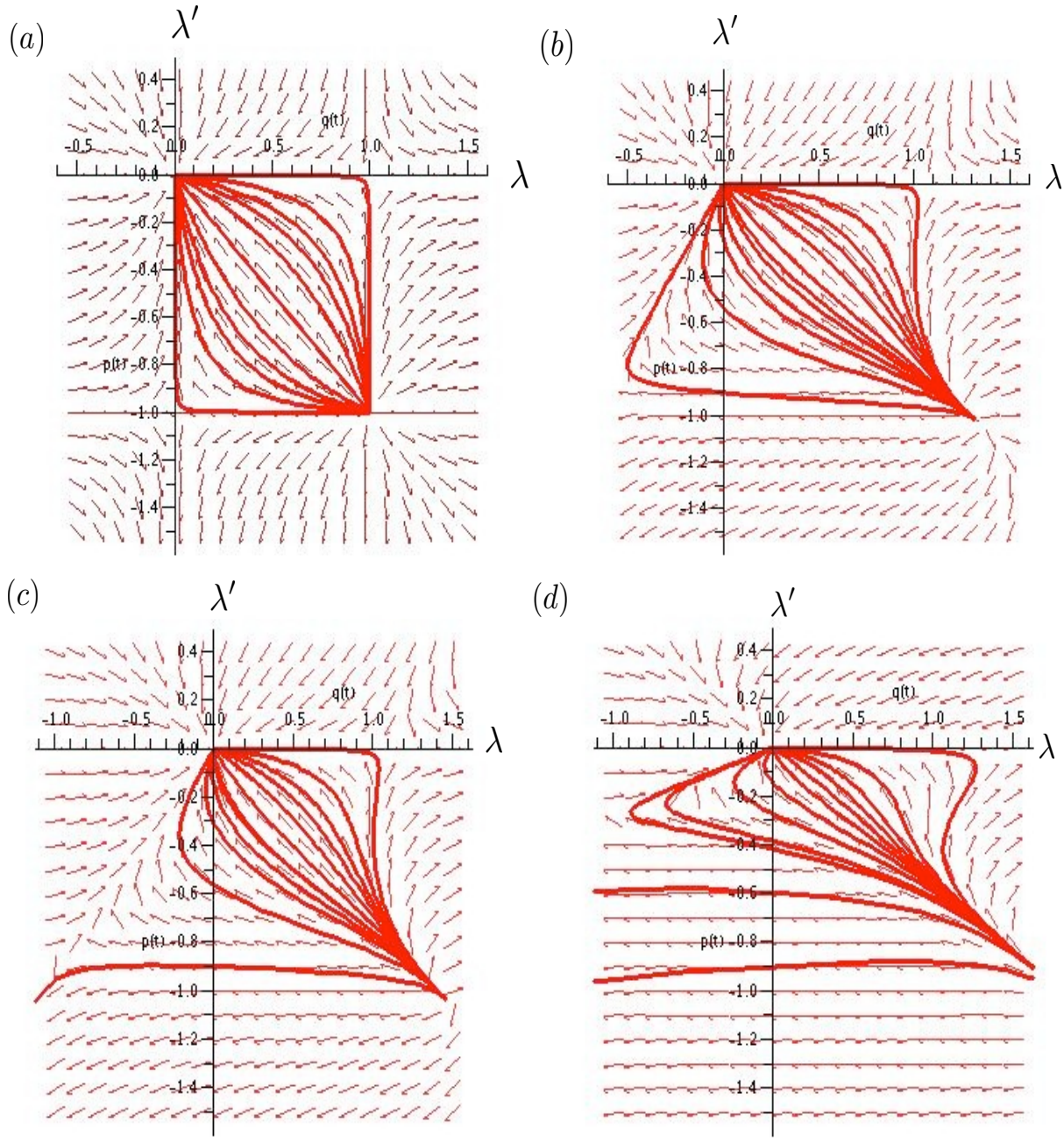

Figure 2.20: Renormalization group flow diagrams for the chiral symmetry breaking strengths, λ and λ' at (a) $\frac{1}{N} = 0.0$, (b) $\frac{1}{N} = 0.1$, (c) $\frac{1}{N} = 0.17$ and (d) $\frac{1}{N} = 1.0$. Below $N = 1$ the results are not physical and the corresponding flow diagrams are not depicted.

.

Using the same Fierz identities that we employed in obtaining the NJL-type gap equation for the Thirring model, Eq.(2.32), Refs.[46][47] have tried to show the existence of a phase transition in the system. One interesting observation from both Refs. is that beginning from a general chiral symmetry preserving model and applying the Fierz identity, the condition of $\lambda = 2\lambda'$ results in the pure NJL form for the whole model - ignoring the parity breaking terms. The Thirring FP which we were following its possible merging to the Gaussian fixed-point is in fact lies very close to the line $\lambda = 2\lambda'$, thus if the RG equations would result in any merging between the Thirring fixed-point and the Gaussian fixed-point, the corresponding flavour number N could automatically be considered as the value of N_c for NJL model too. In any case, our RG analysis has not shown any value for N_c as we already expected since the limit of $N \to \infty$ does not give any chiral symmetry breaking mass. In the next Sec. we add an explicit chiral symmetry breaking term to the chiral symmetry preserving model and try to follow the same logic as the discussion on QED_3, to obtain a value for N_c.

2.9 Massive-gauge field QED_3; Thirring model

In the following we are going to discuss the mass generation mechanism in the Thirring model which through a similar approach as in QED_3 the β-function for the Thirring coupling will lead to the generation of all other chiral symmetry preserving coupling strengths.

Similar to what we did for the QED_3, we introduce a Gross-Neveu type of coupling as a direct chiral symmetry breaking term. The resulting RG equations lead to a complicated coupled equation of all couplings strengths coupled to each other in next-to-the leading order of $1/N$. The fact that both QED_3 and Thirring exhibit similar behaviour with respect to a symmetry breaking perturbation - such as Gross-Neveu type- is however remarkable. The Thirring model can also be considered as the effective field theory for the phase fluctuating superconductor coupled to the singular gauge field $\vec{a}$, in the superconducting phase. In this phase the gauge field is massive and the Lagrangian takes the form,

$$\mathcal{L} = \bar{\Psi}\left(\gamma_\mu \partial_\mu + i a_\mu\right)\Psi + M\vec{a}^2 + \frac{1}{2e^2}(\nabla \times \vec{a})^2. \tag{2.37}$$

M is the mass of the gauge field $\vec{a}$ and comes from the Anderson-Higgs mechanism as discussed in Chapter 1. Upon re-scaling,

$$\sqrt{M \cdot N}\, a_\mu \to a_\mu, \tag{2.38}$$

the Lagrangian looks like,

$$\mathcal{L} = \bar{\Psi}\left(\gamma_\mu \partial_\mu + i\frac{\lambda'}{\sqrt{N}} a_\mu\right)\Psi + \vec{a}^2 + \frac{1}{2e^2}(\nabla \times \vec{a})^2, \tag{2.39}$$

where $\lambda' \sim 1/\sqrt{M}$. Ignoring the dynamics of the gauge field and integrating out the gauge field $\vec{a}$ one reaches to the Thirring model as the effective theory for the d-wave superconductor deep inside the superconducting region,

$$\mathcal{L} = \bar{\Psi}\left(\gamma_\mu \partial_\mu\right)\Psi + \frac{\lambda'}{N}\left(\bar{\Psi}\gamma_\mu \Psi\right)^2. \tag{2.40}$$

It is important to notice that the Thirring interaction coupling appears in the form of charge in the massive gauge field theory. This observation will lead us to treat the dynamical mass generation in Thirring model the same way as we did in QED_3 in previous Sections. The obvious difference is that the charge renormalization fixed-point is replaced with Thirring coupling strength fixed-point. Adding the Gross-Neveu term to the above Lagrangian by a charily symmetric breaking perturbation,

$$\mathcal{L} = \bar{\Psi}(\gamma_\mu \partial_\mu)\Psi + \frac{g}{N}(\bar{\Psi}\Psi)^2 + \frac{\lambda'}{N}(\bar{\Psi}\gamma_\mu \Psi)^2. \tag{2.41}$$

From our next-order RG equations, we can see that coupling of g and λ' induces non-zero g' and λ couplings strengths upon renormalization. Calculating all the diagrams in Fig.(2.18), results in the coupling between almost all the four-fermion coupling strengths and results in a much more sophisticated picture as we originally had for three-dimensional quantum electrodynamics. Below in Eq.(2.42) we report which non-zero couplings generate the other ones is reported. The fact is that there is nothing to prevent the chiral symmetry breaking interactions inducing a chiral symmetry preserving interaction terms in the next order of $1/N$. As a matter of fact the chiral symmetry breaking couplings, g and g' generate chiral symmetry preserving coupling strengths λ and λ' in the $1/N$ order. This means that beginning from Thirring model with an additional Gross-Neveu interaction added to it, all the four possible chiral symmetry preserving and breaking interaction coupling strengths are induced and the β-functions of all the couplings strengths are coupled to each other (unlike the zeroth order case). We have listed how all different couplings contribute to renormalization of the other couplings in the followings,

$$\begin{array}{rcl@{\qquad}rcl}
\dfrac{\lambda'^2}{N} & \to & \lambda_{\rm R}, & \dfrac{g\lambda'}{N} & \to & g'_{\rm R}, \\
\dfrac{g\lambda'}{N} & \to & g'_{\rm R}, & \dfrac{g\lambda'}{N} & \to & g_{\rm R,} \\
\dfrac{gg'}{N} & \to & \lambda'_{\rm R}, & \dfrac{g'^2}{N} & \to & g_{\rm R}, \\
\dfrac{g'\lambda}{N} & \to & g'_{\rm R}, & \dfrac{g'\lambda}{N} & \to & \lambda_{\rm R}, \\
\dfrac{\lambda\lambda'}{N} & \to & \lambda'_{\rm R}, & \dfrac{\lambda^2}{N} & \to & \lambda_{\rm R}, \\
\dfrac{g^2}{N} & \to & g_{\rm R,} & \dfrac{g\lambda}{N} & \to & g_{\rm R}, \\
\dfrac{g'\lambda'}{N} & \to & g_{\rm R}. & & &
\end{array} \tag{2.42}$$

The RG equations will be,

$$\begin{aligned}
\frac{{\rm d}g}{{\rm d}\ln b} &= -g - \left(1 - \frac{1}{4N}\right) g^2 - \frac{1}{2N} g'^2 + \frac{1}{2N} g\lambda - \frac{9}{2N} g\lambda' - \frac{9}{2N} g'\lambda', \\
\frac{{\rm d}g'}{{\rm d}\ln b} &= -g' + \left(1 + \frac{1}{4N}\right) g'^2 - \frac{1}{2N} g\lambda' - \frac{1}{2N} g'\lambda' + \frac{1}{6N} gg', \\
\frac{{\rm d}\lambda}{{\rm d}\ln b} &= -\lambda - \left(1 - \frac{1}{4N}\right) \lambda^2 + \frac{9}{N} \lambda'^2 - \frac{3}{4N} \lambda\lambda' + \frac{3}{2N} g'\lambda + \frac{1}{2N} g\lambda, \\
\frac{{\rm d}\lambda'}{{\rm d}\ln b} &= -\lambda' + \left(1 + \frac{1}{2N}\right) \lambda'^2 + \frac{2}{N} gg' - \frac{1}{2N} \lambda\lambda' - \frac{1}{2N} g'\lambda - \frac{1}{6N} g\lambda'.
\end{aligned} \tag{2.43}$$

Notice that because the chiral symmetry breaking couplings *do* generate chiral symmetry preserving couplings and not vice versa, we do not expect a symmetric look for β_λ and β_g or $\beta_{\lambda'}$ and $\beta_{g'}$ unlike the leading order RG equations. The analysis of the phase transition in the above system is somewhat difficult. There are 16 fixed points which corresponds to Thirring, parity breaking, chiral symmetry preserving and Gross-Neveu chiral symmetry breaking regions. Going back to the idea of treating the Gross-Neveu interaction as a perturbation on the original Thirring theory, we will focus on the $g \neq 0$ and $\lambda' \neq 0$ plane. Assuming that particularly for the Thirring fixed point which at $N = \infty$ is at $\lambda' = 1, \lambda = 0, g = 0, g' = 0$, and the Gross-Neveu fixed-point $\lambda' = 0, \lambda = 0, g = 1, g' = 0$, we can ignore the couplings including the other two parameters λ and g' inside the above RG equations Eq.(2.43) will lead to a simper set of coupled equations,

$$\begin{aligned}\frac{\mathrm{d}g}{\mathrm{d}\ln b} &= -g - \left(1 - \frac{1}{4N}\right) g^2 - \frac{9}{2N} g\lambda', \\ \frac{\mathrm{d}\lambda'}{\mathrm{d}\ln b} &= -\lambda' + \left(1 + \frac{1}{2N}\right) \lambda'^2 - \frac{1}{6N} g\lambda'. \end{aligned} \tag{2.44}$$

Upon decreasing the value of large-N, the $\lambda' = 1, g = 1$, fixed-point will merge with the Thirring fixed point. For some N's after a critical value N_c, the Thirring fixed point will be a completely repulsive one. The flow diagram of the system of the RG equations for different values of N is plotted below in Fig.(2.21).

This will let us estimate a value for the critical N_c for Thirring model,

$$N_c = 4.0. \tag{2.45}$$

This is in accordance with some other previous works using Schwinger-Dyson equations [48][49], which reported $N_c = 4.32$. The numerical calculation, however, has reported $N_c = 6.6$ [50][51].

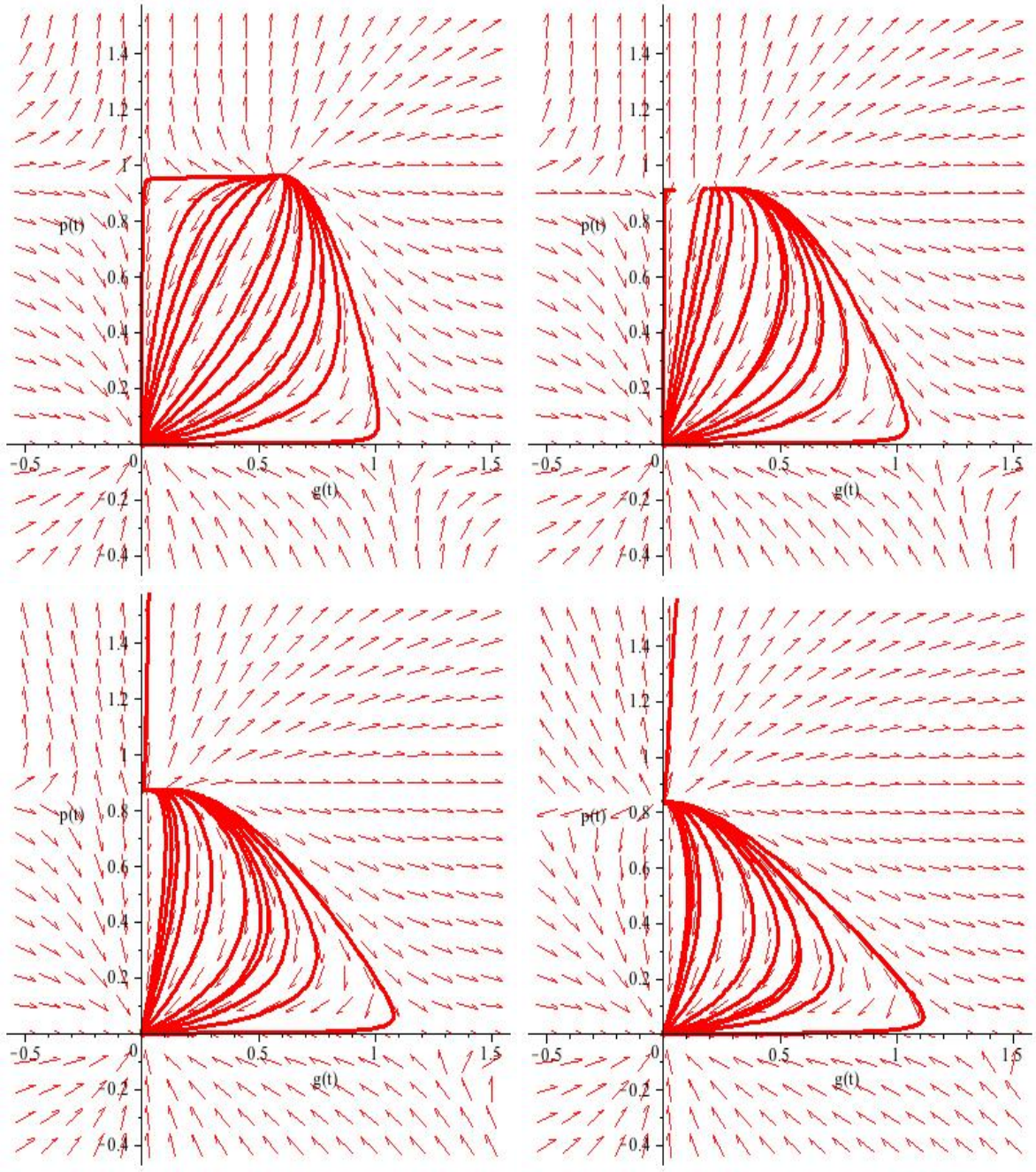

Figure 2.21: Renormalization group flow diagrams for the chiral symmetry breaking strengths, g and Thirring coupling λ' at (a) $1/N = 0.1$, (b) $1/N = 0.2$, (c) $1/N = 0.3$ and (d) $1/N = 0.4$. As it can seen, the nature of the Thirring coupling changes upon passing the critical $N_c \approx 3.0$.

2.10 Further Discussion and Future Directions

2.10.1 Anisotropic RG scheme; 2+1 dimensional quantum electrodynamics

As the reader might have noticed, so far all the RG calculations have been performed by assuming the same cutoff for imaginary time and momenta. This is not exactly the case for the case of underdoped cuprates as the critical point that the quantum fluctuations of the system nearby it should identify the pseudogap region. In this section we apply the same RG techniques to the three-dimensional QED coupled to a Gross-Neveu coupling to the leading order in large-N and derive the RG equations with imaginary-time cutoff taken to infinity. This resembles a system in a 3-ϵ dimensions and might give somewhat different results. The charge renormalization in this scheme can be derived from the calculation of the polarization bubble and the resulting β-function has a different factor in front of the Ne^4 term which might eventually result in a different reading for the value of N_c.

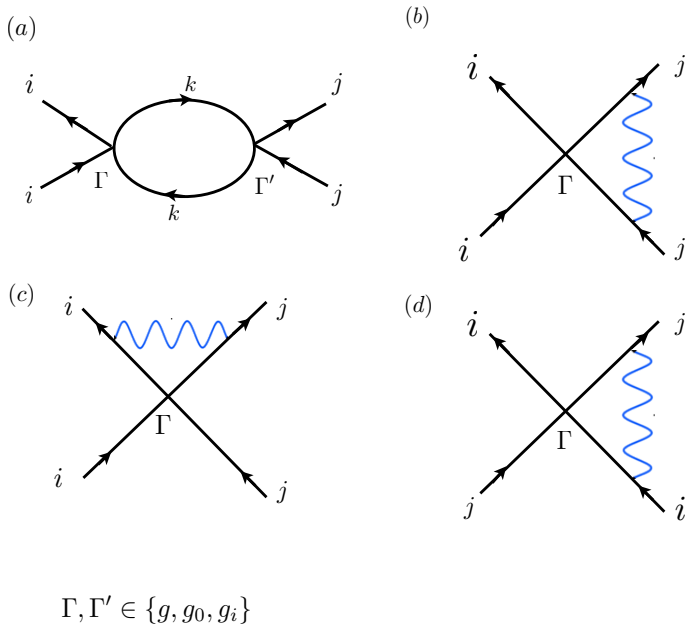

Figure 2.22: Diagrams contributing to the leading order in the anisotropic RG scheme. The main difference is that there are now three coupling strengths appearing in the vertices and there can be cross terms from those couplings in the RG equations even in the leading order of $1/N$.

$$\begin{aligned}
\frac{\mathrm{d}e^2}{\mathrm{d}\ln b} &= e^2 - \frac{N}{6}e^4, \\
\frac{dg}{d\ln b} &= -g - 2g^2 + 4e^2 g + \frac{2}{3}e^2 g' + \frac{3}{8}e^2 g'_0 + \frac{5}{16}e^2 g'_i, \\
\frac{\mathrm{d}g'_0}{\mathrm{d}\ln b} &= -g' + \frac{1}{24}e^2 g'_0 + \frac{3}{8}e^2 g, \\
\frac{\mathrm{d}g'_i}{\mathrm{d}\ln b} &= -g'_i + g'^2_i - \frac{1}{48}e^2 g'_i + \frac{1}{4}e^2 g. \qquad (2.46)
\end{aligned}$$

Analysis of the above RG equations, is left as a future project. Most importantly one has to argue the consistency of the charge renormalization β-function which is now obtained using a field-theoretical approach and momentum-shell renormalization for the interaction coupling strengths.

There is also another straight forward extension of the problems discussed above and that is the next-order in $1/N$ modification to the QED_3 RG equations that was obtained in the beginning of the chapter. Aside from the one-loop particle-particle diagrams that is already calculated to reach at Eq.(2.43), we also need to look at the radiative correction diagrams to the next order. We expect that the value of N_c does not change significantly from the value we calculated $N_c = 6.0$. This should affirm the consistency of our large-N expansion.

2.11 Summary

As the heart of the high-temperature superconducting transition in the underdoped regime is proposed to be explained by dynamical mass generation in Dirac fermionic theories strongly coupled with a gauge field and also in the presence of different four-fermionic couplings we needed to understand the mechanism much better. More importantly we need to have a reliable estimate of the critical number of fermionic flavours, N_c, below which the dynamical mass generation does not happen. Our approach to the dynamical mass generation of fermionic theories in presence of both gauge field and on-site interaction terms is based on a momentum-shell renormalization group analysis using which we can identify when the system (QED_3 in this case), becomes unstable with respect to the introduction of infinitesimal (chiral) symmetry breaking terms.

Next part of the Chapter we proceeded with a similar analysis for Thirring model which effectively describes AF order-parameter generation directly from the d-wave phase (and not from the intermediate pseudogap phase). We show the possibility of dynamical mass generation in Thirring model and derive the value of $N_c = 4.0$ for this transition. The scheme we are discussing will lead

to the conclusion that since there is the possibility of transition to AF phase both from pseudogap and dSC phase there might be an overlap region between the two AF and dSc phases. However, it has been argued before that considering the full theory and including the vortex degrees of freedom the overlap region tends to be zero as upon the mass of the gauge put restriction on momentum cut-off that appears in the calculation of the quasi-particle dynamical mass generation. A fact that has been absent from our RG analysis.

s

Chapter 3

Superfluid Density and Helicity Modulus

3.1 Weakly Interacting Bosons; General Approach

In this section we will review the general theory for superfluids and derive the formulas for condensate fraction and superfluid density for a superfluid either on a lattice or continuum with a general form of dispersion under the Bogluibov approximation. Later on, we will focus on the layered model that is appropriate for the QED_3 theory of nodal high-temperature superconductors and the low-temperature, underdoped form of the superfluid density along both ab-axes and also particularly the c-axis as discussed in the previous sections.

Consider a bosonic theory with both continuous and discrete degrees of freedom in a general form:

$$\begin{aligned} S_0 &= \int_0^\beta \mathrm{d}\tau \int \mathrm{d}^d\mathbf{x} \sum_{ij} (-t_{ij} b_i^*(\mathbf{x},\tau) b_j(\mathbf{x},\tau) + \mathrm{h.c.}) + \sum_i b_i^*(\mathbf{x},\tau) \left(-\partial_\tau - \frac{\nabla^2}{2m} - \mu \right) b_i(\mathbf{x},\tau) \\ &+ \frac{\lambda}{2} (b_i^*(\mathbf{x},\tau) b_i(\mathbf{x},\tau))^2. \end{aligned} \tag{3.1}$$

where bosonic fields, $b(\mathbf{x},\tau)$, are coherent-state bosons at continuous position $\mathbf{x}$, lattice site index i, and imaginary time τ. t_{ij} is the hopping amplitude between the lattice sites i to j, β is the inverse temperature and λ is the on-site interaction strength. To see the spontaneous gauge symmetry breaking in this this theory, as is customary, we introduce a linear symmetry breaking term to the action:

$$S_0 \longrightarrow S_\nu = S_0 + \frac{1}{2} \int \mathrm{d}\tau \mathrm{d}^d\mathbf{x} \sum_i (\nu^* b_i(\mathbf{x},\tau) + \nu b_i^*(\mathbf{x},\tau)), \tag{3.2}$$

where ν is the Bose symmetry breaking field. S_ν can be written in the momentum space representation as

$$S_\nu = \sum_{\omega_n,\mathbf{k}} (-i\omega_n + \xi_\mathbf{k})|b(\mathbf{k},\omega_n)|^2 + \frac{\beta^{1/2}(2\pi)^d}{\mathrm{vol}^{1/2}}\{\nu^* b(0,0) + \nu b^*(0,0)\}, \tag{3.3}$$

where ξ is the energy dispersion of the system measured from the chemical potential. It can take very general forms as we have been considering a very general form of hopping and continuous dispersion initially. By introducing the symmetry breaking field the ambiguity in transforming the sum over momenta into an integral in the thermodynamic limit is removed, since the zero-momentum states are singled out by the field ν and the divergence is removed. The order parameter $\langle b(\mathbf{x},\tau)\rangle$ can be written as the derivative of the free energy with respect to the symmetry breaking field,

$$\begin{aligned} \lim_{\nu\to 0} \frac{\partial \ln Z_\nu}{\partial \nu^*} = \int \mathrm{d}^2\mathbf{x}\mathrm{d}\tau \langle b(\mathbf{x},\tau)\rangle = (\mathrm{vol})(\beta)\langle b\rangle \\ \implies \lim_{\nu\to 0} \frac{\partial f}{\partial \nu^*} = \langle b\rangle = \phi_0, \end{aligned} \tag{3.4}$$

where f is the free energy density of the system.

$$f_\nu = \frac{T}{(\mathrm{vol})} \ln Z_\nu = T\sum_{\omega_n} \int_\mathbf{k} \frac{1}{-i\omega_n + \xi_\mathbf{k}} + \frac{\nu^2}{4\mu}. \tag{3.5}$$

The derivative with respect to chemical potential gives the total number density in terms of the symmetry breaking field and chemical potential and a sum of over momentum occupation numbers:

$$\begin{aligned} -\frac{\partial f_\nu}{\partial \mu} &= n_{\mathrm{tot}} = \int_\mathbf{k} n_B(\xi_\mathbf{k}) + \frac{\nu^2}{4\mu^2}, \\ -\frac{\partial f_\nu}{\partial \nu^*} &= \phi_0, \\ \to \phi_0 &= \frac{\nu}{2\mu}, \end{aligned} \tag{3.6}$$

with n_B being the Bose distribution function. This will lead us to the relation for the total number density,

$$n_{\mathrm{tot}} = \int_\mathbf{k} n_B(\xi_\mathbf{k}) + |\phi_0|^2. \tag{3.7}$$

Now, the non-zero order parameter ϕ_0 can occur at temperatures below some critical Bose-Einstein temperature T_{BE}, under the condition that while both $\nu \to 0$ and $\mu \to 0$ the quantity $\nu^2/4\mu^2$ remains constant.

$$\lim_{\nu\to 0}\lim_{\mu\to 0}\frac{\nu^2}{4\mu^2} = \text{constant} \quad \text{, i.e., } \phi_0. \tag{3.8}$$

3.2 Dilute Bose Gas; Bogoliubov Approximation

In this section we discuss a similar approach to the weakly interacting bosonic superfluid in d-dimensions with a general form of dispersion on either a lattice or in the continuum with weak on-site interactions indicated by the interaction strength λ in Eq.(3.1). To proceed I introduce new bosonic fields:

$$\begin{aligned} b(\mathbf{x},\tau) &\rightarrow b(\mathbf{x},\tau)+\phi_0, \\ b^\dagger(\mathbf{x},\tau) &\rightarrow b^\dagger(\mathbf{x},\tau)+\phi_0^*, \end{aligned} \tag{3.9}$$

where the order parameter $\phi_0 \sim \int b(\mathbf{x},\tau)$, is the zero-momentum part of the bosonic fields. In the absence of interactions, the quantum statistical average of the new field will be zero both below and above the critical $T_{\rm BE}$. Begin with the Hamiltonian of the bosonic theory using the new bosonic fields

$$\begin{aligned} H_{\rm BG} &= \int \mathrm{d}^d\mathbf{x}\sum_{ij}(-t_{ij}(b_i^\dagger(\mathbf{x})+\phi_0^*)(b_j(\mathbf{x})+\phi_0)+\text{c.c.}) \\ &+ \sum_i\left((b_i^\dagger(\mathbf{x})+\phi_0)\left(-\frac{\nabla^2}{2m}-\mu\right)(b_i(\mathbf{x}+\phi_0)\right) \\ &+ \frac{\lambda}{2}\{(b_i^\dagger(\mathbf{x})+\phi_0^*)(b_i(\mathbf{x})+\phi_0)\}^2-\tilde{\mu}|\phi_0|^2 \\ &+ \nu(b_i(\mathbf{x})^*+\phi_0^*)+\nu^*(b_i(\mathbf{x})+\phi_0), \end{aligned} \tag{3.10}$$

where the symmetry breaking term is also included in the Hamiltonian. Now, after the shift in the bosonic operators the divergence that leads to Bose-Einstein condensation has been removed and a perturbation theory is possible in the dilute limit. To do so, we only keep the quadratic and linear terms in the action and drop the rest of the odd and quartic powers. While the dispersion, $\xi_{\mathbf{k}} = \varepsilon_{\mathbf{k}} - \mu + 2\lambda\phi_0^2$, is re-defined to include the Hartee term from the quartic interaction, the corresponding action can be written in a more compact form by introducing two-component Nambu spinors for our bosonic fields.

$$
\begin{aligned}
S_{\rm BG} &= S_0 + S_{\rm qp} + \frac{\beta}{2}\int_{\mathbf{k}} \xi_{\mathbf{k}}, \\
S_0 &\equiv \beta(-\tilde{\mu}|\phi|_0^2 + \frac{\lambda}{2}|\phi|^4), \\
S_{\rm qp} &\equiv \frac{T}{2}\sum_{\omega_n}\int \frac{{\rm d}^d\mathbf{k}}{2\pi^d}
\begin{pmatrix} b^*_{\mathbf{k},\omega_n} & b_{-\mathbf{k},-\omega_n} \end{pmatrix}
\begin{pmatrix} -i\omega_n + \xi_{\mathbf{k}} & \lambda\phi_0^{*2} \\ \lambda\phi_0^2 & i\omega_n + \xi_{-\mathbf{k}} \end{pmatrix}
\begin{pmatrix} b_{\mathbf{k},\omega_n} \\ b^*_{-\mathbf{k},-\omega_n} \end{pmatrix}, \\
S_\nu &\equiv \sum_{\omega_n}\int_{\mathbf{k}} (\nu b^*_{0,0} + \nu^* b_{0,0}).
\end{aligned}
\tag{3.11}
$$

Notice that there is an overall extra term $\xi_{\mathbf{k}}/2$ added to $S_{\mathbf{BG}}$ which comes from writing the bosonic field combinations $bb^\dagger$ in a time-ordered manner $b^\dagger b$ after expanding the $H_{\rm qp}$.
The above action can be diagonalized by a Bogoliubov transform,

$$
\begin{aligned}
\alpha_{\mathbf{k},\omega_n} &= \cosh(\Theta_{\mathbf{k}}) b_{\mathbf{k},\omega_n} + \sinh(\Theta_{\mathbf{k}}) b^*_{-\mathbf{k},-\omega_n}, \\
\alpha^*_{\mathbf{k},\omega_n} &= \cosh(\Theta_{\mathbf{k}}) b^*_{\mathbf{k},\omega_n} + \sinh(\Theta_{\mathbf{k}}) b_{-\mathbf{k},-\omega_n}.
\end{aligned}
\tag{3.12}
$$

This diagonalizes the action if $\tanh(2\Theta_{\mathbf{k}}) = \lambda|\phi_0|^2/\xi_{\mathbf{k}}$ is satisfied. The diagonalized action can be written as,

$$
S_{\rm qp} = \frac{T}{2}\sum_{\omega_n}\int \frac{{\rm d}^d\mathbf{k}}{2\pi^d}
\begin{pmatrix} \alpha^*_{\mathbf{k},\omega_n} & \alpha_{-\mathbf{k},-\omega_n} \end{pmatrix}
\begin{pmatrix} -i\omega_n + E_{\mathbf{k}} & 0 \\ 0 & i\omega_n - E_{\mathbf{k}} \end{pmatrix}
\begin{pmatrix} \alpha^*_{\mathbf{k},\omega_n} \\ \alpha_{-\mathbf{k},-\omega_n} \end{pmatrix}
\tag{3.13}
$$

and the Bogoliubov quasi particle dispersion $E_{\mathbf{k}}$ will be:

$$
E_{\mathbf{k}} = \sqrt{\xi_{\mathbf{k}}^2 - \lambda^2\phi_0^4} = \sqrt{\varepsilon_{\mathbf{k}}(\varepsilon_{\mathbf{k}} + 2\lambda\phi_0^2)}.
\tag{3.14}
$$

The free energy density of the action is easy to calculate since the theory is Gaussian

$$
f(\nu=0) = -\frac{T}{\rm vol}\ln Z = \frac{T}{2}\sum_{\omega_n}\int_{\mathbf{k}} \ln\{\omega_n^2 + \xi_{\mathbf{k}}^2 - (\lambda\phi_0^2)^2\} + \int_{\mathbf{k}} \frac{\xi_{\mathbf{k}}}{2} - \tilde{\mu}|\phi_0|^2 + \frac{\lambda}{2}|\phi_0|^4,
\tag{3.15}
$$

while the same condensate order-parameter ϕ_0 as in the non-interacting limit can still be obtained as the derivative of the free energy with respect to the symmetry breaking field

$$\lim_{\nu\to 0}\left(-\frac{\partial f(\nu)}{\partial \nu}\right)=\phi_0 \tag{3.16}$$

while the particle number density is easily seen to be

$$n_{\rm tot}=-\frac{\partial f}{\partial \mu}=\int_{\mathbf{k}}\left(\frac{T}{2}\sum_{\omega_n}\frac{2\xi_{\mathbf{k}}}{\omega_n^2+E_{\mathbf{k}}^2}+\frac{1}{2}\right)+|\phi_0|^2, \tag{3.17}$$

where the derivative with respect to chemical potential has been replaced with the one with respect to boson energy, $\partial/\partial\mu=\partial/\xi_{\mathbf{k}}$.

3.3 Superfluid Density; Generalized Landau Formula

The superfluid density is a torsional spring constant which provides a response to a helical twist of the order parameter

$$\phi_0\rightarrow\phi_0\, e^{i\mathbf{k_0}\cdot\mathbf{x}}, \tag{3.18}$$

which implies the same twist in the the symmetry-breaking field ν. As argued by Landau for translationally invariant systems, this corresponds to a Galilean transform $v_0=\nabla\theta$. In the new coordinate system which is moving the with the velocity v_0, the kinetic energy of the superfluid can be written as,

$$K(v_0)=K_0+\frac{1}{2}Mv_0^2+\mathbf{P}\cdot\mathbf{v_0}, \tag{3.19}$$

where the cross term, $\mathbf{P}\cdot\mathbf{v_0}$, can be written as

$$\begin{aligned}\mathbf{P}\cdot\mathbf{v_0} &= \int b^\dagger(\mathrm{x})\left(\frac{i\hbar^2}{m}\mathbf{k_0}\cdot\nabla\right)b(\mathrm{x})\\ &= \frac{\hbar}{m}\mathbf{k_0}\cdot\Sigma_{\mathbf{k}}\hbar\mathbf{k}\; b_{\mathbf{k}}^\dagger b_{\mathbf{k}}.\end{aligned} \tag{3.20}$$

The action of this term is to impose a velocity drift on the quasi-particle excitations, $\varepsilon(\mathbf{k})\rightarrow\varepsilon(\mathbf{k})-\mathbf{v_0}\cdot\mathbf{k}$, which give rises to a momentum flux density $\mathbf{P}_{\rm tot}/\mathrm{vol}$. The proportionality constant between total momentum and $\mathbf{k_0}$ defines the normal fluid density, ρ_n. Assuming a two fluid model picture,

$$\rho=\rho_s+\rho_n, \tag{3.21}$$

leads to a definition for the superfluid density.

For a more general case of non-Galilean invariant systems, such as bosons on a lattice or in the presence of external magnetic fields, there is a more rigorous mathematical definition [91][56][55]. One can assume a twist in the boundary conditions of the system has been imposing helical twist in the order parameter and then calculate the change in the free-energy of the system, under the new "twisted" boundary condition. The difference between the old and new free-energies per phase-twist can give us the superfluid density. Here $\mathbf{k_0}$ is taken to be θ/L where L is the system size along the direction for which the superfluid response is being calculated and θ is the value of the boundary condition twist.

$$\rho_s \equiv \frac{m^2}{\hbar^2}\Upsilon_\mu = \lim_{\theta\to 0}\lim_{L\to\infty}\{F(\theta,\mu,T) - F(0,\mu,T)\}. \tag{3.22}$$

where we have defined the so-called "helicity-modulus", Υ_μ[56][55]which is the superfluid density per unit of $(\hbar/m)^2$. Calculating the free-energy in an arbitrary system of bosons with an arbitrary boundary condition twist is a difficult task. We adopt an equivalent method. Instead of the twist in the boundary conditions we merely assume the phase-twist in the symmetry breaking term, $\nu \to \nu\exp(i\mathbf{k_0}\cdot\mathbf{x})$. and define the superfluid density in a similar manner as Eq.(3.22),

$$\rho^{(s)}_{\alpha,\beta} = \lim_{\nu\to 0}\lim_{k_0\to 0}\frac{m^2}{\hbar^2}\frac{\partial^2 F(\mu,T;\mathbf{k_0})}{\partial k_{0,\alpha}\partial k_{0,\beta}}, \tag{3.23}$$

where the superfluid density now takes the form of a tensor. In isotropic models the superfluid density is an scalar.

Applying a gauge transform to make the symmetry breaking field real and constant again, requires that we transform bosonic field same way:

$$\begin{aligned} b(\mathbf{x},\tau) &\to b(\mathbf{x},\tau)\, e^{i\mathbf{k_0}\cdot\mathbf{x}} \\ b^*(\mathbf{x},\tau) &\to b^*(\mathbf{x},\tau)\, e^{-i\mathbf{k_0}\cdot\mathbf{x}} \\ &. \end{aligned} \tag{3.24}$$

The effect of this transform in momentum space is

$$\begin{aligned} b_{\mathbf{k},\omega} &\to b_{\mathbf{k}+\mathbf{k_0},\omega} \\ b_{-\mathbf{k},\omega} &\to b_{-\mathbf{k}+\mathbf{k_0},\omega} \end{aligned} \tag{3.25}$$

and the k_0-dependent action now becomes

$$\begin{aligned} S_0 \to S_0(\mathbf{k}_0) &= (\varepsilon_{\mathbf{k}_0} - \mu)|\phi_0|^2 + \frac{\lambda}{2}|\phi_0|^4, \\ S_{\rm qp} \to S_{\rm qp}(\mathbf{k}_0) &= \sum_{\omega_n} \int_{\mathbf{k}} \begin{pmatrix} b^*_{\mathbf{k},\omega_n} & b_{-\mathbf{k},-\omega_n} \end{pmatrix} \times \\ & \qquad \begin{pmatrix} -i\omega_n + \xi_{\mathbf{k}+\mathbf{k}_0} & \lambda\phi_0^{*2} \\ \lambda\phi_0^2 & i\omega_n + \xi_{-\mathbf{k}+\mathbf{k}_0} \end{pmatrix} \begin{pmatrix} b^*_{\mathbf{k},\omega_n} \\ b_{-\mathbf{k},-\omega_n}. \end{pmatrix} \end{aligned} \tag{3.26}$$

The new action can be diagonalized with a Bogoliubov transform. Now the Bogoliubov coefficients $u_{\mathbf{k}}$ and $v_{\mathbf{k}}$ will have the form

$$\begin{aligned} u_{\mathbf{k}}(\mathbf{k_0}) = \cosh(\Theta_{\mathbf{k}}(\mathbf{k_0})) &= \frac{\bar{\varepsilon_{\mathbf{k}}} + \lambda\phi_0^2}{\sqrt{\bar{\varepsilon}_{\mathbf{k}}(\bar{\varepsilon}_{\mathbf{k}} + 2\lambda\phi_0)}} \\ v_{\mathbf{k}}(\mathbf{k_0}) = \sinh(\Theta_{\mathbf{k}}(\mathbf{k_0})) &= \frac{\lambda\phi_0^2}{\sqrt{\bar{\varepsilon}_{\mathbf{k}}(\bar{\varepsilon}_{\mathbf{k}} + 2\lambda\phi_0)}} \end{aligned} \tag{3.27}$$

and $S_{\rm qp}(\mathbf{k})$ becomes

$$\begin{aligned} S_{\rm qp}(\mathbf{k}) &= T\sum_{\omega_n} \int_{\mathbf{k}} \begin{pmatrix} b^*_{\mathbf{k},\omega_n} & b_{-\mathbf{k},-\omega_n} \end{pmatrix} \\ &\times \begin{pmatrix} -i\omega_n + \Delta\varepsilon_{\mathbf{k}} + E(\bar{\xi}_{\mathbf{k}}) & 0 \\ 0 & i\omega_n - \Delta\varepsilon_{\mathbf{k}} + E(\bar{\xi}_{\mathbf{k}}) \end{pmatrix} \begin{pmatrix} b_{\mathbf{k},\omega_n} \\ b^*_{-\mathbf{k},-\omega_n} \end{pmatrix} \end{aligned} \tag{3.28}$$

where $\bar{\varepsilon}$ and $\Delta\varepsilon$ are defined as

$$\begin{aligned} \bar{\varepsilon_{\mathbf{k}}} &= \frac{1}{2}(\varepsilon_{\mathbf{k}+\mathbf{k_0}} + \varepsilon_{\mathbf{k}-\mathbf{k_0}}), \\ \Delta\varepsilon_{\mathbf{k}} &= (\varepsilon_{\mathbf{k}+\mathbf{k_0}} - \varepsilon_{\mathbf{k}-\mathbf{k_0}}). \end{aligned} \tag{3.29}$$

The free energy density for the phase-twisted system will be

$$\begin{aligned} F(k_{0,\alpha}) = T\sum_{\omega_0} \int_{\mathbf{k}} \ln\left(-i\omega_n + \frac{\partial\xi_{\mathbf{k}}}{\partial k_{0,\alpha}} + E(\bar{\xi}_{\mathbf{k}})\right) + \ln\left(i\omega_n - \frac{\partial\xi_{\mathbf{k}}}{\partial k_{0,\alpha}} + E(\bar{\xi}_{\mathbf{k}})\right) \\ + \int_{\mathbf{k}} \xi_{\mathbf{k}+\mathbf{k_0}} + (\varepsilon_{\mathbf{k_0}} - \mu)|\phi_0|^2 + \frac{\lambda}{2}|\phi_0|^4. \end{aligned} \tag{3.30}$$

Now, the helicity modulus will be simply obtained from the second derivative of the $\mathbf{k}$-dependent free energy.

$$\begin{aligned}\Upsilon_\alpha &= \lim_{\mathbf{k}_0\to 0}\frac{\partial^2 F(\mathbf{k}_0)}{\partial k_{0,\alpha}\partial_{0,\beta}} \\ &= \lim_{\mathbf{k}_0\to 0}\frac{T}{2}\sum_{\omega_n}\int_{\mathbf{k}} -\frac{(\partial_{k_{0,\alpha}}E(\bar{\xi_{\mathbf{k}}})+\partial_{k_{0,\alpha}}\xi_{\mathbf{k}})^2}{\{-i\omega_n+E(\bar{\xi_{\mathbf{k}}})+(\partial_\alpha\xi_{\mathbf{k}})k_{0,\alpha}\}^2}-\frac{(\partial k_{0,\alpha}E(\bar{\xi_{\mathbf{k}}})-\partial k_{0,\alpha}\xi_{\mathbf{k}})^2}{\{i\omega_n+E(\bar{\xi_{\mathbf{k}}})-(\partial_\alpha\xi_{\mathbf{k}})k_{0,\alpha}\}^2} \\ &\quad +\frac{\partial^2_{k_{0,\alpha}}E(\bar{\varepsilon_{\mathbf{k}}})}{\{-i\omega_n+E(\bar{\xi_{\mathbf{k}}})+(\partial_\alpha\xi_{\mathbf{k}})k_{0,\alpha}\}}+\frac{\partial^2_{k_{0,\alpha}}E(\bar{\varepsilon_{\mathbf{k}}})}{\{i\omega_n+E(\bar{\xi_{\mathbf{k}}})-(\partial_\alpha\xi_{\mathbf{k}})k_{0,\alpha}\}} \\ &\quad +\frac{\partial^2}{\partial k^2_{0,\alpha}}(\varepsilon_{\mathbf{k}_0}-\mu)\phi_0^2+\frac{\lambda}{2}\phi_0^4). \end{aligned} \tag{3.31}$$

Taking the limit $\mathbf{k_0}\to 0$ and performing the summation over Matsubara frequencies simplifies the above formula to a generalized Landau formula for the helicity modulus:

$$\begin{aligned}\Upsilon_{\alpha,\beta} = \int_{\mathbf{k}}\left(\frac{\partial\varepsilon_{\mathbf{k}}}{\partial k_\alpha}\right)\left(\frac{\partial\varepsilon_{\mathbf{k}}}{\partial k_\beta}\right)\frac{\mathrm{d}n_{\mathrm{B}}(E_{\mathbf{k}})}{\mathrm{d}E_{\mathbf{k}}}+\int_{\mathbf{k}}\frac{\partial^2\varepsilon_{\mathbf{k}}}{\partial k_\alpha k_\beta}\cdot\left(n_{\mathrm{B}}(E_{\mathbf{k}})\cdot\frac{\varepsilon+\lambda\phi_0^2}{E_{\mathbf{k}}}\right) \\ +\int_{\mathbf{k}}\frac{\partial^2\varepsilon_{\mathbf{k}}}{\partial k_\alpha k_\beta}\cdot\frac{1}{2}\left(\frac{\varepsilon+\lambda\phi_0^2}{E_{\mathbf{k}}}-1\right)+\left(\frac{\partial^2\varepsilon_{\mathbf{k}}}{\partial k^2_{0,\alpha}}\right)_{k_0=0}\times|\phi_0|^2.\end{aligned} \tag{3.32}$$

This will be our starting point to analyze the anisotropic superfluids which will be discussed in the next section. Notice that in terms of the standard language of linear response theory, the first term represents the paramagnetic response of the quasi-particles and represents a current-current correlation function (or similarly a polarization bubble). The second term, on the other hand, is the diamagnetic part of the response which is absent in a translationally invariant model while playing an important role in lattice models. The third term is the zero-temperature superfluid depletion and conventionally part of the diamagnetic response term. Finally the last part is the collective response of the condensate to the phase twist. As expected the component of the dispersion is coupled to the Bose condensate in this term and the introduction of a generalized form of dispersion here might just change the effect of the Bose condensate term by a constant factor $\partial^2\varepsilon(\mathbf{k}=0)/\partial k^2$.

In the language of two fluid model, we can also identify the normal fluid and total fluid density from the above result as follows

$$\Upsilon_{\mathrm{tot},\alpha,\beta} = \Upsilon_{\mathrm{s},\alpha,\beta}+\Upsilon_{\mathrm{n},\alpha,\beta}, \tag{3.33}$$

while the condensate fraction/order parameter, ϕ_0 can also be written in terms of the total particle number density

$$|\phi|^2 = n_{\rm tot} - \int {\rm d}\varepsilon \frac{\partial E}{\partial \varepsilon} n_{\rm tot}(E). \tag{3.34}$$

Restricting ourselves to diagonal elements of the helicity modulus and substituting back for ϕ into Eq.(3.32) yields the normal and total helicity moduli as

$$\begin{aligned}
\Upsilon_{\rm tot} = \Upsilon_{s,\alpha}(T=0) = n_{\rm tot} \cdot \left(\frac{\partial^2 \varepsilon_{\mathbf{k}}}{\partial k_{\alpha,0}^2} \right)_{k_0=0} + \frac{1}{2} \int_{\mathbf{k}} \frac{\partial^2 \varepsilon_{\mathbf{k}}}{\partial k_{\alpha,0}^2} \left(\frac{\partial E_{\mathbf{k}}}{\partial \varepsilon_{\mathbf{k}}} - 1 \right) \\
\Upsilon_{n,\alpha} = \int \left(\frac{\partial \varepsilon_{\mathbf{k}}}{\partial k_\alpha} \right)^2 \cdot \frac{{\rm d}n_{\rm B}(E_{\mathbf{k}})}{{\rm d}E_{\mathbf{k}}} + \int_{\mathbf{k}} \left(\frac{\partial \varepsilon_{\mathbf{k}}}{\partial k_\alpha} - \frac{\partial \varepsilon_{\mathbf{k}=\mathbf{0}}}{\partial k_\alpha} \right) n_{\rm B}(E_{\mathbf{k}}) \cdot \frac{\partial E_{\mathbf{k}}}{\partial \varepsilon_{\mathbf{k}}}.
\end{aligned} \tag{3.35}$$

Thus we obtain the familiar relationship between the superfluid and normal components,

$$\frac{\Upsilon_{\alpha,s}(T)}{\Upsilon_{\alpha,{\rm tot}}} = 1 - \frac{\Upsilon_{\alpha,n}(T)}{\Upsilon_{\alpha,{\rm tot}}}. \tag{3.36}$$

$\Upsilon_{\rm tot}$ has the zero-temperature depletion effect in it, which is typically of $\sim \mathcal{O}(\lambda^{3/2})$. Before doing that there are some points to be considered regarding the form of the superfluid density /helicity modulus tensor. The helicity modulus tensor should be diagonal as can be seen from the following argument. In general this is not the case but in most of the physical problems such as anisotropic bosonic models in a continuum or a tight-binding lattice, the kinetic energy for different degrees of freedom can be divided into independent pieces and there is no coupling. i.e.,

$$\varepsilon_{\mathbf{k}} = \sum_i \varepsilon_{\mathbf{k}}^{(i)} \tag{3.37}$$

where the $\varepsilon_{\mathbf{k}}^{(i)}$ is the dispersion for the i-th degree of freedom. As an example consider the $\varepsilon_{\mathbf{k}} = \varepsilon(x,y) = \varepsilon_1(x) + \varepsilon_2(y)$ where x and y are two momenta. The formula for helicity modulus would look like,

$$\begin{aligned}
\Upsilon_x &= \int \mathrm{d}x\mathrm{d}y \left[-\frac{dn_{\mathrm{B}}(\varepsilon)}{d\varepsilon} \cdot \left(\frac{\partial \varepsilon(x,y)}{\partial x} \right)^2 + \frac{\partial^2 \varepsilon(x,y)}{\partial x^2} \cdot n_{\mathrm{B}}(\varepsilon(x,y)) + \left(\frac{\partial^2 \varepsilon(x,y)}{\partial x_0^2} \right)_{x_0=0} |\phi|2 \right] \\
&= \int \mathrm{d}x\mathrm{d}y \left[\frac{dn_{\mathrm{B}}(\varepsilon(x,y))}{dx} \cdot \left(\frac{\partial \varepsilon}{\partial x} \right)^{-1} + \frac{dn_{\mathrm{B}}(\varepsilon(x,y))}{dy} \cdot \left(\frac{\partial \varepsilon}{\partial y} \right)^{-1} \right] \left(\frac{\partial \varepsilon}{\partial x} \right)^2 \\
&\quad + \frac{\partial^2 \varepsilon(x,y)}{\partial x^2} \cdot n_{\mathrm{B}}(\varepsilon(x,y)) + \left(\frac{\partial^2 \varepsilon(x,y)}{\partial x_0^2} \right)_{x_0=0} |\phi|^2 \\
&= -\int \mathrm{d}x\mathrm{d}y \frac{dn_{\mathrm{B}}(\varepsilon(x,y))}{dx} \cdot \left(\frac{d\varepsilon_1(x)}{dx} \right) + n_{\mathrm{B}}(\varepsilon(x,y)) \cdot \frac{d^2 \varepsilon_1(x)}{dx^2} + \left(\frac{\partial^2 \varepsilon(x,y)}{\partial x_0^2} \right)_{x_0=0} |\phi|^2 \\
&= \left(\frac{\partial^2 \varepsilon(x,y)}{\partial x_0^2} \right)_{x_0=0} |\phi|^2,
\end{aligned} \tag{3.38}$$

where we arrived at the last line through an integration by parts. As one expects, the superfluid density is proportional to the condensate fraction in a non-interacting bosonic model. The anisotropy will only appear in the second derivative term calculated at the zero momentum twist.

The helicity modulus in the simple model we are considering, $\varepsilon_{\mathbf{k}} = \sum_i \varepsilon_{\mathbf{k}}^{(i)}$, is trivially diagonal. The second derivative of the dispersion will vanish if the two components are not equal

$$\frac{\partial^2 \varepsilon(x,y)}{\partial x \partial y} = \frac{\partial}{\partial x} \left(\frac{\partial \varepsilon_2(y)}{\partial y} \right) = 0. \tag{3.39}$$

Actually, in the absence of interaction, the above observations can be stated in a generalized form almost independent of the form of the dispersion. I can state them in the form of a theorem.

Theorem I: In the absence of topological defects, the helicity modulus of a free system of bosons in d-dimensions is always diagonal and the diagonal elements are proportional to the condensate fraction, i.e.,

$$\Upsilon_{\mu\nu}(T) = \left(\frac{\partial^2 \varepsilon_k}{\partial k_\mu k_\nu} \right)_{k=0} \times n_0(T). \tag{3.40}$$

Without loss of generality, we limit ourselves to the case of two momenta (calling them x and y as before) and notice that,

$$\begin{aligned}
\frac{\partial n_{\mathrm{B}}(\varepsilon(x,y))}{\partial x} &= \frac{\mathrm{d}n_{\mathrm{B}}(\varepsilon)}{\mathrm{d}\varepsilon} \cdot \frac{\partial \varepsilon(x,y)}{\partial x} \\
\frac{\partial n_{\mathrm{B}}(\varepsilon(x,y))}{\partial y} &= \frac{\mathrm{d}n_{\mathrm{B}}(\varepsilon)}{\mathrm{d}\varepsilon} \cdot \frac{\partial \varepsilon(x,y)}{\partial y}.
\end{aligned} \tag{3.41}$$

Substituting the above in the formula for the $\Upsilon_{\mu\nu}$ - as we did for additive dispersion ($\varepsilon(x,y) = \varepsilon_1(x) + \varepsilon_2(y)$, after partial integration one finds

$$\Upsilon_x = \int \mathrm{d}y \left[n_{\mathrm{B}}(\varepsilon) \frac{\partial \varepsilon(x,y)}{\partial x} \right]_{\mathrm{boundary}, x=\pm\infty} + \left(\frac{\partial^2 \varepsilon(x,y)}{\partial x^2} \right)_{x,y=0} \cdot |\phi_0|^2. \tag{3.42}$$

The boundary term is basically the total momentum on the boundary and vanishes in the thermodynamic limit. In the presence of topological defects, however, the boundary term does not vanish as is the case for the vortices in a two or three dimensional superfluid.

The corresponding version of the above theorem for fermionic systems can be found in Ref.[57]. The statement is that there has to be a gap in the dispersion of the quasi-particles to have a non-zero superfluid density/helicity modulus. The derivation is pretty much identical to the bosonic version considering there is no BEC condensate contribution in the fermionic models.

Theorem II: For an anisotropic dilute Bose gas, the helicity modulus, $\Upsilon_{\mu\nu}$, vanishes at the same value of critical temperature, T_c as the isotropic case.

$Proof$: Near T_c the BEC fraction, $\phi_0^2 \to 0$. The Bogoliubov spectrum, $\sqrt{\varepsilon_k(\varepsilon_k + \lambda\phi_0^2}$ approaches the free dispersion, ε_k. i.e.,

$$\Upsilon_{\mu\nu}(T \to T_c) = \Upsilon^{(0)}(T \to T_c) = \delta_{\mu\nu} n_0(T \to T_c) \to 0. \tag{3.43}$$

where $T_c = T_{\mathrm{BEC}}$ under the Bogoliubov approximation. Eq.(3.38) similarly can be derived for a weakly interacting fermionic systems using linear response theory techniques. The main source of difference os however the contribution of the condensate ϕ_0^2 everywhere in Eq.(3.38), which is missing from fermionic counter-part [57][58][59].

3.4 Regimes of an Isotropic Superfluid; Cross Over Scaling for the Helicity Modulus

Before we get into the problem of the layered anisotropic superfluid, let us discuss cross over regimes of an isotropic d-dimensional superfluid particularly in two and three dimensions. One can do that by investigating temperature dependence of superfluid density/helicity modulus in different limits. In the following, we will closely follow the discussion in Ref.[91] on the crossover scaling of the superfluid density.

For a non-interacting system of bosons superfluid density scales as

$$\frac{\Delta\rho_s(T)}{\rho_0} = 1 - \left(\frac{T}{T_c}\right)^{d/2}. \tag{3.44}$$

There are three characteristic energy scales in the problem: $\lambda\phi_0^2$, ε_k $(k \sim n_{\rm tot}^{1/d})$ and, T. They can be expressed in terms of corresponding length scales, where the $\lambda_{\rm T} = h/\sqrt{2\pi mT}$ is the thermal wavelength while $a = \sqrt{\hbar^2/m\lambda}$ is the scattering length. We have mentioned the $\hbar$ and $k_{\rm B}$ in the formulas for the sake of familiarity while we consistently assume both to be equal to unity. In terms of these and length scales the superfluid density can be written as a function of dimensionless variables

$$\frac{\Delta\rho_s}{\rho_0} = \tilde{F}\left(\frac{\lambda_{\rm T}}{a}, \frac{T}{T_c}\right) \tag{3.45}$$

where $\tilde{F}(0, \frac{T}{T_c}) = 1 - \left(\frac{T}{T_c}\right)^{d/2}$ describes an ideal Bose gas. Near T_c one can assume a scaling hypothesis for the superfluid density

$$\rho_s(T) = \rho_s^{\rm ideal}(T) \cdot \tilde{Y}\left(\frac{a/\lambda_{T_c}}{t^\phi}\right), \tag{3.46}$$

with $\tilde{t} = 1 - T/T_c$ and asymptotic behaviour as $T \to T_c, y \to \infty, Y(y) \sim y^\zeta$ and also $Y(0) = 1$, which corresponds to $a/\lambda_T \to 0$ as $\tilde{t} \to 0$.

At low temperatures the linear character of Bogoliubov spectrum will dominate when $T \ll T_1 = \lambda\phi_0^2$. This corresponds to the famous $\frac{\Delta\rho_s}{\rho_0} \sim T^{d+1}$ behaviour (Landau's T^4-law in three-dimension), i.e.,

$$\frac{\Delta\rho_s(T)}{\rho_0} = \tilde{F}\left(\frac{\lambda_T}{a}, \frac{T}{T_c} \to 0\right) \sim T^{d+1}. \tag{3.47}$$

Assuming a similar cross over scaling form for superfluid density as $t \to 0$ and defining $t \equiv \frac{T}{T_c}$,

$$\rho_s(T) = \rho^{\rm ideal}(T) \cdot \tilde{Y}_0\left(\frac{a/\lambda_{T_c}}{t^{\phi'}}\right) \tag{3.48}$$

It is natural to assume that the correct low-T scaling should be given by the ratio of T and $T_1 = \lambda\phi_0^2$ thus leading to the fact that the exponent $\phi' = 1$. The width of the quantum critical region near $T = 0$ is given by [91],

$$t \le t_1 = \left(\frac{T_c}{T_1}\right)^{(d-2)/2} \tag{3.49}$$

We have summarized the crossover scaling properties of the superfluid density in a wide range of temperature in the Fig.(3.1).

Now we have all the tools to investigate the particular case of weakly interacting layered bosons, which is suggested to be relevant for the underdoped cuprates . This is the subject of the next Chapter.

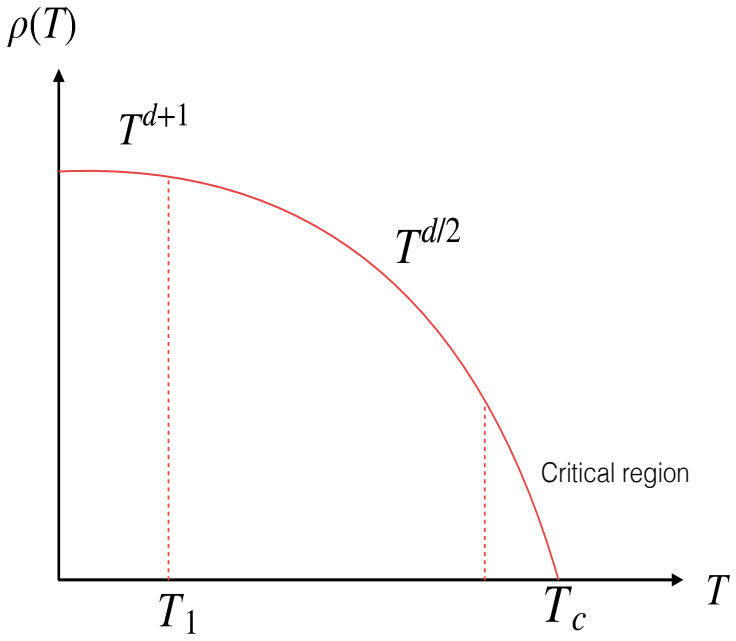

Figure 3.1: The three major crossover temperatures for an isotropic and weakly interacting superfluid.

Chapter 4

C-axis Superfluid Density In Layered Bosonic Models

4.1 Introduction

The original inspiration for writing this section comes from an idea that detailed analysis of the response functions such as superfluid density along different axes can help us to fix the unknown parameters that appear in the field theory constructed for the underdoped cuprates Eqs.(1.65) and (1.68). The focus on the bosonic superfluid density comes from the argument by I.F. Herbut [38] that in the underdoped regime the superfluid density calculated from the bosonic degrees of freedom in the system Eq.(1.68), is dominant in comparison to the fermionic part and also gives the right doping dependence compared with experiments. Ref.[38] has proposed a layered model of bosons with the possibility of inter-layer hopping added to the original field theory. In the BEC limit the ab-plane superfluid density is calculated and shown to fit the observed experimental results. We aimed to generalize the above approach to c-axis superfluid density observations to try to fix unknown parameters appearing in the action, Eq.(1.68). However, as it turns out the bosonic superfluid density cannot give a good match for the c-axis superfluid response in HTS. One can argue that fermionic degrees of freedom and their impurity scattering in inter-layer hopping play a dominant role [59][60].

Hence we will not emphasize the modelling of the HTS superfluid response using our layered model much and rather try to analyze it as an abstract model. We work out all crossover scaling

behaviours for both the ab-plane and c-axis superfluid densities and show that there is a quasi two-dimensional regime that appears in the low-T range where $\rho_s \sim T^{2+\epsilon}$, above the quantum critical point in the vicinity of which $\rho_s \sim T^{d+1}$.

4.2 Layered Quasi Two-Dimensional Superfluids

In high-temperature superconductor materials lattice symmetry and electronic structure basically describes a tight-binding dispersion for electrons. Phenomenologically, we will be adopting a similar dispersion relation for our bosons which are basically the dual-quantum vortex fields in the theory of a phase fluctuating d-wave superconductor. The tight-binding dispersion for bosons will be anisotropic:

$$\varepsilon_{\mathbf{k}} = t_a \sin^2(k_x a) + t_b \sin^2(k_y b) + t_c \sin^2(k_z c), \tag{4.1}$$

where $t_{a,b,c}$ are the values of the hopping amplitude along the a- b- or c-axes. In YBCO and most of the HTS materials the values of a and b lattice spacings are close to each other while the c-axis has a ratio of 10 relative to them.The hopping amplitudes are significantly different. with $t_{ab}/t_c \sim 1000$. This will allow us to assume a somewhat simpler model for the layered bosonic model. We assume

$$\varepsilon_{\mathbf{k}} = \frac{k_x^2 + k_y^2}{2m} + t \sin^2(k_z c) \tag{4.2}$$

with m being the mass of the bosons and t the hopping amplitude for intra-layer jumps. We have noted the axes defining the plane as a and b-axis and the axis perpendicular to them as c-axis and the a, b, and c denote the corresponding lattice spacings.

The condensate fraction can simply be calculated as,

$$n_0(T) = n_0(0) + \int \frac{\mathrm{d}k_z}{2\pi} \int \frac{k \mathrm{d}k}{2\pi} \left(\exp\left[\frac{k^2}{2mT} + \frac{t}{T} \sin^2(k_z c)) - 1 \right] \right)^{-1}. \tag{4.3}$$

The integral can be exactly calculated upon expanding the Bose-function in terms of a geometrical series and the result is

$$\frac{mT}{(2\pi)^2} \sum_{n=1}^{\infty} \int_0^1 \frac{\mathrm{d}\alpha}{\sqrt{1-\alpha^2}} \int_0^{\infty} \mathrm{d}y \cdot \lambda^n e^{-n\{y + \frac{t}{T}\alpha^2\}}, \tag{4.4}$$

where $y \equiv k^2/2$ and $\alpha \equiv \sin(k_z c/2)$, and the λ is the fugacity $\lambda = \exp(\beta\mu)$. Performing the integrals over y and α is straight forward,

$$n(T) = n_0 - \frac{mT}{\pi}\sum_n \frac{\lambda^n}{n} I_0\left(\frac{-nt}{T}\right) e^{\frac{nt}{T}}. \tag{4.5}$$

with $I_0(x)$ being the Bessel function. In the limit of small hopping, $t/T \ll 1$,

$$I_0(tn/T) \simeq 1 + \frac{1}{4}\left(\frac{tn}{T}\right)^2 + \mathcal{O}\left(\frac{tn}{T}\right)^3, \tag{4.6}$$

$$\begin{aligned} \Delta n(T) &= -\frac{mT}{\pi}\ln\left[1-\lambda e^{-\frac{t}{T}}\right] \\ &\simeq \frac{mT}{\pi}\ln\left(\frac{T}{t}\right), \quad \text{for} \lambda = 1. \end{aligned} \tag{4.7}$$

The next order term can also be calculated

$$\begin{aligned} & \frac{mT}{\pi}\sum_n \frac{e^{-nt/T}}{n} \times \left(\frac{nt}{2T}\right)^2 \\ = \quad & \frac{1}{1-e^{-t/T}} \times \frac{mt^2}{4\pi T^2} \simeq \frac{mt}{4\pi T}, \end{aligned} \tag{4.8}$$

which might be of significance in the low temperature limit. If one does the summation before expanding the integral Bessel function there would be an additional contribution, that is linear in temperature,

$$\begin{aligned} \Delta n &= \int_0^1 -\frac{mT}{\pi}\cdot\ln(1-e^{-\frac{t\alpha^2}{T}})\frac{\mathrm{d}\alpha}{\sqrt{1-\alpha^2}} \\ &= \frac{m}{\pi}\cdot T\left(\ln\left(\frac{T}{t}\right) + \pi\ln 2\right). \end{aligned} \tag{4.9}$$

For the sake of completeness I conclude the non-interacting limit calculations by including next-nearest-neighbuor hopping (nnn). The assumed nnn-model is

$$\varepsilon_k = \frac{1}{2m}(k_x^2 + k_y^2) + t\sin^2(k_z/2) + t'\{\sin^2(k_z/2)(k_x^2+k_y^2)\}. \tag{4.10}$$

The condensate fraction can be conveniently calculated,

$$\begin{aligned}
\Delta n(T) &= \int \frac{\mathrm{d}k_z}{(2\pi)} \frac{k\mathrm{d}k}{(2\pi)^2} \left[\exp\left\{ k^2 \left(\frac{1}{2mT} + \frac{t'}{T}\sin^2(k_z/2) \right) + \frac{t}{T}\sin^2(k_z/2) \right\} - 1 \right]^{-1} \\
&= \int \frac{\mathrm{d}k_z}{(2\pi)} \left(\ln\left(\frac{T}{t}\right) + \ln(\sin^2(k_z/2)) \right) \cdot \left(\frac{1}{2mT} + \frac{t'}{T}\sin^2(k_z/2) \right)^{-1} \\
&= \frac{mT}{\pi} \int \mathrm{d}z \frac{1}{1 + 2mt'\sin^2(k_z/2)} \ln\left(\frac{T}{t}\right) \\
&+ \frac{1}{1 + 2mt'\sin^2(k_z/2)} \ln(\sin^2(k_z/2)), \qquad (4.11)
\end{aligned}$$

which leads to

$$\Delta n(T) = \frac{mT}{\pi} \left[\frac{\ln\left(\frac{T}{t}\right)}{\sqrt{1+2mt'}} + \text{constant} \right]. \qquad (4.12)$$

Thus, the modifications for $t'm \ll 1$ are minor.

4.2.1 Regimes of an Anisotropic Superfluid; Crossover Scaling for the Helicity Modulus

In the layered model, the existence of a new energy scale, t (hopping amplitude), changes the low-temperature scaling properties of the superfluid density. The effective dimensionality of the system will vary with temperature. Near $T = 0$ we have 3D behaviour $\Delta\rho_s \sim T^4$ while as T increases it changes into $\Delta\rho_s \sim T^3$ which represents a quasi-two dimensional system.

Similar to the analysis of the isotropic case we write the form of ρ_s as

$$\frac{\Delta\rho_s(T)}{\rho_0} = \tilde{F}\left(\frac{\lambda_T}{a}, \frac{T}{T_c}, \frac{t}{T} \right) \qquad (4.13)$$

while for $\lambda = 0$, $\tilde{F}\left(0, \frac{T}{T_c}, \frac{t}{T}\right)$ will represent the $2+\epsilon$ dimensional Bose-Einstein condensate result,

$$\tilde{F}\left(0, \frac{T}{T_c}, \frac{t}{T}\right) = \left(\frac{T}{T_c}\right)^{\frac{2+\epsilon}{2}} = \frac{T\ln T}{T_c \ln T_c}. \qquad (4.14)$$

Which we have assumed $\ln T \sim T^{\epsilon}$. This will determine the value of ϵ which depends on t/T,

$$\frac{2}{\ln(T_c/t)} = \epsilon. \qquad (4.15)$$

At low-T's but above T_1 ($T > T_1$), we can see from Bogoliubov spectrum that the quasi-particles will be easily excited along the ab-plane but not along c-axis. We ignore the terms $k_x^2/2mT$ and

$k_y^2/2mT$ but retain $t\sin^2(k_z/2)/T$. Inserting this into the quasi-particle dispersion leads to the energy scale $T_1' \equiv \sqrt{t\lambda\phi_0^2}$. An alternative way to derive the crossover temperature T_1' is to assume a scaling ansatz for the superfluid density of the following form

$$\rho_s(T) = \rho^{\rm ideal}(T) \cdot Y_0 \left(\frac{\frac{\lambda_T}{a} \cdot \frac{t}{T}}{T/T_c} \right), \tag{4.16}$$

in analogy with the isotropic model. Eq.(4.16) indicates that ρ_s is a homogeneous function of the dimensionless parameters $\frac{\lambda_T}{a}, \frac{t}{T}, \frac{T}{T_c}$. The scaling behaviour of Y_0, however, is not complete. There might not be an asymptotic form for $Y(y) \to y^\zeta$ as $y \to \infty$. But it will roughly behave as a $2+\epsilon$-dimensional superfluid at low-T, i.e.

$$\begin{aligned} \frac{\Delta\rho_s}{\rho_0} &\sim \tilde{F}\left(\left(\frac{\sqrt{t\lambda\phi_0^2}}{T} \right)^2 \cdot \frac{T_c}{T} \right) \\ &\sim T^{3+\epsilon}. \end{aligned} \tag{4.17}$$

Eq.(4.17) defines T_1' as the upper limit temperature for the interacting quasi-two dimensional regime in our layered model. The regimes of the highly anisotropic layered bosonic model are defined based on the crossover temperatures $T_1, T_1', T_c - \Delta_c T$ and T_c.

4.2.2 Regime I: Interacting 3D Limit ($T < T_1'$)

To calculate the superfluid density/helicity modulus in this regime we will begin with calculating the zero temperature depletion of the condensate fraction. However, since the result are temperature independent they will be used in the rest of the regime I and II calculation of both ab-plane and c-axis superfluid densities.

Consider the the paramagnetic part of the superfluid response along ab-plane given by equation:

$$\rho_{ab}^{\rm n}(T) = -\frac{1}{2}\int \frac{2\pi k {\rm d}k}{(2\pi)^2} \frac{{\rm d}k_z}{2\pi} \frac{{\rm d}n_{\rm B}(E)}{{\rm d}E} \cdot \left(\frac{\mathbf{k}}{m} \right)^2, \tag{4.18}$$

we define new variables x, y and the speed of sound $u = \sqrt{2\lambda\phi_0^2}$,

$$\begin{aligned} y &\equiv \frac{u}{T}\sqrt{\frac{k^2}{2m} + t\sin^2(k_z/2)} \\ x &\equiv \frac{u\sqrt{t}}{T}\sin(k_z/2). \end{aligned} \tag{4.19}$$

The integral can be re-written as

$$\rho^{\rm n}_{ab}(T) = \int_0^\infty \left(\frac{T}{u\sqrt{t}}\right) \cdot \frac{{\rm d}x}{\sqrt{1-\left(\frac{T}{u\sqrt{t}}\right)^2 x^2}} \int_{y=x}^\infty \left(\frac{T}{u}\right)^3 \frac{{\rm d}n_{\rm B}(y)}{{\rm d}y} y^3 {\rm d}y$$
$$-t\int_0^\infty \left(\frac{T}{u\sqrt{t}}\right)^3 \cdot \frac{x^2{\rm d}x}{\sqrt{1-\left(\frac{T}{u\sqrt{t}}\right)^2 x^2}} \int_{y=x}^\infty \left(\frac{T}{u}\right) \frac{{\rm d}n_{\rm B}(y)}{{\rm d}y} y{\rm d}y. \qquad (4.20)$$

To leading order in temperature, T, we take $1/\sqrt{1-(Tx/u\sqrt{t})^2} \sim 1$ to obtain

$$\begin{aligned}\int {\rm d}x \int_{y=x} {\rm d}y n_{\rm B}(y) y^2 &= \int {\rm d}x \int {\rm d}y \sum_{n=1}^\infty e^{-ny} y^2 \\ &= \sum_n \int {\rm d}x \left(\frac{2}{n^3} - \frac{2}{n^2}\frac{\partial}{\partial n} + \frac{1}{n}\frac{\partial^2}{\partial n^2}\right) e^{-nx} \\ &= \sum_n \frac{6}{n^4} = 6\zeta(4), \end{aligned} \qquad (4.21)$$

where ζ is the Reiman zeta-function. Similarly, the other term can be calculated as

$$\int {\rm d}x \cdot x^2 \int_{y=x} {\rm d}y n_{\rm B}(y) = 2\zeta(4), \qquad (4.22)$$

and overall,

$$\rho^n_{ab}(T) = \frac{2}{m\sqrt{t}} \cdot \frac{1}{(2\pi)^2} \cdot \frac{T^4}{u^5} \cdot 8\zeta(4). \qquad (4.23)$$

Now, let us get to the c-axis normal component. The paramagnetic response term looks like,

$$\rho^n_{c,{\rm para}}(T) = -\int_{\alpha\sqrt{t}} \frac{{\rm d}n_{\rm B}(y)}{{\rm d}y} y{\rm d}y \cdot 4\alpha^2\sqrt{1-\alpha^2} \cdot 2{\rm d}\alpha \times \left[\left(\frac{t}{2}\right)^2 \frac{2}{(2\pi)^2}\frac{1}{u}\right], \qquad (4.24)$$

Again, $u\sqrt{t}\alpha/T \to x$ and $uy/T \to y$,

$$
\begin{aligned}
-\left[\left(\frac{t}{2}\right)^2 \frac{2}{(2\pi)^2}\frac{1}{u}\right] \quad \times \quad & \left(\frac{T}{u}\right)\int_{y=x} \frac{\mathrm{d}n_{\mathrm{B}}(y)}{\mathrm{d}y} y\mathrm{d}y \left(\frac{T}{u\sqrt{t}}\right)^3 \cdot 2\sqrt{1-\left(\frac{T}{u\sqrt{t}}\right)^2 x^2}\mathrm{d}x \\
= \quad & \sum_n \int_0 x^3 e^{-nx}\mathrm{d}x + \sum_n \left(\int_{y=x} e^{-nx}\mathrm{d}y\right) x^2 \mathrm{d}x \\
= \quad & \frac{\sqrt{t}}{(2\pi)^2 u^3}\cdot 6\zeta(4). \qquad (4.25)
\end{aligned}
$$

This time we have to add the diamagnetic contribution which appears when there is a lattice structure rather than a continuum.

$$
\begin{aligned}
\rho^n_{c,dia}(T) \quad = \quad & \int \frac{t}{2}\left(1-\cos(k_z)\right) n_{\mathrm{B}}(E)\cdot \frac{\varepsilon+\lambda\phi^2}{E}\cdot \frac{k\mathrm{d}k\mathrm{d}k_z}{(2\pi)^2}\frac{T}{u\sqrt{t}} \\
= \quad & \sum_n \int_{x,y} \frac{t}{2}\left(\frac{T}{u\sqrt{t}}\right)^2 2x^2 \times e^{-ny} \times \left(\frac{\left(\frac{T}{u}\right)^2 y^2 + \frac{u^2}{2}}{Ty}\right)\left(\frac{T}{u}\right)^2 y\mathrm{d}y\left(\frac{T}{u\sqrt{t}}\right)\frac{2\mathrm{d}x}{\sqrt{1-\frac{T^2x^2}{u\sqrt{t}}}} \\
= \quad & \frac{\sqrt{t}}{(2\pi)^2 u^3}\cdot 2\zeta(4)\cdot T^4 \qquad (4.26)
\end{aligned}
$$

To compare the two results, we need to calculate the depletion of the condensate fraction and the superfluid densities at zero-temperature, Δn_0, $\Delta\rho^{\mathrm{dep}}_{ab}$ and, $\Delta\rho^{\mathrm{dep}}_{c}$.

$$
\begin{aligned}
\Delta n_0 \quad = \quad & \frac{1}{2}\int_k \left(\frac{\varepsilon_k+\lambda\phi^2}{\sqrt{\varepsilon_k(\varepsilon_k+\lambda\phi^2)}}-1\right) \\
= \quad & \frac{4\sqrt{2}}{3\pi}\sqrt{\frac{m}{t^2}}\cdot\lambda^{3/2}\phi, \qquad (4.27)
\end{aligned}
$$

while $\Delta\rho^{\mathrm{dep}}_{ab} = \frac{1}{m}\Delta n_0$. A similar calculation shows that the c-axis depletion is also proportional to the condensate fraction by a factor of anisotropy.

$$
\begin{aligned}
\Delta\rho^{\mathrm{dep}}_{c} \quad = \quad & \frac{1}{2}\int_k \frac{t}{2}\cos(k_z)\left(\frac{\varepsilon_k+\lambda\phi^2}{\sqrt{\varepsilon_k(\varepsilon_k+\lambda\phi^2)}}-1\right) \\
\Delta\rho^{\mathrm{dep}}_{c} \quad = \quad & \Delta\rho^{\mathrm{dep}}_{ab}\times\left(\frac{tm}{2}\right)+\mathcal{O}\left(\frac{\lambda\phi^2}{t}\right). \qquad (4.28)
\end{aligned}
$$

Thus the relative values for the ρ_{ab} and ρ_c have the same temperature dependence,

$$\frac{\rho^s_{ab}(T)}{\rho^s_{ab}(0)} = 1 - \frac{\rho^n_{ab}(T)}{\rho^n_{ab}(0)} = 1 - \frac{1}{\rho_0}\frac{T^4}{m\sqrt{t}\pi^2 u^5}\cdot 8\zeta(4),$$
$$\frac{\rho^s_{c}(T)}{\rho^s_{c}(0)} = 1 - \frac{\rho^n_{c}(T)}{\rho^n_{c}(0)} = 1 - \frac{1}{\rho_0}\frac{T^4}{m\sqrt{t}\pi^2 u^5}\cdot 8\zeta(4). \tag{4.29}$$

The two results are proportional and the depletion of the condensate should be included in the c-axis ρ_0.

This is the famous Landau T^4-rule for the interacting region. In this regime the effective dimensionality of the system is three as the temperature is lower than any scale of the system, including the hopping amplitude. As discussed in the previous sections, as temperature increases one expects to see the the quasi-two dimensional nature of the system introduce a T^{d+1}-behaviour for the normal component of the superfluid density - in the ab-plane at least - with $d = 2 + \epsilon$. A similar result can be expected for the c-axis superfluid density with a different effective dimensionality, i.e., $d = 1+\epsilon$.

4.2.3 Regime II: Interacting (2+ϵ)D Limit ($T_1' < T < T_1$)

As one increases the temperature to the range $T_1' \ll T \ll T_1$, i.e. $\lambda\phi^2 \ll T \ll \sqrt{t\lambda\phi^2}$, the layered nature of the system displays itself. To see the behaviour of the superfluid density and/or the helicity modulus we begin with calculating the depletion of the superfluid density in this regime,

$$\Delta\rho^{\rm dep}_{ab} = \frac{1}{m}\int_k (y^2 - t\alpha^2)\frac{{\rm d}n_{\rm B}}{u{\rm d}y}\times\frac{y{\rm d}y}{(2\pi)^2}\cdot\frac{4{\rm d}\alpha}{\sqrt{1-\alpha^2}}. \tag{4.30}$$

The re-scaling of the variables is different now:

$$\begin{aligned} \frac{uy}{T} &\to y, \\ \alpha &\to \alpha, \\ c_1 = \frac{4}{m}\cdot\frac{1}{(2\pi)^2}&. \end{aligned} \tag{4.31}$$

Similarly to previous section, there are two different powers of y that appear in the integral:

$$\begin{aligned} -\frac{T^3}{u^4}\int y^3\frac{{\rm d}n_{\rm B}}{{\rm d}y}{\rm d}y\frac{{\rm d}\alpha}{\sqrt{1-\alpha^2}} &= 3c_1\frac{T^3}{u^4}\left(\zeta(3)\pi + \frac{\pi}{8}\left(\frac{T_1'}{T}\right)^2 + \frac{1}{9}\left(\frac{T_1'}{T}\right)^3\right) \\ &\approx \frac{3\pi\zeta(3)c_1}{u^4}\cdot T^3 + \mathcal{O}\left(\left(\frac{T_1'}{T}\right)^2\right). \end{aligned} \tag{4.32}$$

The second term in Eq.(4.30) gives a different behaviour,

$$\begin{aligned} - \quad & c_1 \cdot \frac{T}{u^2} \int t\alpha^2 \int_a^\infty n_{\rm B}(y){\rm d}y \cdot \frac{{\rm d}\alpha}{\sqrt{1-\alpha^2}} \\ = \quad & -\frac{\pi}{4} c_1 \cdot \frac{T}{u^2} \left[\ln\left(\frac{T}{T_1'}\right) + 0.151697 + \frac{1}{3}\left(\frac{T_1'}{T}\right) + \mathcal{O}\left(\left(\frac{T'}{T}\right)^2\right)\right]. \end{aligned} \tag{4.33}$$

Including the boundary terms which have a linear behaviour in T, the final result for the ab-plane superfluid density in this limit is,

$$\begin{aligned} \Delta\rho_{ab} = \frac{3\pi\zeta(3)c_1}{u^4}\cdot T^3 - \frac{\pi}{4}c_1 \cdot \frac{T\cdot t}{u^2}\left[\ln\left(\frac{T}{T_1'}\right) + 0.1516 + \frac{1}{3} + \mathcal{O}\left(\left(\frac{T_1'}{T}\right)^2\right)\right] + \\ + \frac{\pi}{4}c_1 t \cdot \frac{T}{u^2}\left[\frac{\pi}{4} - \frac{1}{3}\left(\frac{T_1'}{T}\right) + \mathcal{O}\left(\frac{T_1'}{T}\right)\right]. \end{aligned} \tag{4.34}$$

The c-axis superfluid response comes from a similar calculation. This time both paramagnetic and diamagnetic response terms contribute:

$$\begin{aligned} \Delta\rho_c(T) &= \Delta\rho_c^{\rm p}(T) + \Delta\rho_c^{\rm d}(T), \\ \Delta\rho_c^{\rm p}(T) &= -\tilde{c}_1 \int t^2\alpha^2\sqrt{1-\alpha^2}{\rm d}\alpha \cdot \frac{{\rm d}n_{\rm B}}{u{\rm d}y}\cdot y{\rm d}y \\ &= \tilde{c}_1 t^2 \frac{T}{u^2}\left[-\frac{3}{64} - \frac{\pi}{16}\ln(2) + \frac{\pi}{16}\ln\left(\frac{T_1'}{T}\right)\right], \\ \Delta\rho_c^{\rm d}(T) &= \tilde{c}_1 \int t(1-2\alpha^2) n_{\rm B}(y) y \cdot {\rm d}y \cdot \frac{{\rm d}\alpha}{\sqrt{1-\alpha^2}} \\ = \tilde{c}_1 \left(\frac{T}{u}\right)^2 \cdot \frac{\pi^2}{6}. \end{aligned} \tag{4.35}$$

where $\tilde{c}_1 = 1/4\pi^2$, Overall,

$$\Delta\rho_c(T) = \frac{\pi^2}{6}\tilde{c}_1\left(\frac{T}{u}\right)^2 + \tilde{c}_1 t^2 \cdot \frac{T}{u^2}\left(\frac{\pi}{64} + \frac{\pi}{16}\ln\left(\frac{T}{T_1'}\right)\right). \tag{4.36}$$

Thus the behaviours of the both ab-plane and c-axis superfluid densities will have the forms:

$$\begin{aligned} \Delta\rho_{ab}(T) = \quad & aT^3 + bT\cdot(\ln T + c) \\ \Delta\rho_c(T) = \quad & a'T^2 + b'T\cdot(\ln T + c'). \end{aligned} \tag{4.37}$$

4.2.4 Regime III: Ideal Bose Gas Limit; Anisotropic Bose-Einstein Condensate ($T_1 < T < T_c - \Delta_c T$)

In this limit, that for small hopping covers most of the regime of temperature, the interactions can be ignored. The condensate fraction has been derived in detail in the beginning of the chapter and both ab-plane and c-axis superfluid density are proportional to the condensate fraction:

$$\begin{aligned} \frac{\rho_{ab,s}(T)}{\rho_0} &= 1 - \frac{T \ln T}{T_c \ln T_c}, \\ \frac{\rho_{c,s}(T)}{\rho_0} &= mt \left(1 - \frac{T \ln T}{T_c \ln T_c} \right), \end{aligned} \tag{4.38}$$

where the mt indicates the anisotropy along the c-axis. As mentioned before, the relative helicity modulus along the c-axis, $\Upsilon^c(T)/\Upsilon^c_0$ and in the ab-plane, $\Upsilon^{ab}(T)/\Upsilon^{ab}_0$, are identical. Thus the behaviour of both of the values of the superfluid densities versus temperature is almost linear, $T \ln T$, in the absence of interactions. The effect of interactions can be seen as the curvature of both the ab-plane and c-axis responses. Before we consider more detail of the curvature of the superfluid density graphs we will discuss the relationship of the layered bosonic model we have been analyzing to the underdoped phase-fluctuating high temperature superconductor in the next section.

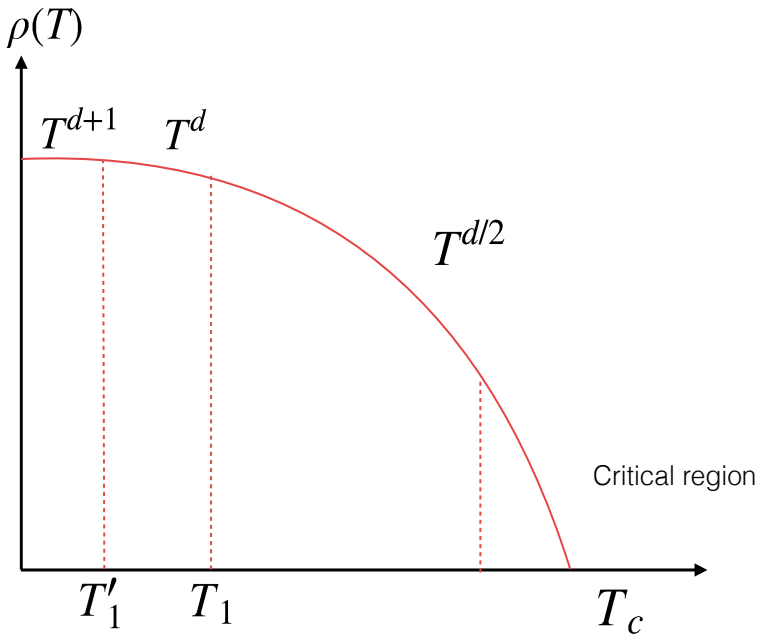

Figure 4.1: The three major crossover temperatures for an anisotropic superfluid. $\rho(T)$ stands for either of the ab-plane or c-axis responses (see text).

4.3 Ioffe-Larkin Rule and the Connection to the Underdoped HTS

In this Section we will discuss the superfluid density response in the high temperature superconductors in the underdoped pseudogap regime the framework of the phase fluctuating d-wave superconductor developed in Chapter1. In principle the depletion of the superfluid density is due to several contributions. The relevant mechanisms in the low energy limit are the order parameter phase fluctuations and depletion of the nodal Dirac quasi-particles, superfluid density. In the following I will construct the superfluid response due to each one of the above mentioned factors and their contribution to the total ab-plane superfluid density. The total superfluid density will have the form:

$$\frac{1}{\rho^{s,ab}(T)} = \frac{1}{\rho_{\rm B}^{s,ab}(T)} + \frac{1}{\rho_{\rm F}^{s,ab}(T)}, \tag{4.39}$$

where $\rho_{\rm B}$ indicates order parameter superfluid response, $\rho_{\rm F}$ is the quasi-particle superfluid density and ρ_s is total superfluid density. This relationship is known as Ioffe-Larkin rule. the generalization

of Ioffe-Larkin rule to the c-axis superfluid densities is not obvious however. Derivation of such a relationship, if any, is left as a future direction of work.

There is a simple logic for the Ioffe-Larkin rule which we will argue below. It basically represents the fact that the external gauge-field does not couple to the bosonic/vortex section of the theory and only appears in the fermionic part. Assuming $e_{\rm F}$ and $e_{\rm B}$ as the gradient of the gauge fields that is coupled to either bosonic or fermionic degrees of freedom (in the model constructed in Chapter 1, both of $e_{\rm F} = e_{\rm B} = \nabla\vec{v}$). Assuming a linear response for small applied electromagnetic field the fermionic and bosonic currents read off as,

$$j_{\rm F} = \sigma_{\rm F} e_{\rm F}, \qquad j_{\rm B} = \sigma_{\rm B} e_{\rm B}, \tag{4.40}$$

where the σ's are the superfluid/Drude responses respectively. *assume* that on the fermionic and bosonic sections of the action, they change upon applying an external electric-field E. The gauge field itself is the same for fermionic and bosonic sectors the external electromagnetic field is only coupled to the fermionic sector:

$$\begin{aligned} e_{\rm F} &\rightarrow e + E, \\ e_{\rm B} &\rightarrow e. \end{aligned} \tag{4.41}$$

The fermionic and bosonic current responses $j_{\rm F}$ and $j_{\rm B}$ are induced respectively, Assuming $j_{\rm F} + j_{\rm B} = 0$ [1] leads to,

$$e = -\frac{\sigma_{\rm F}}{\sigma_{\rm F} + \sigma_{\rm B}} E. \tag{4.42}$$

The physical current $j = j_{\rm F} = -j_{\rm B}$ is given by

$$j = \frac{\sigma_{\rm F}\sigma_{\rm B}}{\sigma_{\rm B} + \sigma_{\rm F}} E. \tag{4.43}$$

The σ's, as is known from the linear response theory, are merely polarization functions or current-current correlation functions $\Pi^{\rm B,F}_{\mu\nu}$ of the either bosonic or fermionic degrees of freedom. In a linear response approximation with only transverse external field applied $\Pi_{\mu\nu} \sim \Upsilon_{\mu\nu} \sim \rho_\mu$. The calculation of the current-current correlation function will be done later. But the above argument and Eq.(4.43) which is essentially the Ioffe-Larkin formula is enough for our current discussion.

[1] In t-J model this corresponds to the fact that bosons represent holes and thus their currents should be opposite of the the fermions

A more formal way of deriving the physical electromagnetic response is as follows. If the external gauge field A_μ in the effective theory appears in the form,

$$S_{\rm eff}(v_\mu, A_\mu) = \Pi(q)^{\rm F}_{\mu\nu}(v_\mu(q) + A_\mu)(v_\nu(-q) + A_\nu(-q)) + \Pi^{\rm B}_{\mu\nu}(q)v_\mu(q)v_\nu(-q), \tag{4.44}$$

then after integrating over the gauge field v_μ, we end up with

$$S_{\rm eff} = \Pi_{\mu\nu}A_\mu(q)A_\nu(-q) \tag{4.45}$$

with the physical superfluid response function,

$$\Pi^{-1} = \left(\Pi^{\rm F}(q)\right)^{-1} + \left(\Pi^{\rm B}(q)\right)^{-1}. \tag{4.46}$$

This can be in fact be derived from the effective field theory of the underdoped regime for HTS constructed in Chapter 1. The Lagrangian for dual theory of the Eqs.(1.72) and (1.73) [38], has the form of,

$$\begin{aligned}\mathcal{L}_\Phi &= \frac{K_\mu}{2}(v_\mu + A_\mu)^2 + h\sum_{n=1,2} b^*(\tau,\mathbf{x})\left[\partial_\tau - iv_0(-)^n a_\tau\right] b_n(\tau,\mathbf{x}) + \frac{1}{2}\sum_n \left([\partial_\mu - i(v_\mu(-)^n a_\mu)]\right)^2 \\ &+ \left(\alpha - \frac{h}{2}\right)^2 \sum_n |b_n(\tau,\mathbf{x})|^2 + \frac{\beta_1}{2}\left(\sum_n |b_n(\tau,\mathbf{x})|^2\right)^2 + \frac{\beta_2}{2}\left(\sum_n |b_n(\tau,\mathbf{x})|^4\right),\end{aligned} \tag{4.47}$$

where h is the chemical potential for the dual theory, K_μ is the stiffness along the μ-direction, A_μ is the external gauge field and $\vec{a}$ and $\vec{v}$ are the singular gauge fields. α and $\beta_{1,2}$ are parameters to be determined from experiment. Integrating out the bosonic fields $b_{1,2}(\tau,\mathbf{x})$ and assuming $\alpha > 0, \beta_{1,2} > 0$, and minimizing the action one finds $|\langle b_1\rangle|^2 = |\langle b_2\rangle||^2 = (h^2 - h_c^2)/2(2\beta_1 + \beta_2)$. To quadratic order $\mathcal{L}_\Phi$ reduces as,

$$\mathcal{L}_{\rm ch} = iJ_\mu \cdot (v_\mu + A)_\mu + \frac{K_\mu}{2}(v_\mu + A_\mu)^2 + \frac{\rho_{\rm b}(T)}{2}(v_\mu^2 + a_\mu^2) - ihn_{\rm b}v_0, \tag{4.48}$$

where J_μ is the physical current defined in the Chapter 1 and $\mu = 0, 1, 2$. $\rho_{\rm b}$ indicates the superfluid density of the bosons and the $n_{\rm b}$ is the total density if the bosons. Setting $A_0 = 0$ and integrating over v_0 yields:

$$\frac{(J_0 - hn_{\rm b})^2}{2(2K_0 + \rho_{\rm b})} + i\vec{J}\cdot(\vec{v} + \vec{A}) + \frac{K}{2}(\vec{v} + \vec{A})^2 + \frac{\rho_{\rm b}(T)}{2}\vec{v}^2. \tag{4.49}$$

This form of the effective action exactly satisfies the condition for the Ioffe-Larkin rule, Eq.(4.44). The first term with J_0^2 is a short-range repulsion between fermions and irrelevant at low energies. The renormalized chemical potential is, $\mu(T) = -h\rho_{\rm b}(T)/(K_0 + \rho_{\rm b})$ with charge renormalization factor as $z = \rho_b/(\rho_b + K_0)$.

Since doping, $x \sim \mu(0)$, it follows that $x \sim \rho_{\rm b}(0)$. Integrating out the fermions we get:

$$\mathcal{L} \sim \frac{K(T)}{2}(\vec{v} + \vec{A})^2 + \frac{\rho_{\rm b}(T)}{2}\vec{v}^2, \tag{4.50}$$

where $K_\mu(T) \sim \Pi^{\rm F}_\mu(q \to 0)$ and $\rho_{\rm b} \sim \Pi^{\rm B}_\mu(q \to 0)$. Finally, integrating out the gauge field v leads to the Ioffe-Larkin rule as expected, Eq.(4.39), where K represents the fermionic superfluid density.

The fermionic current-current correlation function can straight forwardly calculated using the Dirac dispersion for the fermions,

$$\begin{aligned}
\Pi^{\rm F}_{\mu\nu}(q) &= -\frac{1}{\rm vol}\int_0^{1/T} {\rm d}\tau \langle J_\mu(q,\tau) J_\nu(-q,0)\rangle \\
&= \frac{1}{\rm vol}\sum_k \left(\frac{\partial \varepsilon_k}{\partial k}\right)^2 \frac{{\rm d}n_{\rm F}(E)}{{\rm d}E} \\
&= \frac{v_{\rm F}}{v_\Delta} 2\ln 2 \cdot \frac{T}{\pi}.
\end{aligned} \tag{4.51}$$

We expect that the bosonic superfluid density to behave as the 3D XY model and the condensate originates from a Kosterlitz-Thouless type of transition which lead to a T^3 temperature dependence. Writing down the Ioffe-Larkin rule and keeping the leading order terms in temperature,

$$\begin{aligned}
\rho_{\rm s,tot} &= \frac{\rho_s^{\rm B}\cdot\rho_s^{\rm F}}{\rho_s^{\rm B}+\rho_s^{\rm F}} \\
&= \frac{(\rho_s^{\rm B}(0)+\Delta\rho_s^{\rm B})(\rho_s^{\rm F}(0)+\Delta\rho_s^{\rm F})}{\rho_s^{\rm B}(0)+\rho_s^{\rm F}(0)} \\
&\sim z\frac{v_{\rm F}}{v_\Delta}\cdot\frac{2\ln 2}{\pi}\cdot T.
\end{aligned} \tag{4.52}$$

However, since the charge renormalization factor is proportional to the doping, x, we conclude that the slope of the superfluid density vs. T graph be x-dependent. As a matter of fact it is easy to show the slope is proportional to x^2. This contradicts recent measurements of the superfluid density of the highly underdoped cuprates that reported ta constant slope and doping independent [61][62]. This is our inspiration to consider a quasi- three dimensional bosonic theory for which

the contribution for the superfluid density comes from Bose-Einstein condensation rather than a Kosterlitz-Thouless mechanism in the 3D XY model which we had before. As has been discussed previously in this chapter the bosonic superfluid density decreases linearly with temperature and cannot be ignored at low temperatures. More importantly the slope of the bosonic superfluid density is doping independent [38]. The results from Ref.[61] are depicted in Fig.(4.2) which clearly shows the constant slope of the superfluid density for different dopings (i.e. different T_c).

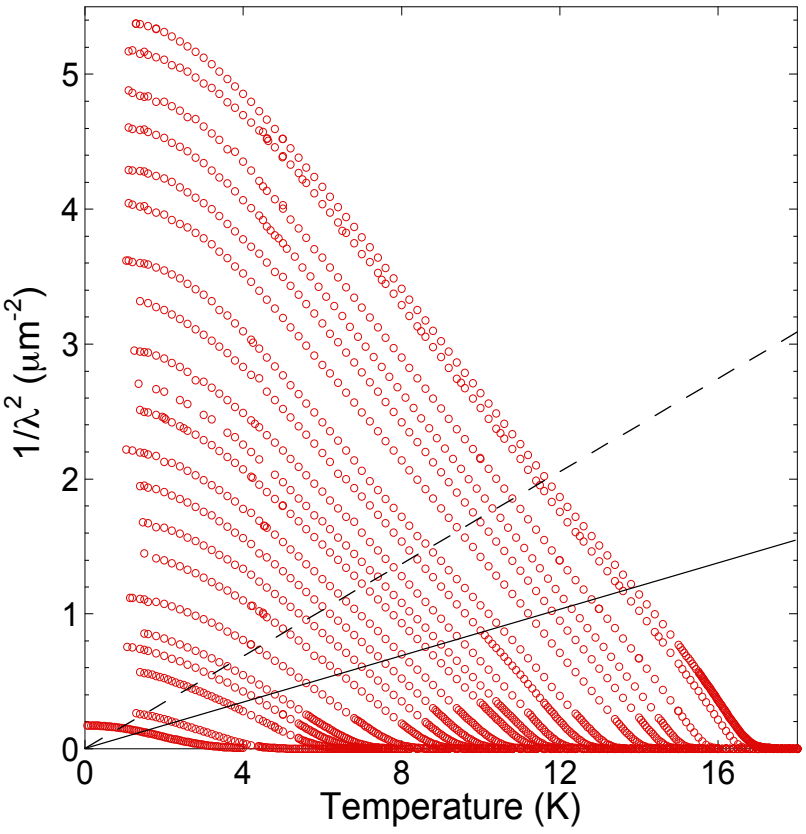

Figure 4.2: The plot of in-plane superfluid density of YBCO versus temperature for different values of of doping $4K^\circ < T_c < 16K^\circ$ [61].

Although the layered bosonic model can explain the experimental observation of the doping-independent slope of the in-plane superfluid density the relevance of the layered model to HTS is

limited to the in-plane superfluid density. It is easy to observe that the argument for the Ioffe-Larkin rule does not hold for the c-axis superfluid density. Experimental observations suggest that unlike the ab-plane superfluid density the c -axis decreases with an almost power-law $\sim T^{2.5}$[63][64][60]. In the next section we show some numerical results for the layered bosonic model while the hopping strength and interaction couplings varies and we also try to fit the results with the HTS superfluid density observations.

4.4 Numerical Results

The integrals in the Landau formula for both ab-plane and c-axis superfluid densities can be calculated numerically. We can change some of the values including hopping amplitude, t, interaction strength, λ, while keeping some others like the inter-layer spacing constant.

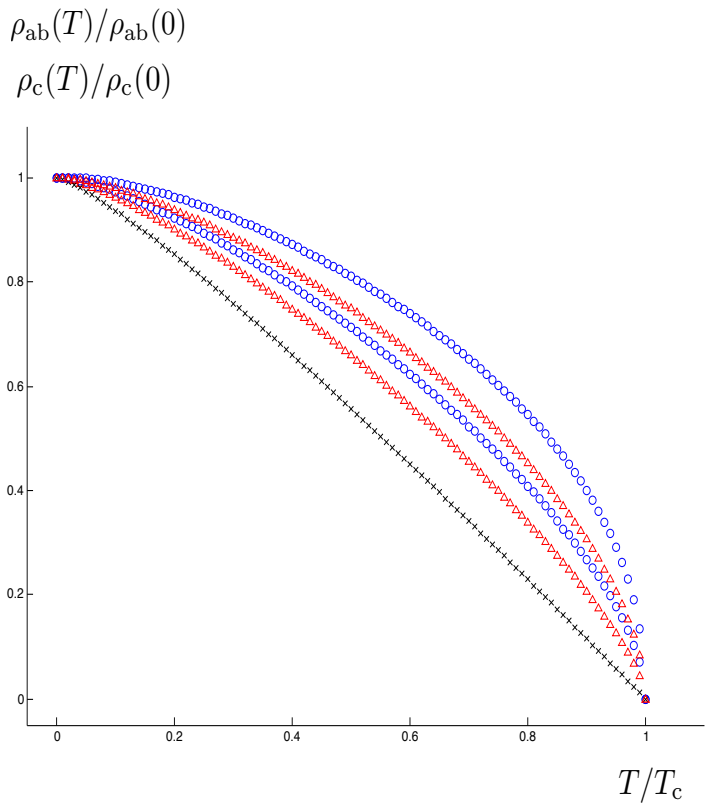

Figure 4.3: in-plane (triangle) and c-axis (circles) superfluid densities plotted as a function of temperature for different values of interaction coupling $\lambda = 0.0, 0.05, 0.02$ for highly underdoped case $T_c = 10$K. The c-axis hopping is assumed 1/10 of the ab-plane (2m): $t = 0.1$.

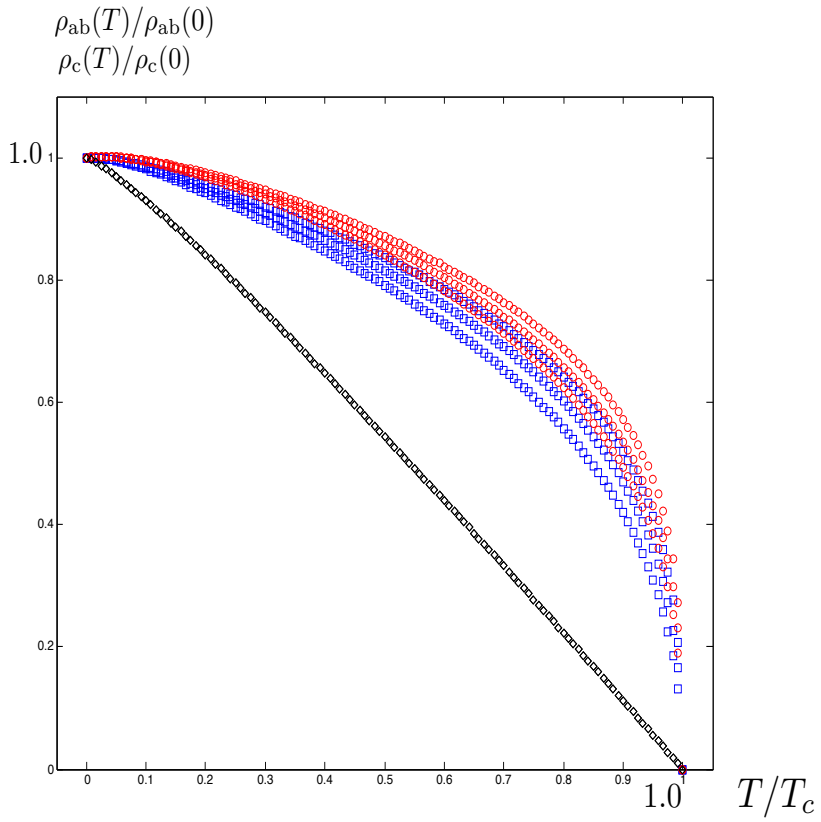

Figure 4.4: in-plane (square) and c-axis (circles) superfluid densities plotted as a function of temperature for different values of hopping amplitude $t = 0.1, 0.05, 0.02$, the diamonds represent the BEC result for a comparison. Value of the interaction coupling is kept at $\lambda = 0.1$. As can be seen the change in the hopping does not dramatically change the temperature dependence of both ab-plane or c-axis superfluid densities.

Fig(4.4) shows that both of the superfluid densities are not very sensitive to the change in the anisotropy. This is understandable based from the discussion we had on the values of c-axis and ab-plane superfluid densities in the BEC limit, i.e., $\rho_{ab}^{(0)}(T)/\rho_{ab}^{(0)}(0) = \rho_c^{(0)}(T)/\rho_c^{(0)}(0)$. By changing interaction between the bosons, Fig.(4.3), both of the superfluid density graphs get slight curvature which is related to the value of the interaction (weak).

In Fig.(4.5), the reader can notice that for a range of weak-interaction couplings one can find a

fit for ab-plane superfluid response of higher T_c samples while the constant-slope BEC result can well explain the very underdoped regime. However, the same is not true for the c-axis result and one cannot find any fit between the experimental observation and the layered bosonic results.

The result above can be compared with the experimental results from microwave cavity measurements of the London penetration depth. In the Fig.(4.5), the ab-plane superfluid density of the bosonic model can fit well for highly underdoped cases with BEC results and as the doping increases, tuning the interaction can give a fit for higher doping up to $T_{\rm c} = 55{\rm K}$ with $t = 0.1$ and $\lambda = .002$ in our bosonic model. The corresponding c-axis response, however, does not match with the same parameters. In the Fig.(4.6), we have reported the case of $\lambda = 0.02, t = 0.1$ as the upper limit of interaction strength value - derived from ab-plane fitting - in comparison with the experimental results. As can be seen there is a mismatch and this leads us to conclude that unlike the in-plane superfluid response, the out-of- plane response must to be a combination of both quasi-particle and bosonic degrees of freedom. Since we do not have a firm Ioffe-Larkin rule for c-axis superfluid densities we do not speculate on this matter much more and leave this as a future direction of research.

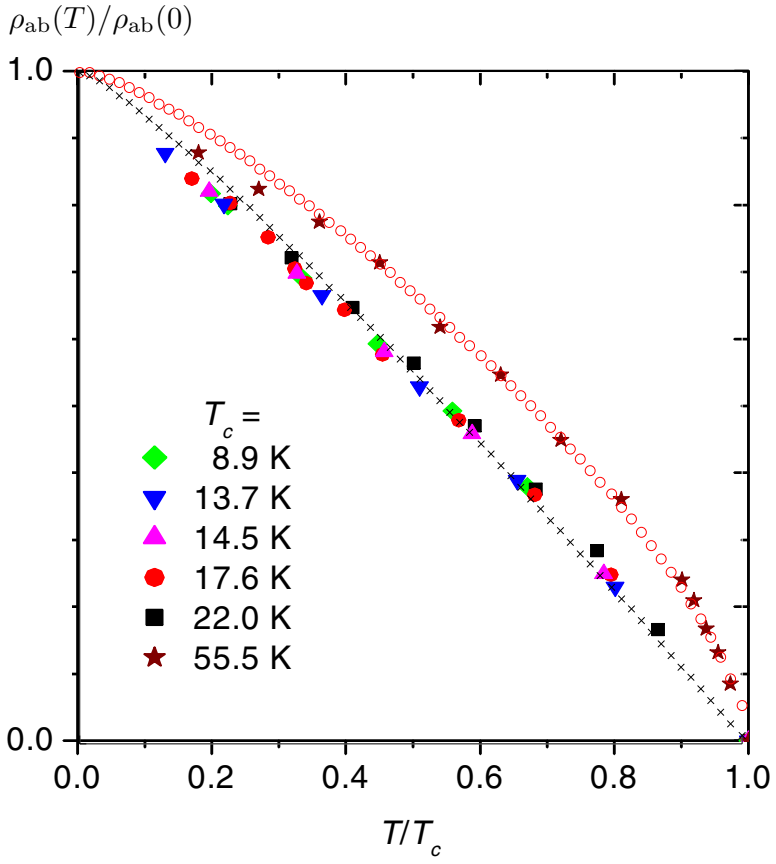

Figure 4.5: ab-plane superfluid density for YBCO [62] (scattered points) and the bosonic superfluid response fit.The best fit for the low-T_c graphs is the linear BEC graph. The circles correspond to $\lambda = 0.02, t = 0.1$, shows an approximate match for $T_c = 55.5K°$.

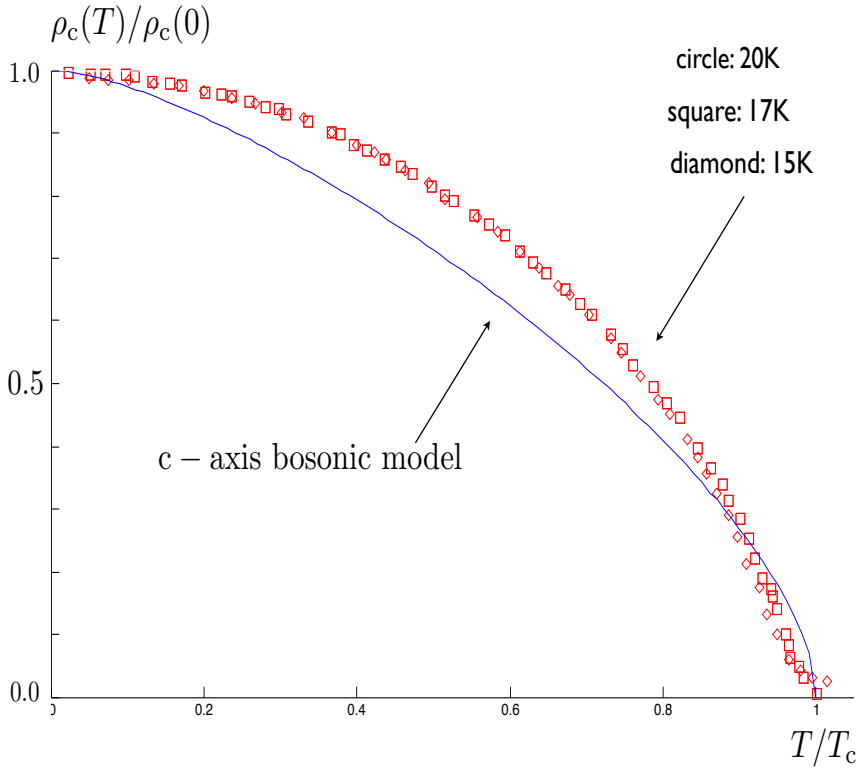

Figure 4.6: The c-axis superfluid response plotted from experiment [61] for three different doping values $T_c = 20K, 17K, 15K$. The solid curve is the c-axis response from the bosonic model with $\lambda = 0.02, t = 0.1$ and $T_c = 20K$.

We also tried a match for higher T_c values for both ab-plane and c-axis superfluid densities which is depicted in the Figs.(4.7) and (4.8). The normalized values of superfluid densities now match with $\lambda = 0.02$ partially as before. The $\lambda = .02$ c-axis superfluid response however does not give a good match, while there is not a proper scaling of the normalized values of c-axis superfluid densities for different doping values.

We do not consider the c-axis graphs a match as the corresponding ab-plane graphs does not fit the experimental observation.

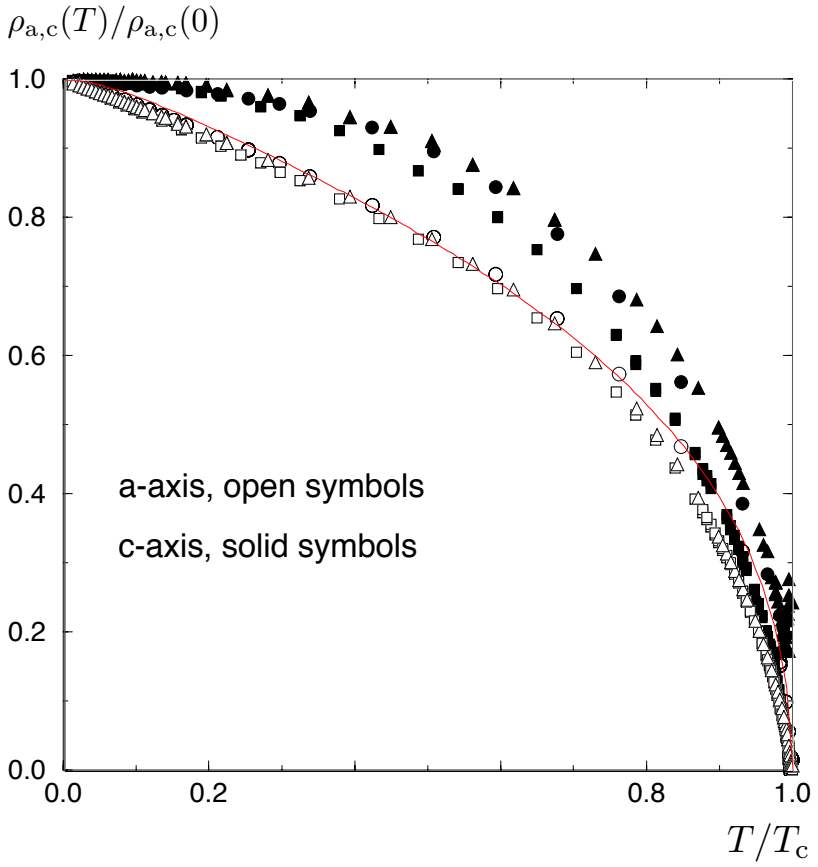

Figure 4.7: Experimental values for both a-axis, i.e., ab-plane (open symbols) and c-axis (solid symbols) for higher doping values [65] and the fit for $\lambda = 0.02, t = 0.1$ and $T_c = 60\mathrm{K}^\circ$.

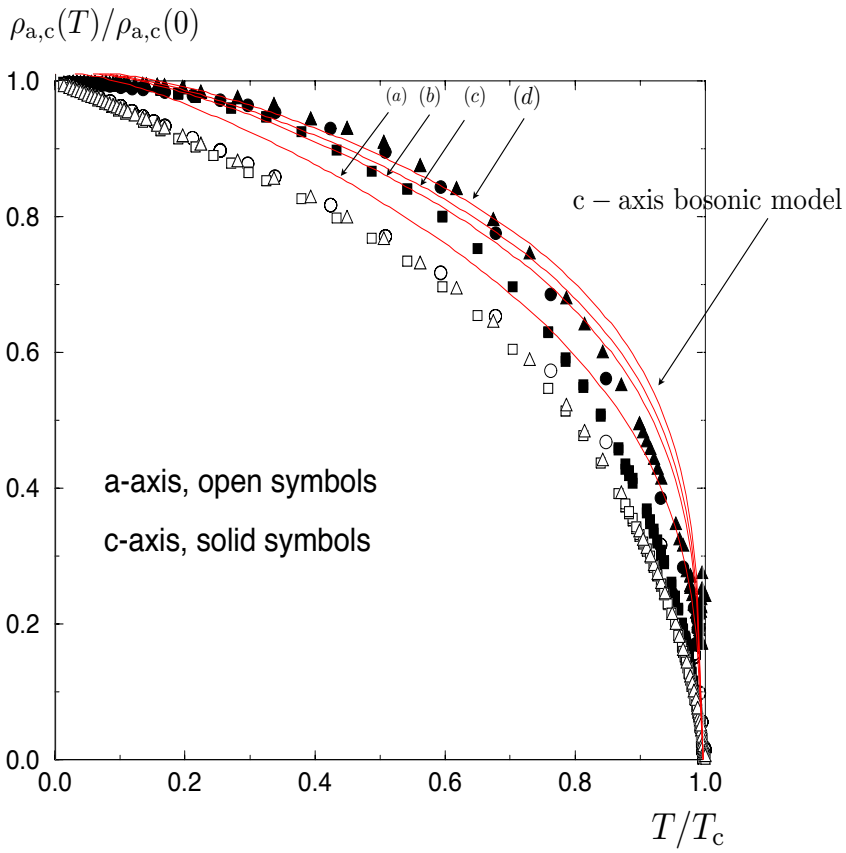

Figure 4.8: Experimental values for both ab-plane and c-axis from [65] and theoretical prediction from bosonic model (solid lines) for c-axis. different graphs correspond to different interaction strengths λ and same hopping amplitude and $T_c : t = 0.1, T_c = 60\mathrm{K}^\circ$. (a) $\lambda = 0.02$. (b)$\lambda = 0.05$ (c) $\lambda = 0.1$. (d) $\lambda = 0.12$.

Chapter 5

Birefringent Break Up of Dirac Fermions in a Square Optical Lattice

This Chapter contains work previously published with M. Kennett et. al [66]. and is somewhat out of line with the previous discussions, not having direct bearing on the subject of superconductivity. However, it discusses a very unique construction of chiral symmetry breaking for Dirac fermions on optical lattices by introducing anisotropy in the kinetic energy. The Sections 5.1 and 5.2 which introduces the theory includes the previous works of M. Kennett and N. Komeilizadeh. The author acknowledges M. Kennett for letting the author to present some of their work here. My contribution lie mainly in Sec. 5.3.

5.1 Introduction

The discovery of graphene [67] and topological insulators [68] has led to much recent interest in systems whose low energy excitations can be described with Dirac fermions. In parallel there has been exploration of the possibility of generating artificial magnetic fields for cold atoms confined in an optical lattice. Neutral bosonic cold atoms cannot couple to a magnetic field directly, so there have been numerous proposals [69, 70] of approaches to couple atoms to an artificial gauge field, several of which have been implemented experimentally [71].

Quantum particles in a uniform magnetic field on a lattice have the well-known Hofstadter spectrum [72]. We study a Hamiltonian with a tunable Hofstadter-like spectrum that arises from the

combination of hopping and an artificial magnetic field with a non-zero mean that are both periodically modulated in the x *and* the y directions. The presence of spatial periodicity in the *amplitude* as well as the phase of the hopping is the key difference between the model we consider here and previous work on the spectrum of particles in the presence of magnetic fields that are periodic in both the x and y directions [73]. This difference facilitates the unusual Dirac-like spectrum that we discuss here.

Our main result is that in the lattice model we introduce [Eq. (5.3)], when there is an average of half a flux quantum per plaquette, and at half-filling, the low energy degrees of freedom can be described by a Dirac Hamiltonian with the unusual property that chiral symmetry is broken in the kinetic energy rather than via mass terms. This has the consequence that the doubly degenerate Dirac cone for massless fermions splits into two cones with tunable distinct slopes, analagous to a situation in which there are two speeds of light for fermionic excitations, similar to birefringence of light in crystals such as calcite. We discuss the meaning of broken chiral symmetry in our effective model and explore the effects of various perturbations, such as staggered potentials, domain walls, and interactions between fermions.

The Chapter is structured as follows: in Sec. 5.2 we discuss a possible scheme to realize the Hamiltonian Eq. (5.3), illustrate its Hofstadter-like spectrum and demonstrate that there are Dirac points in the spectrum when there is an average of half a flux quantum per plaquette. In Sec. 5.3 we discuss the low energy theory in the vicinity of the Dirac points, and give brief conclusions and discussion in Sec. 5.4.

5.2 Effective Hamiltonian

We use a generalization of the approach introduced by Sørensen *et al.* [70] to obtain an artificial magnetic field. However, our results regarding the spectrum of the model are independent of any particular experimental scheme used to realize the model. The scheme in Ref. [70] was presented for bosons but applies equally well to a starting point of spinless fermions (corresponding to only one available hyperfine state for cold atoms) with Hamiltonian

$$H = -\mathcal{J} \sum_{\langle i,j \rangle} (\hat{c}_i^\dagger \hat{c}_j + \hat{c}_j^\dagger \hat{c}_i), \tag{5.1}$$

where $\hat{c}_i^\dagger$ and $\hat{c}_i$ are fermionic creation and annihilation operators respectively at site i and the notation $\langle i, j \rangle$ indicates that we restrict the sum in the hopping term to nearest neighbours only. There

can be no Hubbard-like interaction for spinless fermions, and since nearest neighbour interactions in an optical lattice system are weak, we initially ignore interactions.

In Ref. [70], two steps are required to generate an artificial magnetic field. First, a time-varying quadrupolar potential $V(t) = V_{qp}\sin(\omega t)\hat{x}\hat{y}$ is applied to the system, and second, the hopping is modulated as a function of time. During the course of one oscillation of the quadrupolar potential, hopping in the x direction is turned on for a very short period of time $\tau \ll t_0 = \frac{2\pi}{\omega}$ at times $t = nt_0$, where n is an integer, and hopping in the y direction is turned on for time τ around $t = \left(n + \frac{1}{2}\right) t_0$. Due to the periodic oscillation in the Hamiltonian, the time evolution operator after m periods may be written as $U(t = mt_0) = U(t = t_0)^m$.

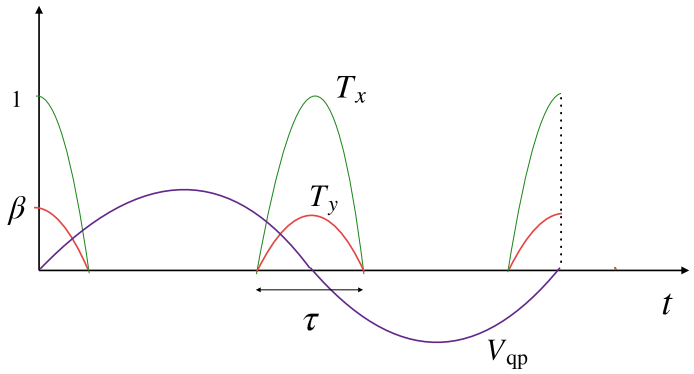

Figure 5.1: Time dependence of the hopping and the quadrupolar potential during the course of one period of the quadrupolar potential.

Our modification to the proposal in Ref. [70] is that when hopping is turned on in the x-direction at time $t = nt_0$, hopping is also turned on in the y-direction with an amplitude $0 \leq \beta \leq 1$ relative to the hopping in the x-direction. At time $t = \left(n + \frac{1}{2}\right) t_0$, hopping is turned on in the y direction, and hopping in the x-direction is turned on with amplitude β relative to the hopping in the x-direction as illustrated in Fig. 5.1.

The operator for hopping in the x direction is $\hat{T}_x = -\mathcal{J}\sum_{x,y}\left(\hat{c}^\dagger_{x+1,y}\hat{c}_{x,y} + \text{h.c.}\right)$ with a similar expression for $\hat{T}_y$. We may write the time evolution operator as

$$\begin{aligned} U\left(t = mt_0\right) \quad = \quad & \Big[e^{-\frac{i\tau}{2\hbar}\left(\beta\hat{T}_x + \hat{T}_y\right)} e^{2\pi i\alpha\hat{x}\hat{y}} e^{-\frac{i\tau}{\hbar}\left(\hat{T}_x + \beta\hat{T}_y\right)} \\ & \times e^{-2\pi i\alpha\hat{x}\hat{y}} e^{-\frac{i\tau}{2\hbar}\left(\beta\hat{T}_x + \hat{T}_y\right)}\Big]^m, \end{aligned} \tag{5.2}$$

where $\alpha = V_{qp}/\pi\hbar\omega$ and we have set the lattice constant to unity. To lowest order in $\mathcal{J}\tau/\hbar$ we can

write this in the form

$$\begin{aligned} U &= e^{-\frac{iH_{\rm eff}t}{\hbar}}, \\ H_{\rm eff} &= -J_0 \sum_{x,y} \Big\{ \Big[\left(1+\beta e^{2\pi i\alpha x}\right) \hat{c}^\dagger_{x,y+1} \hat{c}_{x,y} + \text{h.c.} \Big] \\ &\quad + \Big[\left(\beta + e^{2\pi i\alpha y}\right) \hat{c}^\dagger_{x+1,y} \hat{c}_{x,y} + \text{h.c.} \Big] \Big\}, \end{aligned} \tag{5.3}$$

with $J_0 = \tau\mathcal{J}/t_0$.

5.2.1 Hofstadter-like spectrum

A more conventional way to write this Hamiltonian is in the form

$$H_{\rm eff} = -\sum_{ij} \left[t_{ij} e^{\frac{ie}{\hbar}\int_j^i \mathbf{A}\cdot d\mathbf{l}} \hat{c}^\dagger_i \hat{c}_j + \text{h.c.} \right], \tag{5.4}$$

from which we may identify the amplitude of the hopping and the artificial magnetic field

$$t_{x+1,y} = J_0\sqrt{1+\beta^2+2\beta\cos(2\pi\alpha y)}, \tag{5.5}$$

$$t_{x,y+1} = J_0\sqrt{1+\beta^2+2\beta\cos(2\pi\alpha x)}, \tag{5.6}$$

and the artificial magnetic field

$$B_z = \frac{2\pi\alpha\hbar}{e}\left\{ \frac{\beta^2+\beta\cos(2\pi\alpha x)}{1+\beta^2+2\beta\cos(2\pi\alpha x)} - \frac{1+\beta\cos(2\pi\alpha y)}{1+\beta^2+2\beta\cos(2\pi\alpha y)} \right\}. \tag{5.7}$$

This field is the sum of a spatially uniform piece with magnitude $\frac{2\pi\hbar\alpha}{e}$ and a piece that is spatially periodic in both the x and y directions. If $\beta = 0$, the hopping amplitude is J_0 and the field is uniform with strength $\frac{2\pi\hbar\alpha}{e}$, corresponding to a flux of $\alpha\phi_0$ per plaquette (where ϕ_0 is the flux quantum) as found in Ref. [70] and there is a Hofstadter spectrum. If $\beta = 1$, then $B_z = 0$, but the hopping parameters are still spatially periodic. At β intermediate between 0 and 1, both the hopping and the magnetic field are spatially periodic in x and y. This illustrates the essential difference between the model we consider and previous work on quantum particles in a periodic magnetic field on a lattice – there is spatial periodicity of $1/\alpha$ in the amplitude of the hopping as well as in the magnetic field. For finite β the spectrum (illustrated for $\beta = 1$ in Fig. 5.2) as a function of α is reminiscent of the Hofstadter spectrum.

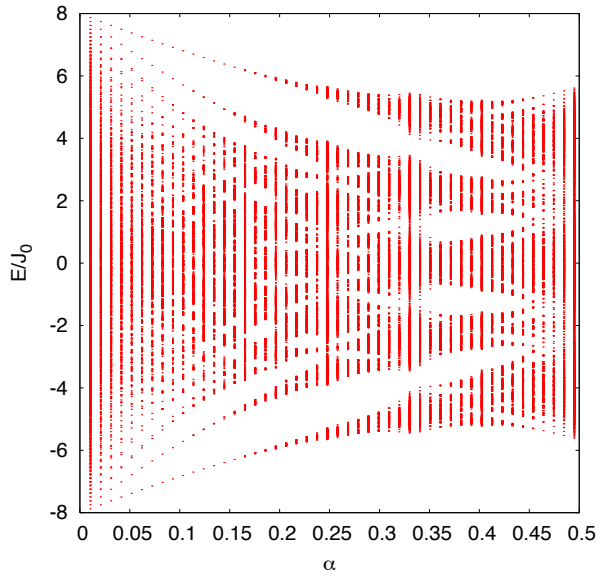

Figure 5.2: Spectrum as a function of α when $\beta = 1$: obtained by exact diagonalization on a 97×97 site lattice: there is no artificial magnetic field, yet due to the periodic hopping, the spectrum has some similarities with the Hofstadter spectrum [credit to Peter Smith].

5.2.2 Half a flux quantum per plaquette

When $\alpha = 1/2$ there is an average of half a flux quantum per plaquette and H_{eff} simplifies to a tight binding model with four sites in the unit cell as shown in Fig. 5.3 a).

Labelling the four sites in the unit cell as A, B, C, and D, and Fourier transforming in space, we may rewrite the effective Hamiltonian in the following form:

$$H = \sum_{\mathbf{k}} \psi_k^\dagger [E_k - \mathcal{H}_k] \psi_k, \tag{5.8}$$

with

$$\mathcal{H}_k = 2 \begin{pmatrix} 0 & J_+ \cos k_y & J_+ \cos k_x & 0 \\ J_+ \cos k_y & 0 & 0 & -J_- \cos k_x \\ J_+ \cos k_x & 0 & 0 & J_- \cos k_y \\ 0 & -J_- \cos k_x & J_- \cos k_y & 0 \end{pmatrix},$$

where $J_\pm = J_0(1 \pm \beta)$ and $\psi_k^T = (c_{Ak}, c_{Bk}, c_{Ck}, c_{Dk})$. We find that the dispersion is

$$E_k = \pm J_\pm \sqrt{\cos^2 k_x + \cos^2 k_y},$$

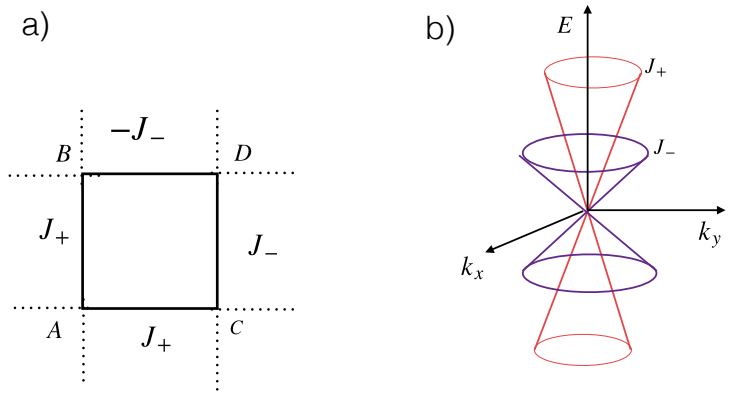

Figure 5.3: a) Unit cell of tight binding model with hopping parameters indicated. b) Dirac cones corresponding to J_+ and J_- bands.

and we note that when $\beta = 1$, $J_- = 0$, so there will be a flat band at $\epsilon = 0$ and a dispersing band associated with J_+. We can also see that in the vicinity of the points $\mathbf{K}_{\pm,\pm} = \left(\pm\frac{\pi}{2}, \pm\frac{\pi}{2}\right)$, the spectrum is linear

$$E_q = \pm J_\pm \sqrt{q_x^2 + q_y^2}, \tag{5.9}$$

where $\mathbf{q} = \mathbf{k} - \left(\pm\frac{\pi}{2}, \pm\frac{\pi}{2}\right)$, and there are cones with two different slopes, corresponding to $J_\pm$ respectively as illustrated in Fig. 5.3 b). When $\beta = 0$, the two slopes are identical, whereas as $\beta \to 1$, the J_- band becomes flat, and the J_+ band remains conical. Several authors recently considered lattice models closely related to the $\beta = 1$ limit of our model, in which there are three bands, one flat, and one Dirac like [74]. The $\beta = 1/2$ spectrum matches that of Weyl fermions considered in Refs. [75, 76]. When $\beta \neq 1$, the underlying Dirac structure of the problem is exposed, which allows us to use a symmetry approach to understand this unusual dispersion.

5.3 Low Energy Theory

We expand around the Dirac points and represent the low energy theory (with $\mathbf{k}$ measured with respect to $\mathbf{K}$) as

$$H_k = 2J_0 \left[\left(\gamma^0\gamma^1 + i\beta\gamma^3\right) k_x + \left(\gamma^0\gamma^2 + i\beta\gamma^5\right) k_y \right], \tag{5.10}$$

where we use a non-standard representation of the gamma matrices in which $\gamma^0 = \sigma_3 \otimes \sigma_3$, $\gamma^1 = i\sigma_2 \otimes I_2$, $\gamma^2 = i\sigma_3 \otimes \sigma_2$, $\gamma^3 = -i\sigma_1 \otimes I_2$, and $\gamma^5 = -\gamma^0\gamma^1\gamma^2\gamma^3 = -i\sigma_3 \otimes \sigma_1$. The matrices γ^0,

γ^1, γ^2 and γ^3 satisfy the Clifford algebra $\gamma^\mu\gamma^\nu + \gamma^\nu\gamma^\mu = 2g^{\mu\nu}$ with Minkowski metric $g^{\mu\nu}$.

The dimension of the minimal representation of a Euclidean Clifford algebra in 2+1 dimensions is 2, allowing for the 2×2 Pauli matrices as a choice for the γs. A non-minimal 4×4 representation as we have used above leads to a freedom in the choice of the γ^0 matrix, i.e. a matrix with $\left(\gamma^0\right)^2 = I_4$ that anticommutes with γ^1 and γ^2. Candidates for γ^0 are then $\{\gamma^0, \gamma^0\gamma^3, \gamma^0\gamma^5, \gamma^1\gamma^2\}$. The matrices $\{\gamma^0, \gamma^0\gamma^3, \gamma^0\gamma^5\}$ form a triplet and $\gamma^1\gamma^2$ forms a singlet with respect to the SU(2) "chiral"-symmetry group with generators $\{\frac{i}{2}\gamma^3, \frac{i}{2}\gamma^5, \frac{i}{2}\gamma^{35}\}$ (where $\gamma^{35} \equiv \gamma^3\gamma^5$). Each different choice of γ_0 corresponds to a different labelling of the four sites in the unit cell. The elements of the chiral group generate transformations between each labelling. For example, the generator γ^5 translates the plaquette indices to the labelling of the neighboring lattice cell along the y-direction, whilst γ^3 translates the plaquette indices to the neighbouring cell in the x-direction.

$$e^{\frac{\pi}{2}\gamma^5}\begin{pmatrix} c_A \\ c_B \\ c_C \\ c_D \end{pmatrix} = i\begin{pmatrix} c_B \\ c_A \\ -c_D \\ -c_C \end{pmatrix}, e^{\frac{\pi}{2}\gamma^3}\begin{pmatrix} c_A \\ c_B \\ c_C \\ c_D \end{pmatrix} = i\begin{pmatrix} c_C \\ c_D \\ c_A \\ c_B \end{pmatrix}. \tag{5.11}$$

Similarly, γ^{35} translates the plaquette one lattice cell along the x- and one lattice cell along the y-direction. When $\beta = 0$, the elements of the chiral group are symmetries of H_k. When $\beta \neq 0$, the γ^3 and γ^5 terms in H_k break the chiral symmetry and shifts along either the x- or y-directions do not leave H_k invariant. We emphasise that this manifest chiral symmetry breaking is inherently different from the conventional notion of spontaneous chiral symmetry breaking in field theoretical models which is the signature of mass generation [41].

An additional discrete symmetry of H_k (that arises from the hopping structure in $\mathcal{H}_k$) that holds even when $\beta \neq 0$ is

$$\Gamma = \frac{i}{2}\left(\gamma^1\gamma^3 + \gamma^2\gamma^5\right) - \frac{i}{2}\left(\gamma^2\gamma^3 - \gamma^1\gamma^5\right),$$

which corresponds to a reflection about the diagonal AD in the unit cell, with $c_A \to c_A$, $c_B \to c_C$, $c_C \to c_B$ and $c_D \to -c_D$. The action of Γ on H_k is to exchange k_x and k_y.

5.3.1 Fermion birefringence

As illustrated in Fig. 5.3 b) the dispersion Eq. (5.9) admits massless fermions with two different "speeds of light" controlled by β. The eigenvectors (written as row vectors) for the positive and negative energy J_+ bands are $\Psi_1^{\mathrm{T}} = \frac{1}{\sqrt{2}}(1, -\sin\theta, -\cos\theta, 0)$ and $\Psi_2^{\mathrm{T}} = \frac{1}{\sqrt{2}}(1, \sin\theta, \cos\theta, 0)$; whilst

the eigenvectors for the J_- bands are $\Psi_3^{\mathrm{T}} = \frac{1}{\sqrt{2}}(0, \cos\theta, -\sin\theta, 1)$ and $\Psi_4^{\mathrm{T}} = \frac{1}{\sqrt{2}}(0, -\cos\theta, \sin\theta, 1)$, where we write $k_x = k\cos\theta$ and $k_y = k\sin\theta$. The linear combinations $\Psi_1 + \Psi_2$ and $\Psi_3 + \Psi_4$ have non-zero amplitude only on A and D sites respectively. Any other state will break up into fast (J_+) and slow (J_-) fermionic excitations, analogous to fast and slow modes in an optically birefringent medium.

5.3.2 Staggered potentials

Staggered on-site potentials are a natural perturbation to H_k in the context of cold atoms on an optical lattice. The most general form of such a potential is

$$\begin{aligned}\Delta &= \sum_k \psi_k^\dagger \left[\Delta_0 I_4 + \Delta_1\gamma^0 + \Delta_2(i\gamma^1\gamma^3 + i\gamma^2\gamma^5)\right. \\ &\qquad \left. +\Delta_3(i\gamma^1\gamma^3 - i\gamma^2\gamma^5)\right]\psi_k, \end{aligned} \tag{5.12}$$

where we may set $\Delta_0 = 0$ since this just corresponds to a uniform shift of the chemical potential. The Δ_1 term violates chiral symmetry in the usual way but is Lorentz invariant and hence introduces a gap in the dispersion of the fermions

$$E_k = \pm\sqrt{\Delta_1^2 + 4J_\pm^2 k^2}. \tag{5.13}$$

When $\beta = 1$ there are flat bands at $E = \pm\Delta_1$ that intersect the J_+ bands only at $(k_x, k_y) = (0, 0)$. The birefringence property discussed above is unaffected by the Δ_1 term. We combine $i\gamma^1\gamma^3$ and $i\gamma^2\gamma^5$ into a Lorentz invariant term (Δ_2) and a Lorentz violating term (Δ_3). There are two cases in which we have obtained simple analytic solutions for the spectrum: case I): $\Delta_1 \neq 0$, $\Delta_2 \neq 0$, $\Delta_3 = 0$, for which

$$E_k = \begin{cases} \Delta_2 \pm \sqrt{(\Delta_1 + \Delta_2)^2 + 4J_+^2 k^2} \\ -\Delta_2 \pm \sqrt{(\Delta_1 - \Delta_2)^2 + 4J_-^2 k^2} \end{cases},$$

and case II): $\Delta_1 \neq 0$, $\Delta_2 = 0$, $\Delta_3 \neq 0$, for which

$$E_k = \begin{cases} \Delta_3 \pm \sqrt{(\Delta_1 - \Delta_3)^2 + 4J_+^2 k_y^2 + 4J_-^2 k_x^2} \\ -\Delta_3 \pm \sqrt{(\Delta_1 + \Delta_3)^2 + 4J_+^2 k_x^2 + 4J_-^2 k_y^2} \end{cases}.$$

In case I) the dispersion is isotropic in momentum space and there are flat bands when $\beta = 1$, whereas in case II), the dispersion is anisotropic, with the anisotropy governed by β through $J_\pm$. In both cases, there is a shift in the spectrum and at least one set of massive modes (however in both cases there can be a set of massless modes whose dispersion is given by the upper half of a cone if $\Delta_1 = \pm\Delta_{2,3}$ and $\Delta_0 = \mp\Delta_{2,3}$).

5.3.3 Interactions

As we consider spinless fermions, there will be no on-site Hubbard interaction, so we consider nearest neighbour interactions of the extended Hubbard type (for cold atoms in an optical lattice these will generally be weak or can be engineered to be weak):

$$H_{\rm int} = \sum_{\langle ij \rangle} V_{ij} n_i n_j. \tag{5.14}$$

Setting all of the $V_{ij} = V_0$, we can write the interaction Hamiltonian in terms of spinors as

$$H_{\rm int} = \frac{V_0}{4} \sum_k \left[(\bar{\psi}_k \gamma^0 \psi_k)^2 - (\bar{\psi}_k \psi_k)^2 \right], \tag{5.15}$$

with $\bar{\psi}_k = \psi_k^\dagger \gamma^0$. The identity and γ^0 that appear in the kernels of the quartic interaction terms are the only elements of the Clifford algebra that either commute or anticommute with all of the elements of the Lorentz group and the chiral group, ensuring that the interactions remain invariant under any rotation of the lattice by the Lorentz group or relabelling of the plaquette indices by the chiral group. At the mean field level, the $(\bar{\psi}\psi)^2$ term breaks chiral symmetry by introducing an effective mass term $m_0\gamma^0$, and the $(\bar{\psi}\gamma^0\psi)^2$ term renormalizes the chemical potential as δI_4. For weak interactions, the mean field interaction Hamiltonian is:

$$\begin{aligned} H_{\rm int}^{\rm MF} &= \sum_k \psi_k^\dagger \left[(\delta I_4 + m_0 \gamma^0) + (m_1 \gamma^0 \gamma^1 + m_2 \gamma^0 \gamma^2 \right. \\ &\qquad \left. + m_3 i\gamma^3 + m_5 i\gamma^5) \right] \psi_k, \end{aligned} \tag{5.16}$$

where $\delta = \langle n_A \rangle + \langle n_B \rangle + \langle n_C \rangle + \langle n_D \rangle$, and the order parameter for staggered charge density wave order $m_0 = \langle n_A \rangle - \langle n_B \rangle - \langle n_C \rangle + \langle n_D \rangle$ arise from the Hartree term. The remaining masses, m_1, m_2, m_3 and m_5 arise from the Fock term – if these are dropped and $\beta = 0$, we recover the mean-field approximation of the Gross-Neveu model [77]. Similarly to a $\Delta_1\gamma^0$ staggered potential, the Hartree term leads to massive excitations, but does not destroy fermion birefringence. The detailed study of interactions when $\beta \neq 0$ is a topic for future investigation.

For small values of β, when $H_{\rm int}$ is added to Eq. (5.3) there is a mapping between the weak interaction strength regime considered above to the strong interaction strength limit that preserves the property of birefringence:

$$E_k(\beta, V_0) = \beta E_k(\beta^{-1}, \beta^{-1} V_0). \tag{5.17}$$

This arises from the appearance of the chiral symmetry generators, γ^3 and γ^5 in the kinetic energy and their duality with Lorenz group generators $\gamma^0\gamma^1, \gamma^0\gamma^2$. Upon choosing a different representation of Clifford algebra elements, one can transform $\gamma^0\gamma^1 \leftrightarrow \gamma^3, \gamma^0\gamma^2 \leftrightarrow \gamma^5$.

5.4 Discussion

The model we introduce here has the unusual feature of low energy excitations that are birefringent massless fermions arising from broken chiral symmetry. We suggested a particular procedure based on Ref. [70] as a way to realize this model with cold atoms in an optical lattice. This might not be the only route to realize the model: recent work by Lan *et al.* [76] on cold atoms suggested a procedure that gives a model with the same spectrum as the $\alpha = 1/2$, $\beta = 1/2$ version of our model. Additionally, as noted in a similar context [78] it might be possible to engineer an appropriate semiconductor heterostructure.

An important feature of the birefringent fermion dispersion that we find here is that the slopes of the J_+ and J_- bands can be controlled by the parameter β. Possible applications of birefringent properties might include a filter for Dirac fermions in cold atom systems (via spatially varying β) or birefringent Klein tunnelling [76]. Flat bands such as Landau levels enhance interactions, suggesting that the flat bands we observe here when $\beta = 1$, which are robust to the addition of a staggered potential and weak interactions may allow for interesting correlated phases when interactions beyond mean field are taken into account [79]. Future avenues for research on this model could include the study of such correlated phases when $\beta \neq 0$. Generalizing the model to fermions with spin would allow for on-site Hubbard interactions, that could require an approach similar to those used to study QED_3 in high temperature superconductors [**?**][5][11][12].

Chapter 6

Phase Diagram of Superconductor-Insulator Transition at Weak Disorders

In this chapter we focus on problem of a quantum phase transition in a disordered system. In particular, the problem of the Superconductor-Insulator (SI) transition in two spatial dimensions in the presence of a disorder potential. Similarly to high temperature superconductors (HTS) - which has been the subject of previous chapters - the quantum phase fluctuations of the superfluid order parameter in such systems is responsible for the phase transition in disordered superconductors.[80][81]. Most importantly the disordered superconductors also share the type of phases that appear for the underoped cuprates: a superconducting phase, an insulating phase through strong correlation, Mott Insulator (MI), in the system and a medium phase disordered phase (pseudogap). The form of phase diagram of the system in low disorder and weak interactions is the main subject of this Chapter.

First, we construct an effective bosonic action for a BCS superconductor in high-disorder and generalize it to arbitrarily low-disorders. Our focus is to derive the phase-diagram of the system for arbitrarily low disorder and (electronic) interaction couplings. Our findings differ from some of the previous numerical results that suggested the transition between a superconductor to a phase-disordered glassy phase persists in that regime. From the form of the phase diagram we offer an argument for discrepancy in the previous findings in the literature. Our main finding is based on a variable-range disorder-dependent hopping bosonic Hamiltonian that we suggest for the low-disorder limit. The exact derivation of suggested model, beginning with an electronic Hubbard

model is left for future works. In the last part of this Chapter, we address a different problem by applying the same approach to the Bose-Hubbard model in low-disorder and weak interactions. There, we prove that the localization-delocalization transition is independent of the form of disorder distribution and merely depends on the disorder-strength and other physical quantities in the system (chemical potential, hopping and interaction strength).

6.1 Superconductor-Insulator Transition

It is known that weak non-magnetic impurities do not affect the transition temperature of s-wave superconductors [84]. In the presence of disorder translational symmetry is broken and momentum k is not a proper quantum number with which to construct the BCS variational ground state. However, time-reversed states of electrons pair up to make Cooper pairs. Anderson's theorem, as this is known, is so strong that until the limit of site-localized states the BCS ground state has a lower energy than the non-superconducting one. This site localized phase is a gapless insulator of tightly bound electron pairs and known as a bosonic Mott insulator (MI). A Mott insulator is incompressible and distinguished by its gap in its low-energy excitations.

On the other hand, It is well-known that all states of non-interacting particles in the presence of a random potential are localized in dimensions $D = 1, 2$ (in the infinite system-size limit) [86]. The localization phenomena leads to less uncertainty of the number operator and the phase-number uncertainty relation requires that disorder in low-dimensional systems enhances the quantum phase fluctuations which eventually should be responsible for a Kosterlitz-Thouless type of transition in this case. This disordered phase still has Cooper pairs and a finite superconducting order parameter amplitude but the phase of order parameter does not have long-range order. Such a phase is called a Bose glass (BG) and is a gapless insulator with finite compressibility [87]. With three distinct phases and two different mechanisms for transitions, the phase diagram of the theory is somewhat difficult to derive. A bosonic model on a lattice with short-range interactions has been suggested by Fisher *et al.* [87] to study the properties of the SI transition. They have argued that the direct Mott-insulator (MI) to superfluid (SF) transition is unlikely and the two phases are always separated by Bose glass phase. If any direct MI to SF transition exists, it is expected to happen at integer fillings (commensurate). More recently Ref. [90], has shown that all the transitions between fully gapped and gapless ground states in disordered systems result in a insulating gapless state, which supports the original conjecture by Fisher *et al.*

The bosonic theory of the Superconductor-Insulator transition has been extensively studied and

has been successful in explaining the critical behaviour of the transition and universality of the conductivity[87][81][82]. However, the nature of the transition in the low-disorder limit has been a source of debate. There are arguments that weak disorder is irrelevant and would prevent the formation of the phase-disordered Bose glass and there is the possibility of a direct Mott-insulator to superfluid transition [96][98][87].

The validity of the bosonic theory in the weak-interaction limit is also an important issue. The bosonic theory assumes that electron pairs do not dissociate at the point of transition. A different mechanism of the Superconductor-Insulator transition has been suggested for weak-disorder which argues that the disorder will enhance the effect of Coulomb interactions to the point that the net interaction between electrons become repulsive and leads to pair-breaking. Thus a direct superconductor to electronic Mott-insulator transition has been suggested [88][89]. We will return to this issue and the possibility of pair-breaking in the low-U, low-disorder bosonic Hubbard model later in the Chapter.

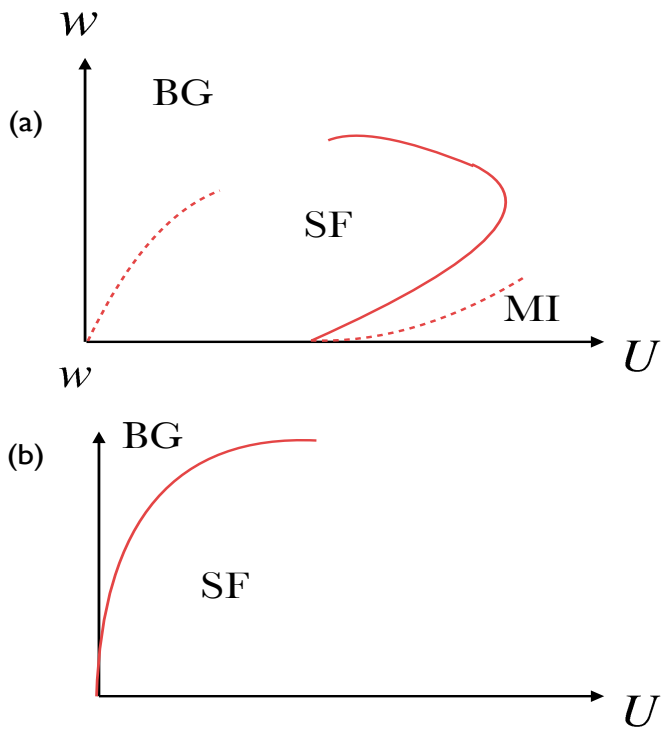

Figure 6.1: Possibilities for the phase boundary in the low disorder limit: (a) phase diagram suggested in Ref.[81] (see also [100]) and heuristic arguments mentioned there to guess the form of phase-boundary in low-disorder (b) Our result with an exponentially small Bose glass region in the limit of $U \to 0$ which explains why there has been debate over the phase diagram between the above two scenarios.

6.2 Derivation of the Bosonic Model

We will begin with a system of lattice fermions in a random potential with onsite attractive Hubbard interaction,

$$H = -t \sum_{\langle i,j\rangle,\sigma=\uparrow,\downarrow} c^{\dagger}_{i,\sigma} c_{j,\sigma} + \sum_{i,\sigma} \tilde{V}_i n_{i,\sigma} - U \sum_{i} n_{i,\uparrow} n_{i,\downarrow}. \tag{6.1}$$

$\tilde{V}_i$ is a random potential with a given distribution $P(\tilde{V})$ - whose form we will discuss later - with second moment, W, which will indicate the disorder strength, and n_i is occupation number

operator. When W/t is small the single-particle states of the Hamiltonian are close to plane waves and the usual BCS variational ground state might be a good candidate to minimize free energy in the mean-field limit (and there is usual the Cooper instability for small $U > 0$). When disorder increases, however, the states are localized and one can write the lattice fermionic states in terms of Anderson localized eigenstates:

$$\begin{aligned} c_{i,\sigma} &= \sum A_n^i c_{n,\sigma} \\ c_{i,\sigma}^\dagger &= \sum A_n^{*i} c_{n,\sigma}^\dagger. \end{aligned} \tag{6.2}$$

The Hamiltonian can thus be written in terms of these localized states as

$$H = \sum_{nm} \varepsilon_n n_{n,\sigma} - \sum_n U_{nn,nn} n_{n,\uparrow} n_{n,\downarrow} - \sum_{nm,kl} U_{nm,kl} c_{n,\uparrow}^\dagger c_{k,\downarrow}^\dagger c_{m,\downarrow} c_{l,\downarrow}. \tag{6.3}$$

In the strong disorder limit, the exact eigenstates of the random single-particle part of the Hamiltonian approach the site-localized wave-function, $|n\rangle \to |i\rangle$, and $U_{nn,nn} \to U$, and the last term involving the overlap between different strongly localized terms can be treated as small perturbation. In the limit of $W/t \to \infty$ the last term is zero and the ground-state is simply the product of composite bosons:

$$\Psi = \prod c_{n,\downarrow}^\dagger c_{n,\uparrow}^\dagger |0\rangle, \tag{6.4}$$

A crucial observation is that the low-energy excitations above this ground state are purely *bosonic*. To create a pair of electrons at the next available energy level does not cost any energy while to create a single electron there costs a finite amount of energy $U/2$. Despite the single particle gap, the ground state does not have any off-diagonal long-range order characteristic of a superfluid. This is the result of the fact that the states are either fully occupied with a pair or empty and in fact an insulator. i.e., there is no hopping/kinetic energy to enable the Bose-Eintsein condensation of these composite bosons and thus off-diagonal long range order.

A mean-field treatment of the interaction term as a small perturbation around a BCS/Anderson variational ground state introduces different terms: (i) a hopping term (for $n = m$ and $k = l$) (ii) a Hartree potential diagonal term ($n = k, m = l$) and similarly (iii) $n = l, m = k$ which represents pair-breaking.

We will drop the pair-breaking term as for energies much lower than U it will be insignificant. These considerations lead to a simple bosonic theory with the effective Hamiltonian

$$H_{\rm b} = -\sum_{nm} J_{nm} b_n^\dagger b_m + V_n b_n^\dagger b_n. \tag{6.5}$$

The parameters $V_n = 2\varepsilon_n - U$, and $J_{nm} = U_{nn,mm}$ and each of the bosonic operators are defined as

$$b_n = c_{n,\uparrow} c_{n,\downarrow}. \tag{6.6}$$

The inclusion of Pauli principle along with the composite nature of these bosons introduces an on-site interaction between the bosons. We can simplify the above theory by assuming that all the J_{nm} are the same and not random variables. In principle the randomness should be kept in both the diagonal term V_n and the hopping J_{nm}. However for the sake of simplicity we assume diagonal disorder only. The above mapping now takes the lattice electrons to a new virtual lattice which is labeled by the energy quantum number n of the localized states. All the complications of the theory - which is now defined on a virtual lattice - is kept in two main features, (i) the exact form of overlap integrals J_{nm} and (ii) the hard-core nature of the interaction.

Remarkably, the same construction of a bosonic Hamiltonian works for bosonic holes,as excitations of a commensurate MI ground state. When hopping is strong the hole excitations hopping around - on top of a MI ground state - can undergo a BEC and lead to a superfluid order parameter. If the solutions remain localized for all of the excitation spectrum in Eq.(6.5) - for strong disorder - the long-range order between these localized excitations acting as seeds of superfluid order is lost through quantum phase-fluctuations. This strong-disorder situation describes a Bose-Glass. The above scenario can come to a clear light by considering a uniform superfluid order-parameter through a infinite-range hopping limit which we will discuss in the next Section.

The above construction of a bosonic theory was originally suggested by Lee and Ma [93] [94]. They, however, did not discuss the phase disordering phase transition of such a system, i.e. SF-BG transition, and merely showed that the superconducting ground-state survive in the high-disorder limit, in what they called a “localized superconductor”.

We have to emphasize that although the construction of the bosonic model was in the strong disorder limit, the procedure is completely general. In weak disorder, since the localization length is large, the overlaps between the localized states are large and can create long-range hopping terms in the bosonic model, Eq.(6.3). The form of the ground state and excitations that accompany it will be also a lot more complicated as the site-localized case will never be reached.

6.3 Infinite-Range Hopping Limit

One of the commonly used mean-field approaches to a system of highly interacting bosons or fermions on a lattice is the infinite-range hopping approximation[87][97]. In the following we investigate the solutions of the infinite-range hopping model in detail both in the interacting and non-interacting cases. For us, however, the infinite-range limit is not an approximation. Rather, we are going to use the exact solutions of the infinite-range problem to map the weak-disorder and dilute model to a high-disorder limit. The infinite-range Hamiltonian,

$$H[b, b^\dagger] = -J \sum_{i,j} b_i^\dagger b_j + \sum_i (V_i - \mu) b_i^\dagger b_i, \tag{6.7}$$

can exactly be diagonalized. Decoupling the hopping term by introducing a superfluid order parameter, m,

$$H_{\text{eff}}\left[m, b_i^\dagger, b_i\right] = -\frac{N}{4J}|m|^2 + \sum_i \left[m b_i^\dagger + m^* b_i + \left(V_i b_i^\dagger b_i\right)\right]. \tag{6.8}$$

The infinite-range assumption is a systematic way of introducing the mean-field assumption of uniform order parameter in the system. For superfluid transition the order parameter is $\langle b_i \rangle$, so the infinite-range hopping assumption is needed to decouple the hopping term through introducing the order parameter into the Hamiltonian.

The hard-core constraint restricts the bosonic occupation numbers to 1 or 0 per site and writing the trace in the $|1\rangle$ and $|0\rangle$ basis in calculating the partition function, we arrive at the effective form for free energy in terms of the order parameter,

$$\langle F \rangle_{\text{dis}} = \frac{m^2}{J} - \frac{\mu}{2} - T \int \mathrm{d}V P(V) \ln \left[\cosh\left(\frac{\sqrt{(V-\mu)^2 + 4m^2}}{2T}\right)\right]. \tag{6.9}$$

$P(V)$ is the disorder distribution and $\langle \cdots \rangle_{\text{dis}}$ indicates average over disorder. For small m's near the transition point Eq.(6.9) can be expanded in powers of m,

$$
\begin{aligned}
H_{\rm b}\left[m\right] &= \int {\rm d}V P(V) \left\{ \ln\left(\frac{e^{(V-\mu)/T}+1}{2} \right) - (V-\mu) \right\} \\
&+ \left\{ -\frac{1}{J} + \int {\rm d}V P(V) \frac{1}{2(V-\mu)} \tanh\left(\frac{V-\mu}{T} \right) \right\} \times m^2 \\
&+ \left\{ \int {\rm d}V P(V) \left\{ T^2 \frac{1+4e^{(V-\mu)/T} - e^{2(V-\mu)/T}}{8(V-\mu)^4 (e^{(V-\mu)/T}+1)^2} \right) \right\} \times m^4 \\
&+ \mathcal{O}(m^6). \qquad (6.10)
\end{aligned}
$$

The mean-field equations for the above model are derived by taking the derivative over the superfluid order parameter, m, which leads to

$$
1 = J \int P(V) {\rm d}V \frac{\tanh\left(\sqrt{(V-\mu)^2+4m^2}/2T \right)}{\sqrt{(V-\mu)^2+4m^2}}, \qquad (6.11)
$$

The transition temperature is obtained from the mean-field equation with $m = 0$. This is in essence the coefficient in the quadratic term put equal to zero,

$$
1 = J \int P(V) {\rm d}V \frac{\tanh((V-\mu)/2T_c)}{V-\mu}. \qquad (6.12)
$$

One of the important limits of the theory is the dilute limit when the hard-core interaction is less important. The condensate state is a Bose-Einstein condensate now, and the question is how the interplay between BEC and localization determines the transition. In the infinite-range limit the energy spectrum of the theory can be worked out for any *arbitrary* form of disorder distribution. The disorder averaged density of states, $\rho(\varepsilon)$, has an interesting form. It consists of two sections, the ground state is *extended* and appears as an isolated δ-function while the rest of the excitations are *localized* and have the exact form of the distribution of the random potential $P(V)$,

$$
\langle \rho(\varepsilon) \rangle_{\rm dis} = \delta(\varepsilon - \varepsilon_0) + P(\varepsilon). \qquad (6.13)
$$

We prove this result in the following. Beginning with one-particle Hamiltonian,

$$
H_{\rm b} = \sum_{ij} \left(-\frac{J}{N} + \delta_{ij}(V_i - \mu) \right) b_i^\dagger b_j, \qquad (6.14)
$$

the disorder-averaged density of states $\langle \rho \rangle_{\rm dis}$ is the imaginary part of the free-particle Green's function at zero momentum,

$$\langle \rho(\omega) \rangle_{\rm dis} = \frac{1}{2\pi N} \left\langle {\rm Im} \sum_i \mathcal{O}_{ij}^{-1} \right\rangle_{\rm dis} . \tag{6.15}$$

The kernel $\mathcal{O}_{ij} = -J/N + \delta_{ij}(V_i - \mu) = 1 + \delta_{ij}\alpha_i$. Expanding the determinant of $\mathcal{O}$, using Saurus' rule for determinant expansion, we obtain:

$$\det \mathcal{O} = (\Pi_k \alpha_k) \left(1 + \sum_l \frac{1}{\alpha_l} \right) \tag{6.16}$$

and the trace of inverse $\mathcal{O}_{ii}^{-1}$,

$${\rm Tr}\mathcal{O}^{-1} = \sum_i \frac{1}{\alpha_i} - \frac{1}{1 + \sum_m \frac{1}{\alpha_m}} \sum_i \frac{1}{\alpha_i^2} \tag{6.17}$$

Notice that the second term is negligible in the thermodynamic limit. The disorder average can be straightforwardly calculated using Cauchy's integral theorem and it gives rise to Eq.(6.13). The most important feature of the form of the density of states in the dilute regime is that the extended ground state's energy ε_0 depends on the disorder distribution,

$$1 - J \int_{-\infty}^{\infty} {\rm d}V \frac{P(V)}{V_i - \mu - \varepsilon_0} = 0, \tag{6.18}$$

where $(1/N)\sum_i$ is replaced with disorder average $\langle \cdots \rangle_{\rm dis}$. This is the same equation as the mean-field equation, Eq.(6.11) in the limit of $T \to 0$. The eigenvector for the ground-state is

$$\phi_0(i) = \frac{m}{V_i - \mu - \varepsilon_0} \sim \frac{1}{\sqrt{N}}, \tag{6.19}$$

and $m = (1/N)\sum_i \phi_n(i)$, is the superfluid order parameter. For a uniform disorder distribution,

$$P(V) = \begin{cases} \frac{1}{2W}, & -W \le V \le W \\ 0, & \text{otherwise,} \end{cases} \tag{6.20}$$

Eq.(6.18), and the normalization condition, give us,

$$\varepsilon_0 = W \ln \left(\frac{W}{J} \right), \tag{6.21}$$

$$m = \frac{1}{\sqrt{N}} \left(\varepsilon_0^2 - W^2 \right)^{\frac{1}{2}} . \tag{6.22}$$

For low-disorder, ($W \ll 1$)

$$m \approx \frac{J}{\sqrt{N}} \left\{ 1 - \frac{1}{6} \left(\frac{W}{J} \right)^2 \right\} \approx \frac{J}{\sqrt{N}}. \tag{6.23}$$

The excitations come from the same eigenvalue equation - however $(1/N) \sum_i$ is not replaced with an average over disorder. The result is simple and the excitation energy value is close to the one of the V_i's,

$$\varepsilon_n = V_i - \mu - \frac{J}{N}. \tag{6.24}$$

The excitations also have the same functional form as the ground-state,

$$\phi_n(i) = \frac{m_n}{V_i - \mu - \varepsilon_n} \sim \frac{1}{N}, \tag{6.25}$$

$$m_n \approx \frac{J}{N}. \tag{6.26}$$

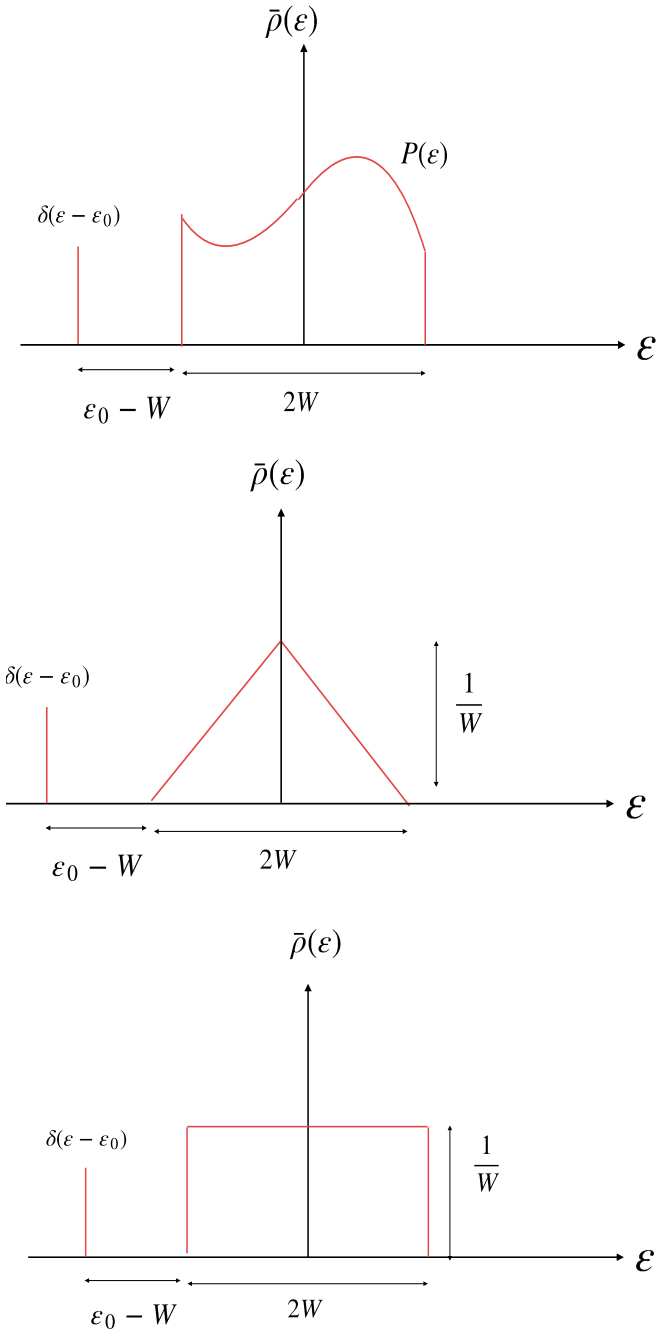

Figure 6.2: (a) The general form of the averaged disorder density of states, $\bar{\rho}(\varepsilon)$, for a bounded disorder distribution with disorder strength W. (b) and (c) The same form for the uniform and triangular distributions Eq.(6.20) and Eq.(6.57). For the triangular distribution, upon increasing disorder strength the extended ground state indicated by $\delta(\varepsilon - \varepsilon_0)$, can reach the lower edge of the density of states.

(The $m_n = J/N$ comes from assuming a site-localized form for $\phi_n(i), \phi_n(i) \sim \delta(i - i_n), n \neq 0$). As discussed before, in the weak-disorder limit the value of the normalization factors is important and determines the nature of the wave-functions. The isolated ground state has $1/\sqrt{N}$ normalization which is the signature of an *extended* coherent-state while the excitations are all normalized as $1/N$ as a sign being of perfectly *localized*. The fact that ground-state is extended and excitations are localized (in the thermodynamic limit) can be more rigorously proved [95].

As a matter of fact the existence of an extended ground state with gapped excitations depends on the behaviour of the disorder distribution near its lower edge, i.e. the IR behaviour of the gap equation - Eq.(6.18). It is easy to see that a distribution weaker than linear does not give a finite integral value in Eq.(6.18), and for the linear function $P(V) \sim V$ near the edge the existence of a solution depends on the slope of the distribution. Notice that if the solutions of gap equation, Eq.(6.18), do not result in a gapped spectrum, then the system is missing the extended ground state. Thus, if a form of disorder distribution can let the isolated ground state merges with the lower edge of the excitation spectrum upon increasing disorder, we can interpret it as a *localization-delocalization* transition. This is in fact what happens for the triangular distribution:

$$P(V) = \begin{cases} \frac{1}{W^2}V + \frac{1}{W}, & -W \leq V \leq 0, \\ -\frac{V}{W^2} + \frac{1}{W} & 0 \leq V \leq W. \end{cases} \tag{6.27}$$

The lowest eigenvalue will satisfy the following relation,

$$\frac{W^2}{J} = \ln\left(\frac{\varepsilon_0 - W}{|\varepsilon_0|}\right)(|\varepsilon_0| - W) + \ln\left(\frac{|\varepsilon_0| + W}{|\varepsilon_0|}\right)(|\varepsilon_0| + W) \tag{6.28}$$

Taking the limit of $\varepsilon_0 \to -W$ leads to a critical values for disorder strength,

$$W_c = 2J \ln 2, \tag{6.29}$$

and the slope of the distribution near the lower edge would be inverse of this value $1/(2J \ln 2)$.

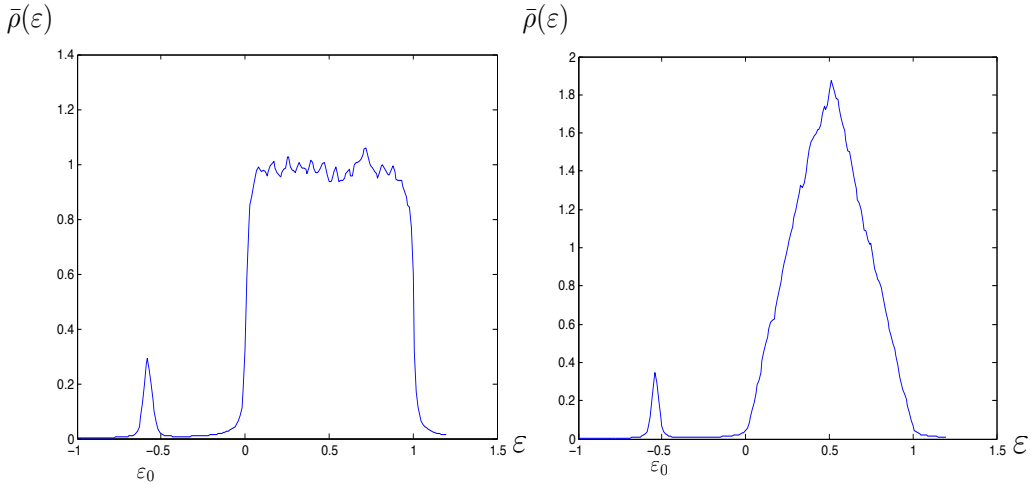

Figure 6.3: Numerical calculation of disorder-averaged density of states, $\bar{\rho}(\varepsilon)$, for both triangular and uniform disorder distributions. The disorder strength, W, is 0.5 and hopping,J, is 1.0.

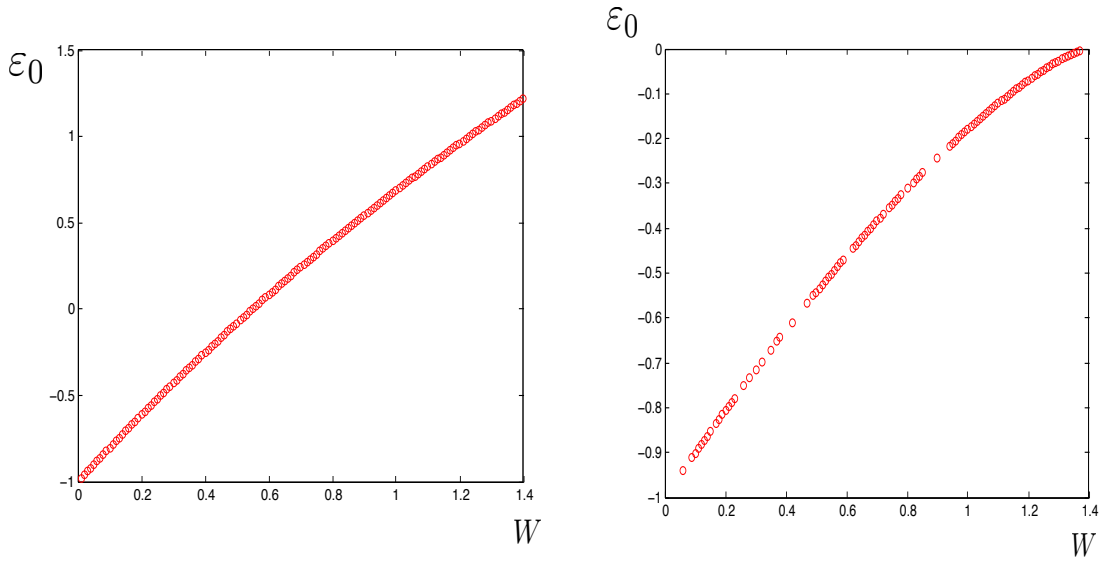

Figure 6.4: Numerical solutions for ground-state energy of both uniform and triangular distributions as a function of disorder. Notice the ground-state energy merges to lower edge of the distribution - $V = 0.0$ in the figure - for the triangular distribution as disorder reaches the critical value $2\ln 2$.

The above picture of ground-state and localized excitations can explain the three phases in our original theory as follows: The free bosonic Hamiltonian Eq.(6.14) explains the dynamics of *holes* around the MI ground state of the hard-core bosons. When the functional form of the disorder distribution lets an extended state exist, as the chemical potential reaches $\varepsilon_0 \sim W$ transition to a superfluid state happens, to be precise, holes undergo a Bose-Einstein condensation. Before that, the insulating phase can be identified as a Mott insulating phase as the spectrum is gapped. For distributions with smooth behaviour on their lower edge, there is no gap in the density of states and both ground-state and excitations are localized. This can be interpreted as a candidate for a Bose glass phase in the BEC limit.

Before concluding this section, let us address the finite soft-core interactions for the sake of completeness. The gap equations that we discussed for the non-interacting model so far are also very similar to the equation for the phase-boundary in the Bose-Hubbard model. In the Bose-Hubbard model a perturbation expansion for small hopping amplitude around the Mott insulating state leads to a similar condition as the gap equation, Eq.(6.11),

$$\frac{1}{J} = \sum_i \left[\frac{U(n_i+1)}{Un_i - (V_i - \mu + J)} + \frac{Un_i}{V_i - \mu + J - U(n_i - 1)} \right]. \tag{6.30}$$

The discrete values of occupation numbers, n_i can be treated as the the density of states or some *screened* disorder distribution $\tilde{P}(V)$. Because of the nature of bosonic onsite interaction, they are discrete values unlike our case. A similar approach is in principle possible for the hard-core model in mid-densities by considering the expansion of the free energy in the powers of superfluid order parameter, Eq.(6.10). However the order parameter is not a real bosonic field anymore and the dynamics of the screening would be somewhat different.

6.4 Mapping of the Hamiltonian Between Low-Disorder and High-Disorder Limits

The case of weak disorder in the bosonic Hamiltonian, Eq.(6.5), is somewhat straight-forward. We can simplify the form of hopping J_{ij} into a step-function form where the hopping between the particles closer than a characteristic lengths, l_{w}, is J and outside that length the hopping amplitude is zero. The characteristic length is of the order of the localization length. The integral that determines the hopping depends on the overlap of the localized states, $J_{ij} \approx \int \phi_i^*(x)\phi_j(x)$, in two-dimensions,

Anderson localization implies permanent localization of all single-particle states with an exponentially decaying form,

$$\phi_i(x) \approx e^{-\frac{x}{l_{\rm w}}}. \tag{6.31}$$

The overlap integral for the hopping amplitude will be dominant inside $x \leq l_{\rm w}$ region. At weak disorder, the localization length is large and sensitive to the value of disorder strength. Its dependency can be approximated by the non-analytic form,

$$l_{\rm w} \approx \exp\left\{-\frac{c}{W}\right\}. \tag{6.32}$$

Thus, for a hard core bosonic theory in weak-disorder, we propose a disorder-dependent J_{ij}:

$$H_{\rm b} = -J \sum_{i_x - j_x, i_y - j_y \leq l_{\rm w}} b^\dagger(i)b(j) + \text{h.c.} + (V_i - \mu)b^\dagger(i)b(i). \tag{6.33}$$

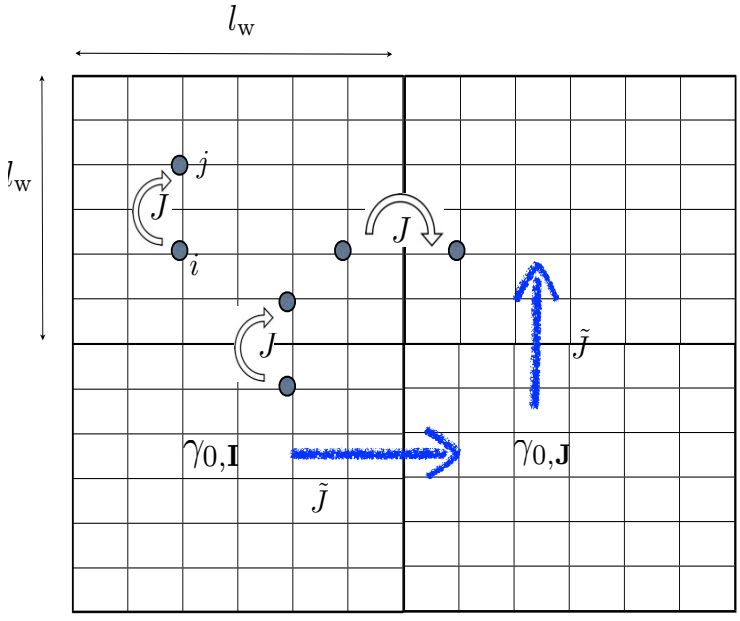

Figure 6.5: The coarse graining procedure of mapping the lattice into large blocks of the localization length size, $l_{\rm w}$. The operators $\gamma_0(\mathrm{I})$ (or $\gamma_0(\mathrm{J})$) represents the local, extended ground-state of the block/cell indexed I (or J)

$l_{\rm w}$ now determines the hopping range and c is a number with units of energy and we will assume it to be of order 1 for simplicity. The non-analytic dependence of the localization length is an indication that the clean limit cannot be considered as a limiting case of this model. The interplay between disorder and interaction in the original fermionic theory is now translated into a bosonic theory which in the dilute limit can be treated as a free system.

Now, we suggest a *coarse graining* procedure by dividing the lattice into a much larger lattice with lattice spacing for which the unit cells are of the size of the hopping range, i.e., the localization length $l_{\rm w}$. Inside each two-dimensional box of size $l_{\rm w}$, we re-write the bosonic operators in terms of the infinite range hopping model solutions. This can be justified as for arbitrarily low disorder the localization length is exponentially large. The hopping between each of these neighbouring coarse-grained cells is mainly dominated by the superfluid extended ground state indicated by energy ε_0. As the last step, one needs to integrate out the excitation degrees of freedoms inside each block and we will be left with an effective theory for the inside-the-block-extended local ground states which now have the nearest neighbour hopping between each cells. This will let us to make a direct mapping between a low-disorder theory with long-range hopping and the nearest-neighbour hopping high-disorder limit of the dirty bosonic theory. The values of these nearest neighbour hopping amplitudes between local superfluid states are however different from original hopping J and should be calculated through the coarse-graining procedure. The same goes for the effective disorder strength in each block. In the following we will demonstrate this in a systematic way,

Let us begin with transforming the bosonic operator to the solutions of the infinite range hopping model,

$$\begin{aligned}\gamma_n &= \sum_i \phi_n(i) b_i, \\ \gamma_n^\dagger &= \sum_i \phi_0^*(i) b_i^\dagger,\end{aligned} \tag{6.34}$$

while the wave functions $\phi_n(i) \sim 1/(\varepsilon_n - V_i)$ were derived in the previous Section, Eqs.(6.19) and (6.26). The operators $\gamma_0^\dagger(\mathrm{I})$ and $\gamma_0(\mathrm{I})$ are the creation and annihilation operators for the single *extended* state inside each block/cell of size $l_{\rm w}$.

The Hamiltonian in terms of the infinite-range hopping operators can be written as

$$H_b = -\frac{J}{N}\sum_{i,j<l_{\rm w}}\sum_{\langle {\rm IJ}\rangle}\phi_n^*(i)\phi_m(j)\gamma_n^\dagger({\rm I})\gamma_m({\rm J}) + \sum_{\rm I}(\varepsilon_n-\mu)\gamma_n^\dagger({\rm I})\gamma_n({\rm I}). \tag{6.35}$$

The capital indices I and J label neighbouring cell blocks while i, j indices label internal sites for each individual cell. To integrate out the excitations, I first write down the Hamiltonian keeping terms with γ_0 in them,

$$\begin{aligned} H_{b=} &- NJ\sum_{nm}\sum_{\rm IJ}\langle\phi_0\rangle^2_{\rm dis}\cdot\left\{\gamma_0^\dagger(I)\gamma_0(J)+{\rm h.c.}\right\} \\ &+\sum\sum_{\rm I}\varepsilon_0(I)\gamma_0^\dagger(I)\gamma_0(I)+\sum_{\rm I}\sum_n\varepsilon_n\gamma_n^\dagger(I)\gamma_n(I) \\ &-NJ\sum_{IJ}\langle\phi_0\rangle\langle\phi_0\rangle\cdot\left\{\gamma_0^\dagger(I)\gamma_n(J)+\gamma_n^\dagger(I)\gamma_0(J)\right\}. \end{aligned} \tag{6.36}$$

The Hamiltonian is Gaussian and integrating out the excitations leads to a coarse-grained Hamiltonian with "renormalized" parameters $\tilde{J}$ and $\tilde{W}$ and chemical potential $\tilde{\mu}$,

$$H_{\rm b} = \tilde{J}\sum_{\langle {\rm IJ}\rangle}\left\{\gamma_0^\dagger(I)\gamma_0(J)+\gamma^\dagger(J)\gamma_0(I)\right\}+(\tilde{V}_{\rm I}-\tilde{\mu})\gamma_0^\dagger({\rm I})\gamma_0({\rm I}), \tag{6.37}$$

with the new effective nearest-neighbour hopping amplitude $\tilde{J}$ and random potential $\tilde{V}$,

$$\begin{aligned} \tilde{J} &= \frac{1}{N}\left(\sum_{ij}\phi_0^*(i)\phi_0(j)\right)\cdot J = NJm^2 \\ \tilde{V} &= \varepsilon_I \approx \frac{1}{N}\sum_{i\in {\rm I_{th}cell}} V_i \\ \tilde{\mu} &= \mu+\sum_n\frac{m^2J^4}{\varepsilon_n}\approx \mu+W^2J^3. \end{aligned} \tag{6.38}$$

N is the number of lattice sites in each cell block and proportional to $l_{\rm w}^2$ in two dimensions. Using the value of m obtained for a uniform distribution, Eq.(6.22), and substituting for the solutions of ε_0 one gets,

$$\tilde{J} = J \cdot W^2 \left\{ \coth^2 \left(\frac{W}{J} \right) - 1 \right\}, \tag{6.39}$$

Crudely, $\tilde{J}$, can be approximated with J - at least it is independent of cell size, N.

Calculating the effective value of the disorder strength is more tedious. This is basically to calculate the distribution of the ε_0. This is similar to calculating the standard deviation of the mean, using the central limit theorem, while the mean is calculated over a large but *finite size* cell. Now we expect the extended superfluid state, which in the infinite range hopping and thermodynamic limit was an isolated δ-function at energy ε_0 given by the Eq.(6.18), now to be a Gaussian around the same value with the second moment of the Gaussian now indicating the effective disorder strength $\tilde{W}$.

We can also derive the coarse-grained disorder strength by considering the second term in the Eq.(6.17). Including only that term in the density of states' form and averaging over disorder we will have,

$$\langle \delta\rho(\omega) \rangle_{\rm dis} = \frac{1}{2\pi} {\rm Im} \left\langle \frac{1}{1 + \sum_m \frac{1}{\alpha_m}} \sum_i \frac{1}{\alpha_i^2} \right\rangle_{\rm dis}. \tag{6.40}$$

The average over disorder can be written as,

$$\begin{aligned} \langle \delta\rho(\omega) \rangle_{\rm dis} &= \int \sum_i \frac{P[V]\mathcal{D}V}{\alpha_i^2} \delta \left[1 + \sum_j \frac{1}{\alpha_j} \right] \\ &= \int \frac{{\rm d}k}{2\pi} \int P[V]\mathcal{D}V \cdot \left(\frac{1}{N} \sum_i \frac{1}{\alpha_i^2} \right) \cdot \exp \left\{ ik \cdot \left(1 + \frac{1}{N} \sum_i \frac{1}{\alpha_i^2} \right) \right\}. \end{aligned} \tag{6.41}$$

Since in the low-disorder limit the hopping range increases faster than exponentially, we can look at the large-N limit of the above integrals over the disorder. Expanding the exponential function and applying Sterling's approximation one ends of with the following Gaussian form for the $\tilde{P}(V)$, the effective disorder distribution:

$$\tilde{P}(V) = \exp \left\{ -\frac{1}{2J^2} \left(1 + J \left\langle \frac{1}{V - \varepsilon_0} \right\rangle_{\rm dis} \right)^2 \cdot \frac{N}{\left\langle \frac{1}{V - \varepsilon_0} \right\rangle^2} \right\}. \tag{6.42}$$

Now let us insert the values of the averages over the $\langle \phi^2 \rangle$ and $\langle \phi^4 \rangle$ for the uniform distribution, into Eq.(6.42),

$$\left\langle \frac{1}{(\cdots)} \right\rangle / \left\langle \frac{1}{(\cdots)^2} \right\rangle = \ln\left[\frac{|\varepsilon_0|+W}{|\varepsilon_0|-W}\right] \cdot \frac{\varepsilon_0^2 - W^2}{2W}, \tag{6.43}$$

and thus the coarse-grained disorder strength, $\tilde{W}$ will have the form,

$$\tilde{W}(W) = W \cdot \ln\left[\frac{\coth(W/J)+1}{\coth(W/J)-1}\right] \cdot \frac{\coth^2(W/J)-1}{2} \cdot e^{-\frac{1}{2W}}. \tag{6.44}$$

This will lead to the known result that the $\tilde{W} \sim W/\sqrt{N}$. The fact that N has also a non-analytic dependence on disorder strength actually make the above result quite interesting. We could have used the intuitive argument that the coarse-grained disorder distribution is

$$\tilde{W} = W \cdot \exp\left\{\frac{1}{2W}\right\}. \tag{6.45}$$

In the next section we will apply the results obtained above to estimate the phase boundary.

6.5 Phase Diagram of the Theory

We begin by an estimate of the phase-boundary in the strong disorder limit. In strong disorder all the states of the system are localized and the wave function decays exponentially within the range of the slocalization length. This leads to a effective hopping energy/kinetic energy of the form of the neighbouring wave functions overlap integral,

$$\mathrm{K} \sim \exp\left[a \cdot \left(\frac{W}{t}\right)^2\right], \tag{6.46}$$

where a is a numerical factor. Near the transition point, this kinetic energy part should be comparable with value of the interaction energy in the system which is of order the interaction strength, U in Eq.(6.1). This leads to an estimate for phase boundary in the strong-disorder limit

$$\frac{U}{t} \sim \exp\left[a\left(\frac{W}{t}\right)^2\right]. \tag{6.47}$$

Notice that as argued before, in the strong disorder limit $U/t \sim J$. We now substitute the values of the effective hopping strength, $\tilde{J}$ and effective disorder strength, $\tilde{W}$, into Eq.(6.47), and obtain a similar estimate for the phase boundary in the low-disorder limit. The fact that the characteristic energy associated with disorder, W is exponentially suppressed makes an interesting and non-trivial

phase-boundary. Since the value of hopping in the bosonic model is proportional to the electronic interaction strength, we will use J instead of that. The result reads,

$$J^3W^2\left\{\coth^2\left(\frac{W}{J}\right)-1\right\}e^{-\frac{4}{W}}\sim\exp\left[\left(W\cdot\ln\left[\frac{\coth(W/J)+1}{\coth(W/J)-1}\right]\cdot\frac{\coth^2(W/J)-1}{2}\cdot e^{-\frac{1}{2W}}\right)^2\right] \tag{6.48}$$

The value of disorder, W, plotted as a function of interaction strength, J, is an exteremely sharp function. However it is analytic and also smooth near the origin. This can be the reason that some numerical calculations and some experiments have previously suggested that in the low-disorder limit the Bose-glass to superfluid transition is not possible and only a Mott-insulator to superfluid transition through a pair-breaking mechanism would be allowed. That argument would lead to a constant value for W as J reaches zero. In our scheme, we think, we can argue that Bose-glass state still survive for very low interaction and low disorder values although in an exponentially narrow region around the $W=0$ axis. In the following we are going to argue, however, that the form of the phase-boundary in low-disorder is independent of the details of the phase-boundary in high-disorder. If instead of the Eq.(6.47), we had used a simpler approximation,

$$J\sim W, \tag{6.49}$$

We would end up with a smoother phase-boundary, coming for the equation,

$$J=\frac{\exp\left(-\frac{c}{2W}\right)}{W\left(\coth^2(\frac{W}{J}-1\right)}. \tag{6.50}$$

Fig.(6.6), shows the solution to the above equation,

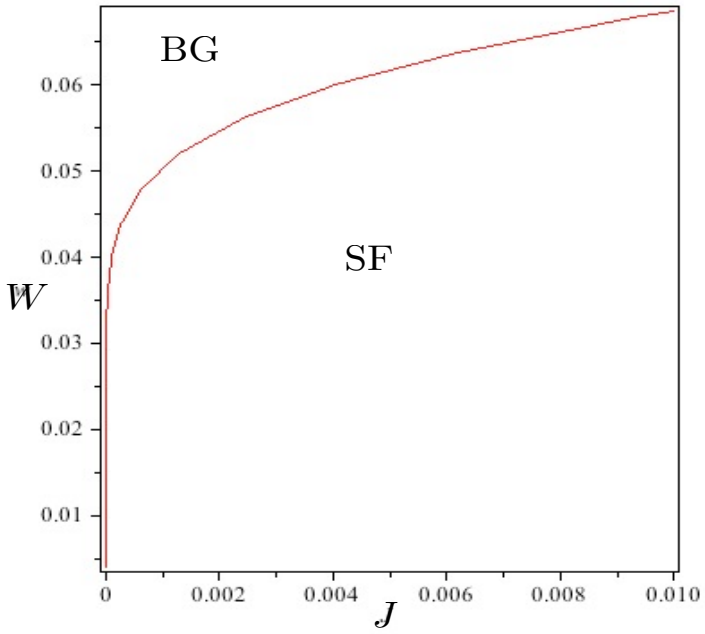

Figure 6.6: Phase-boundary of the superfluid and BG phases near the arbitrary weak disorder and interaction strength (both of the W and J are written relative to original electronic hopping t).

Although the author is not aware of any numerical work on the weak-disorder limit of the phase-boundary for the superconductor-insulator problem, our result is consistent with the heuristic arguments in Ref.[81]. At the same time we can explain why some other works have predicted a MI-SF transition through a pair dissociation mechanism. The BG region is so small that it can be easily missed.

The nature of three different phases in our theory is somewhat easier to explain in this long-range hopping model. The Mott-insulating phase is preferred when the local ground state of each site is a gapped insulator. When the local superfluid ground-state is reached, then the coarse grained Hamiltonian ground state, Eq.(6.15) can explain long-range order in thermodynamic limit (SF) or having a phase disordered state (BG).There is however another possibility and that is when the form of the disorder potential prohibits an extended ground state to exist. This means that even inside each block will see a local superfluid to Bose glass transition. The superfluid ground state is now an overlap of localized states and not a modified BEC. This is what has been described as *localized superconductors* by Ma and Lee [93].

The difference between the two possible mechanisms of the formation of superfluid and insulating states in low- and high densities requires a careful inclusion of the interaction. In the next section we will include the interaction for a Bose-Hubbard model Hamiltonian and show that the original mechanism assumed holds and the formation of localized superconductors and a localized Bose-glass ground state does not happen in the weak-interaction limit of our model. In other words, the mechanism of the phase transition is independent of the form of the disorder distribution.

6.6 Screening of the Disorder Potential in the Bose-Hubbard Model in the Weak Interaction Limit

Inspired by the above discussion it is worth to consider the effect of interactions in a soft-core bosonic model with a Bose-Hubbard (BH) type of interaction. As before, the hopping term for bosons is assumed to have a long range which depends on the disorder non-analytically ,

$$H = \frac{J}{N} \sum_{i_x, i_y \leq l_{\rm w}} \left(b_i^\dagger b_j + b_j^\dagger b_i \right) + \sum_i \left((V_i - \mu) b_i^\dagger b_i + \frac{\lambda}{2} \left(b_i^\dagger b_i \right)^2 \right) \tag{6.51}$$

The main feature of the screening, which we are in interested to investigate, is whether it affects the behaviour of the disorder potential at the lower-edge. As discussed before, if $P(V)$, has a linear - or weaker - form near the edge - like the triangular distribution - there is the possibility of having localized ground states inside each cell.

Steps of the coarse graining procedure can be exactly followed as before. Transforming the bosonic operators, $b_i^\dagger, b_i$ into the solutions of a non-interacting model $\gamma^\dagger, \gamma$, Eq.(6.34), the Hamiltonian can be written as,

$$\begin{aligned} H_b &= -\frac{J}{N} \sum_{\substack{i \in {\rm I_{th}cell} \\ j \in {\rm J_{th}cell}}} \sum_{\langle {\rm IJ} \rangle} \phi_n^*(i) \phi_m(j) \gamma_n^\dagger({\rm I}) \gamma_m({\rm J}) - J \sum_{ij \in {\rm I_{th}cell}} \sum_{I,nm} \phi_n^*(i) \phi_m(j) \gamma_n^\dagger({\rm I}) \gamma_m(I, nm) \\ &+ \sum_{\rm I} \sum_i (V_i - \mu) \phi_n^*(i) \phi_m(j) \gamma_n^\dagger({\rm I}) \gamma_m({\rm I}) \\ &+ \frac{\lambda}{2} \sum_{\rm IJKL} \sum_{ijkl} \sum_{nmpq} \phi_n(i) \phi_m(j) \phi_p(k) \phi_q(l) \gamma_n^\dagger(I) \gamma_m^\dagger(J) \gamma_p(K) \gamma_q(L). \end{aligned} \tag{6.52}$$

The above form can be simplified by considering the fact that the dominant wave-function overlaps come from the condensate. Ignoring the terms with an odd number of condensate operator in them we arrive at the Bogoliubov Hamiltonian written in terms the Anderson localized solutions,

$$
\begin{aligned}
H_{\rm b} &= H_0 + H_{\rm exc} + H_{\rm hopping}, \\
H_0 &= \sum_{\rm I} \varepsilon \gamma^\dagger_{0,I}\gamma_{0,I} + \frac{\lambda}{2}\langle\phi_0^4\rangle(\gamma^\dagger_{0,I}\gamma_{0,I})^2, \\
H_{exc,} &= \sum_{\rm I}\sum_{n}(\varepsilon_n + 4\lambda\langle\phi_0^2\phi_n^2\rangle\langle\gamma^\dagger_{0,I}\gamma_{0,I}\rangle)\gamma^\dagger_{n,I}\gamma_{n,I} + \langle\phi_0^2\phi_n^2\rangle\langle\gamma^\dagger_{0,I}\gamma^\dagger_{0,I}\rangle\gamma_{n,I}\gamma_{n,I}, \\
&\quad + \langle\phi_0^2\phi_n^2\rangle\gamma^\dagger_{n,I}\gamma^\dagger_{n,I}\langle\gamma_{0,I}\gamma_{0,I}\rangle, \\
H_{\rm hopping} &= \tilde{J}\sum_{\langle IJ\rangle}\gamma^\dagger_{0,I}\gamma_{0,J} + {\rm h.c.}.
\end{aligned} \tag{6.53}
$$

Notice that the validity of the approximation now relies on the fact that ground state is the only extended state in the theory and for large enough block sizes, the overlap integrals in the Hartree-Fock approximation of Eq.(6.52), are dominated by γ_0. The Bogoliubov transform results in a new spectrum for the excitations in the low-energy limit. This will be of particular interest for us as the screening of the original disorder potential can result in different solutions of the gap equation, Eq.(6.18), and possibly the disappearance of the extended ground state. One should also notice that the coefficients $\langle\phi_0^4\rangle$ and $\langle\phi_0^2\phi_n^2\rangle$ now will give rise to two different values for the effective interaction strength in H_0 and $H_{\rm exc}$.

The Bogoliubov dispersion for quasi-particles is,

$$E_n = \sqrt{\varepsilon_n\left(\varepsilon_n + 2\lambda\langle\phi_0^2\phi_n^2\rangle n_0\right)}, \tag{6.54}$$

where $n_0 = \langle\gamma_0^\dagger\gamma_0\rangle$ is the superfluid condensate and is obtained by minimizing the condensate part of the Hamiltonian, H_0,

$$n_0 = \frac{\varepsilon_0}{N\lambda\langle\phi_0^4\rangle}. \tag{6.55}$$

Notice that ε_0 plays the role of chemical potential μ. The phononic part of the dispersion is of particular interest to us. If the new quasi-particles model considered, their density of states can be treated as the screened disorder potential. For energies very close to zero, i.e., the edge of the disorder distribution.

$$E_n = \sqrt{\frac{2\langle\phi_n^2\phi_0^2\rangle\cdot\varepsilon_0}{N\langle\phi_0^4\rangle}}\cdot\sqrt{\varepsilon_n} \tag{6.56}$$

This is in fact the prescription for a triangular distribution, if the original distribution- in this case ε_n - is a uniform one,

$$P_{\rm tri}(V_{\rm tri}) = \begin{cases} \sqrt{\frac{W^2}{2} V_{\rm uni}}, & 0 < V < W/2 \\ W - \sqrt{1 - V_{\rm uni}/W)\frac{W^2}{2}} & W/2 < V < W. \end{cases} \tag{6.57}$$

which implies that the factor $\sqrt{\varepsilon_0}$ now should determines the value of the the disorder strength of the screened disorder potential W'. The main point to see from this observation is that upon closing the gap, i.e., $\varepsilon_0 \to 0$, the effective disorder strength, W', also goes to zero which indicates that one might not reach the critical disorder $W_c/J = 2\ln 2$ - for the triangular distribution - through this mechanism, this is a significant result in the sense that in weak interaction and disorder limit, where the hopping ranges are long and the coarse graining procedure is possible. The mean-field Bogoliubov spectrum determines the form of the screened disorder distribution and this new screened distribution always keeps a gapped spectrum.

6.7 Concluding Remarks

In conclusion, we addressed the problem of a bosonic model with finite-range hopping as the effective model for the S-I transition at low-disorder and weak interaction strength. We considered both hard-core and Hubbard interactions independently and derived the form of the phase boundary for the hard-core model using a mapping between low-disorder and strong-disorder limits of the model. The exponentially small region of BG phase that we obtained for the phase diagram in the low-disorder limit, was considered the reason that why some of the numerical works have missed it in their simulations. For the Bose-Hubbard model we showed that using the same coarse graining technique we were able to show that the screening of the disorder potential by the interaction now happens in such a manner that it keeps the gap for the extended local ground states. This prevents double mechanisms for the MI-BG and BG-SF transitions in this limit.

Appendix A

Representations of Gamma-Matrices in 2+1 Dimensions

In this appendix we show a construction for all the possible representations of the γ-matrices in 2+1 dimensions assuming a $\mathrm{SU}(2) \otimes \mathrm{SU}(2)$ symmetry for the action. For the case of underdoped cuprates one $\mathrm{SU}(2)$ sector corresponds to the Lorentz group and the other SU(2) is the group of chiral rotations.

To begin, we conjecture the following form for the γ-matrices,

$$\gamma_\mu \in \{\mathbf{1}, \vec{\sigma}\} \otimes \{\mathbf{1}, \vec{\sigma}\}, \tag{A.1}$$

there is some freedom in choosing the form of the γ_μ's, while knowing the generators of one of the $\mathrm{SU}(2)$s one can predict the elements of the other $\mathrm{SU}_c(2)$ (in our case the chiral symmetry group). Given γ_3 the Clifford algebra is complete and other elements of the $\mathrm{SU}_c(2)$ can be obtained easily as

$$\begin{aligned} \gamma_5 &= \gamma_0\gamma_1\gamma_2\gamma_3 \\ \gamma_{35} &= i\gamma_3\gamma_5. \end{aligned} \tag{A.2}$$

There is a freedom in choosing γ_3, however. One can exchange γ_3 and γ_5 since γ_5 anti-commutes with all γ_μ's and squares to unity too. The other freedom is that one can rotate all the γ_μ's ($\mu = 0, 1, 2$) between each other. more importantly one can rotate the γ_μ's among each other while this time $\mu = 1, 2, 3$.

The simplest representation would be

$$\gamma_0 = \begin{pmatrix} \sigma_3 & \\ & -\sigma_3 \end{pmatrix}, \quad \gamma_3 = \begin{pmatrix} & \mathbf{1} \\ \mathbf{1} & \end{pmatrix},$$
$$\gamma_1 = \begin{pmatrix} \sigma_1 & \\ & -\sigma_1 \end{pmatrix}, \quad \gamma_{35} = \begin{pmatrix} \mathbf{1} & \\ & -\mathbf{1} \end{pmatrix},$$
$$\gamma_2 = \begin{pmatrix} \sigma_2 & \\ & -\sigma_2 \end{pmatrix}, \quad \gamma_5 = \begin{pmatrix} & -i \\ i & \end{pmatrix}.$$

The representation that we used in Ch.1, however, is somewhat different and can be easier to deal with,

$$\gamma_0 = \begin{pmatrix} & \mathbf{1} \\ \mathbf{1} & \end{pmatrix}, \quad \gamma_3 = \begin{pmatrix} & -i\sigma_2 \\ i\sigma_2 & \end{pmatrix},$$
$$\gamma_1 = \begin{pmatrix} & -i\sigma_3 \\ i\sigma_3 & \end{pmatrix}, \quad \gamma_{35} = \begin{pmatrix} & \sigma_2 \\ -\sigma_2 & \end{pmatrix},$$
$$\gamma_2 = \begin{pmatrix} & i\sigma_1 \\ -i\sigma_1 & \end{pmatrix}, \quad \gamma_5 = \begin{pmatrix} \mathbf{1} & \\ & -\mathbf{1} \end{pmatrix}.$$

In the following we will proceed to construct the complete set of the $\gamma_\mu u$'s that are generators of both $\mathrm{SU}(2)$ and $\mathrm{SU}_c(2)$. Consider two elements of the Algebra A and B and propose the forms:

$$\begin{aligned} A &= \sigma_\nu \otimes \sigma_\mu, \\ B &= \sigma_\rho \otimes \sigma_\kappa. \end{aligned} \tag{A.3}$$

The condition $A^2 = B^2 = \mathbf{1}$ is automatically satisfied. The anti-commutation between A and B would enforce that either (i): σ_ν and σ_ρ commute and σ_μ and σ_κ anti-commute or (ii): vice versa. (i) leads to

$$\text{case } (i) \rightarrow \begin{cases} \sigma_\rho = \sigma_\nu = \mathbf{1}, \\ \text{or} \\ \rho = \nu, \end{cases} \tag{A.4}$$

$$\text{case } (ii) \rightarrow \begin{cases} \sigma_\mu = \sigma_\kappa = \mathbf{1}, \\ \text{or} \\ \mu = \kappa, \end{cases} \tag{A.5}$$

The possible $\gamma_\mu u$'s would be

$$\begin{aligned} &(i) \quad \gamma_\mu u = \sigma_i \otimes \vec{\sigma}, \\ &(ii) \quad \gamma_\mu u = \mathbf{1} \otimes \vec{\sigma}. \end{aligned} \tag{A.6}$$

Mixtures are also possible. For example one can have- case (iii):

$$\begin{aligned} \gamma_0 = \mathbf{1} \otimes \sigma_i \rightarrow \begin{cases} [\sigma_\nu, \sigma_\rho] = 0 \quad (\text{commute}), \\ \{\sigma_\mu, \sigma_\kappa\} = 0 \quad (\text{anti}-), \end{cases} \\ \gamma_1 = \sigma_l \otimes \sigma_j \rightarrow \begin{cases} [\sigma_\nu, \sigma_\rho] = 0 \quad (\text{anti}-), \\ \{\sigma_\mu, \sigma_\kappa\} = 0 \quad (\text{commute}), \end{cases} \\ \gamma_2 = \sigma_l \otimes \sigma_k \rightarrow \begin{cases} [\sigma_\nu, \sigma_\rho] = 0 \quad (\text{anti}-), \\ \{\sigma_\mu, \sigma_\kappa\} = 0 \quad (\text{commute}), \end{cases} \end{aligned} \quad . \tag{A.7}$$

where $i \neq j \neq k = \{1, 2, 3\}$ and l is some fixed index.

According to the above construction there are complementary sets of generators of the chiral group $\mathrm{SU}_c(2)$, i.e., $\gamma_3, \gamma_5, \gamma_{35}$.

$$(i) \quad \begin{cases} \gamma_0 = \sigma_l \otimes \sigma_i, \\ \gamma_1 = \sigma_l \otimes \sigma_j, \\ \gamma_2 = \sigma_l \otimes \sigma_k, \end{cases} \rightarrow \begin{cases} \gamma_3 = \sigma_{l'} \otimes \sigma_i, \\ \gamma_5 = \sigma_{l'} \otimes \sigma_j, \\ \gamma_{35} = \sigma_{l''} \otimes \sigma_k. \end{cases} \tag{A.8}$$

where $l, l', l'' = \{1, 2, 3\}$ are different indices, while i, j, k are the same notation as used before. Similarly:

$$
\begin{aligned}
(ii)\quad & \begin{cases} \gamma_0 = \mathbf{1} \otimes \sigma_i, \\ \gamma_1 = \mathbf{1} \otimes \sigma_j, \\ \gamma_2 = \mathbf{1} \otimes \sigma_k, \end{cases} \rightarrow \begin{cases} \gamma_3 = \text{does not exist}, \\ \gamma_5 = \cdots, \\ \gamma_{35} = \cdots, \end{cases} \\
(iii)\quad & \begin{cases} \gamma_0 = \mathbf{1} \otimes \sigma_i, \\ \gamma_1 = \sigma_l \otimes \sigma_j, \\ \gamma_2 = \mathbf{1} \otimes \sigma_k, \end{cases} \rightarrow \begin{cases} \gamma_3 = \sigma_{l'} \otimes \sigma_j, \\ \gamma_5 = \sigma_{l''} \otimes \sigma_j, \\ \gamma_{35} = \sigma_l \otimes \mathbf{1}. \end{cases}
\end{aligned} \tag{A.9}
$$

Appendix B

Fierz Identities and Generality of the Interaction Lagrangian

In this section we will construct the linear relationship between the quartic terms invariant under a unitary $\mathrm{U}(N)$ group, known as Fierz identities. These are the direct consequences of the completeness relation for the generators of the symmetry group.

Defining $\mathrm{Tr}(A \cdot B)$ as the inner product between matrices A and B, we write down the completeness relation for the basis constructed out of generators of a $\mathrm{U}(N)$ group, $\{\lambda^\alpha, \mathbf{1}\}$, as

$$\frac{1}{N}\delta_{ab}\delta_{cd} + \frac{1}{2}\sum_{\alpha}^{N^2-1} \lambda^\alpha_{ab}\lambda^\alpha_{cd} = \delta_{ad}\delta_{cb}. \tag{B.1}$$

A the special case of $\mathrm{U}(2)$, using Pauli matrices, Eq. (B.1) simplifies to

$$\delta_{ab}\delta_{cd} + \sum_{\alpha} \sigma^\alpha_{ab}\sigma^\alpha_{cd} = 2\delta_{ad}\delta_{cb}. \tag{B.2}$$

Using the above relations one can derive the requisite linear relationship between different quartic terms. First, it is convenient to represent the $4N$-component spinor Ψ in terms of $2N$-component ones as

$$\Psi = \begin{pmatrix} \chi^i \\ \phi^i \end{pmatrix}. \tag{B.3}$$

It is then possible to apply to above completeness relations to the quartic terms of the form

$$\sum_{\alpha} (\bar{\chi}^i_a \lambda^\alpha_{ij} \chi^j_a)(\bar{\chi}^k_b \lambda^\alpha_{kl} \chi^l_b), \tag{B.4}$$

where χ^i stands for both χ^i and ϕ^i. (The spinor index is indicated by subscripts.) Applying Eq. (B.2) for spinor degrees of freedom and Eq. (B.1) for flavour degrees of freedom, one ends up with the following identity

$$(1+\frac{1}{N})(\bar{\chi}\chi)^2+\sum_{\mu}(\bar{\chi}\sigma_\mu\chi)^2+\sum_{\alpha}(\bar{\chi}\lambda^\alpha\chi)^2=0, \tag{B.5}$$

where we have suppressed both the spinor and flavour (large-N) indices for convenience, and replaced N with $2N$, since QED_3 is $\mathrm{U}(2N)$-symmetric. Similarly, beginning with the quartic term

$$\sum_{\alpha,\mu}(\bar{\chi}^i_a\lambda^\alpha_{ij}\sigma^\mu_{ab}\chi^j_b)(\bar{\chi}^k_c\lambda^\alpha_{kl}\sigma^\mu_{cd}\chi^l_d), \tag{B.6}$$

it is easy to derive the other identity [44]

$$\sum_{\alpha,\mu}(\bar{\chi}\lambda^\alpha\sigma_\mu\chi)^2+\sum_{\alpha}(\bar{\chi}\lambda^\alpha\chi)^2+\frac{1}{N}\sum_{\mu}(\bar{\chi}\sigma_\mu\chi)^2 +(4+\frac{1}{N})(\bar{\chi}\chi)^2=0. \tag{B.7}$$

The above identities applied to a $\mathrm{U}(2N)$-symmetric theory with the S_{int} of the form

$$\tilde{g}_1(\bar{\chi}\chi)^2+\tilde{g}_2(\bar{\chi}\lambda^\alpha\chi)^2+\tilde{g}_3(\bar{\chi}\sigma_\mu\chi)^2+\tilde{g}_4(\bar{\chi}\sigma_\mu\lambda^\alpha\chi)^2, \tag{B.8}$$

leave only two of the terms as independent. Noticing that the Eq. (B.8) is equivalent to the interaction term written in $4N$-component representation: $g_1|\mathbf{A}|^2+g_2|\mathbf{B}_\mu|^2+g_3|C_\mu|^2+g_4|C_{35}|^2$, we can see that our choice of C_μ and C_{35} as the most general CSP quartic terms is justified.

CSB case is not very different. One can consider the interaction of the form in Eq. (B.8) for each $\mathrm{U}(N)$ sector separately (i.e. χ and ϕ). Repeating the same argument would reduce the number of independent interaction couplings in each sector to two, so that the overall number of independent couplings will be four, as assumed in Eq. (2.9).

Similarly, for the 4×4 representation, we can use completeness Eq.(B.1), written in the form:

$$\frac{1}{4}\sum_{A=1}^{16}\Gamma^A_{ml}\Gamma^A_{ik}=\delta_{mk}\delta_{il}. \tag{B.9}$$

Multiplying the Eq.(B.9) to a four-Fermi term, $\bar{\Psi}^a\Gamma_A\Psi^b\bar{\Psi}^c\Gamma_A\Psi^d$, we find,

$$\left(\bar{\Psi}^a\Gamma_A\Psi^b\right)\left(\bar{\Psi}^c\Gamma_A\Psi^d\right)=\sum_{B=1}^{16}C_{AB}\left(\bar{\Psi}^a\Gamma_B\Psi^d\right)\left(\bar{\Psi}^c\Gamma_B\Psi^b\right) \tag{B.10}$$

with the $\Gamma_{A,B}$, belonging to the set of the whole three dimensional Clifford algebra:

$$\Gamma_A, \Gamma_B = (\mathbf{1}, \gamma_\mu, i\gamma_3, \gamma_\mu\gamma_{35}, \gamma_\mu\gamma_3, \gamma_\mu\gamma_5, \gamma_{35}, i\gamma_5)\,. \tag{B.11}$$

The coefficient matrix C_{AB} is given by

$$C_{AB} = \frac{1}{4}\begin{pmatrix} -1 & -1 & 1 & 1 & -1 & 1 & -1 & 1 \\ -3 & 1 & -3 & 1 & 1 & 1 & -3 & -3 \\ 1 & -1 & -1 & 1 & 1 & -1 & -1 & 1 \\ -3 & 1 & 3 & 1 & -1 & -1 & -3 & 3 \\ 3 & 1 & 3 & -1 & 1 & -1 & -3 & -3 \\ 3 & 1 & -3 & -1 & -1 & 1 & -3 & 3 \\ -1 & -1 & -1 & -1 & -1 & -1 & -1 & -1 \\ 1 & -1 & 1 & -1 & 1 & 1 & -1 & -1 \end{pmatrix}. \tag{B.12}$$

The following cases are useful for Chapter 2,

$$\begin{aligned} -(\bar{\Psi}^a\gamma_\mu\Psi^a)^2 - (\bar{\Psi}^a\gamma_{35}\Psi^a)^2 = (\bar{\Psi}^a\Psi^b)(\bar{\Psi}^b\Psi^a) + (\bar{\Psi}^a i\gamma_3\Psi^b)(\bar{\Psi}^b i\gamma_3\Psi^a) \\ +(\bar{\Psi}^a i\gamma_5\Psi^b)(\bar{\Psi}^b i\gamma_5\Psi^a) + (\bar{\Psi}^a\gamma_{35}\Psi^b)(\bar{\Psi}^b\gamma_{35}\Psi^a) \end{aligned} \tag{B.13}$$

and

$$\begin{aligned} (\bar{\Psi}^a\gamma_\mu\Psi^b)^2 - 3(\bar{\Psi}^a\gamma_{35}\Psi^a)^2 = (\bar{\Psi}^a\gamma_\mu\Psi^b)(\bar{\Psi}^b\gamma_\mu\Psi^a) + (\bar{\Psi}^a\gamma_\mu\gamma_{35}\Psi^b)(\bar{\Psi}^b\gamma_\mu\gamma_{35}\Psi^a) \\ +(\bar{\Psi}^a\gamma_\mu\gamma_3\Psi^b)(\bar{\Psi}^b\gamma_\mu\gamma_3\Psi^a) + (\bar{\Psi}^a\gamma_\mu\gamma_5\Psi^b)(\bar{\Psi}^b\gamma_\mu\gamma_5\Psi^a). \end{aligned} \tag{B.14}$$

Bibliography

[1] J. G. Bednorz and K. A. Muller, Zeitschrift fur Physik B **64**, 189 (1986).

[2] W. N. Hardy, D. A. Bonn, D. C. Morgan, R. Liang, and K. Zhang, Phys. Rev. Lett. **70**, 3999 (1993).

[3] Campuzano, J. C., M. Norman, and M. Randeria, 2003, in *Physics of Conventional and Unconventional Superconductors*, edited by K.H. Bennemann and J.B. Ketterson (Springer, Berlin).

[4] J. M. Kosterlitz and D. J. Thouless, J. Phys. C 6, 1181 (1973); J. M. Kosterlitz, J. Phys. C 7, 1046 (1974).

[5] Igor F. Herbut, Phys. Rev. **B 66**, 094504 (2002).

[6] Dominic J. Lee, Igor F. Herbut, Phys. Rev.**B 67**, 174512 (2003).

[7] I. F. Herbut, Phys. Rev. Lett. **88**, 047006 (2002).

[8] B. H. Seradjeh and I. F. Herbut, Phys. Rev. **B66**, 184507 (2002).

[9] M. Franz, and Z. Tesanovic, Phys. Rev. Lett. **87**, 257003 (2001).

[10] O. Vafek, A. Melikyan, M. Franz, Z. Tesanovic, Phys. Rev. **B63**, 134509 (2001).

[11] M. Franz, Z. Tesanovic, and O. Vafek, Phys. Rev.**B66**, 054535 (2002).

[12] Z. Tesanovic, O. Vafek, and M. Franz, Phys. Rev. **B65**, 180511R (2002).

[13] M. Peskin, Ann. Phys. (N.Y.)**113**, 122 (1978).

[14] C. Dasgupta and B.I. Halperin, Phys. Rev. Lett. **47**, 1556 (1981); A. Nguyen and A. Sudbo, Phys. Rev. **B60**, 15307 (1999).

[15] Igor F. Herbut, J. Phys.A **30**:423-430 (1997).

[16] T.W. Appelquist, M. Bowick, D. Karabali, and L.C.R. Wijewardhana, ibid. Phys. Rev. **D33**, 3704 (1986).

[17] T.W. Appelquist, D. Nash, and L.C.R. Wijewardhana, Phys. Rev. Lett. **60**, 2575 (1988).

[18] R.D. Pisarski, Phys. Rev. **D29**, 2423(1984).

[19] J. Villain, J. Phys. (Paris) **36**, 581 (1975).

[20] D. Nash, Phys. Rev. Lett. **62**, 3024 (1989).

[21] O.Vafek, Z. Tesanovic, M. Franz, Phys. Rev. Lett. **89** 157003 (2002).

[22] D.J. Lee, I.F. Herbut, Phys. Rev. **B66** 094512 (2002).

[23] Jacqueline A. Bonnet, Christian S. Fischer, and Richard Williams, Phys. Rev. **B84**, 024520 (2011).

[24] R. D. Pisarski, Phys. Rev.**D29**, 2423 (1984).

[25] T. W. Appelquist, M. Bowick, D. Karabali, and L. C. R. Wijewardhana, Phys. Rev.**D33**, 3704 (1986); T. W. Appelquist, D. Nash,, and L. C. R. Wijewardhana, Phys. Rev. Lett.**60**, 2575 (1988).

[26] Z. Tešanović, O. Vafek, and M. Franz, Phys. Rev. **B65**, 180511 (2002).

[27] B. H. Seradjeh and I. F. Herbut, Phys. Rev.**B66**, 184507 (2002).

[28] P. Maris, Phys Rev.**B54**, 4049 (1995); C. S. Fischer, R. Alkofer, T. Dahm, and P. Maris, Phys. Rev.**D70**, 073007 (2004).

[29] T. W. Appelquist, A. G. Cohen, and M. Schmaltz, Phys Rev.**D60**, 045003 (1999).

[30] S. J. Hands, J. B. Kogut, and C. G. Strouthos, Nucl. Phys.**B645**, 321 (2002); S. J. Hands, J. B. Kogut, L. Scorzato, and C. G. Strouthos, Phys. Rev. **B70**, 104501 (2004).

[31] V. P. Gusynin and M. Reenders, Phys. Rev.**D68**, 025017 (2003).

[32] For these and related issues see a recent review, N. E. Mavromatos and J. Papavassiliou, Rec. Res. Dev. in Phys. **5**, 369 (2004) (preprint cond-mat/0311421).

[33] O. Vafek, Z. Tešanović, and M. Franz, Phys. Rev. Lett. **88**, 157003 (2002).

[34] D. J. Lee and I. F. Herbut, Phys. Rev.**B66**, 094512 (2002).

[35] Babak.H. Seradjeh, Ph.D. Thesis, Simon Fraser University Library (2006)

[36] See also, S. Hands and I. O. Thomas, preprint hep-th/0412009.

[37] I. F. Herbut and D. J. Lee, Phys. Rev. B **68**, 104518 (2003).

[38] Igor F. Herbut, Phys. Rev. Lett. **94**, 237001 (2005).

[39] T. Appelquist, M. J. Bowick, D. Karabali, and L. C. R. Wijewardhana, Phys. Rev. D **33**, 3774 (1986).

[40] C. Vafa and E. Witten, Commun. Math. Phys. **95**, 257 (1984).

[41] V. A. Miransky, *Dynamical Symmetry Breaking in Quantum Field Theories*, (World Scientific, Singapore, 1993), Ch. 10 and references therein.

[42] H. Terao, Int. J. Mod. Phys. A, **16**, 1913 (2001).

[43] D. K. Hong and S. H. Park, Phys. Rev.**D49**, 5507 (1994); S. J. Hands, Phys. Rev.**D51**, 5816 (1995).

[44] M. Gomes, V. O. Rivelles, and A. J. da Silva, Phys. Rev.**D41**, R1363 (1990).

[45] I.F.Herbut, D.J.Lee, Phys. Rev.**B68**, 104518 (2003).

[46] H. Gies, L. Janssen, Phys. Rev.**D82**, 085018 (2010).

[47] I.F. Herbut, V. Juricic, B. Roy, Phys. Rev. **B79**, 085116 (2009).

[48] T. Itoh, Y. Kim, M. Sugiura , K. Yamawaki, Prog. Theor. Phys. **93** 417 (1995).

[49] D.K. Hong, S.H. Park, Phys. Rev.**D49** 5507 (1994).

[50] S. Hands, Phys. Rev. D **51** 5816 (1995).

[51] S. Christofi, S. Hands, C. Strouthos, Phys. Rev. D **75** 101701 (2007).

[52] K. Kond, Nucl. Phys. B P**450** 251 (1995).

[53] I.F. Herbut, Dominic J. Lee, Phys. Rev. **B68** 104518 (2003)

[54] P.B. Weichman, Phys. Rev. **B38** 8739 (1988).

[55] M. E. Fisher, M. Barber, D. Jasnow, Phys. Rev.**A8**, 1111 (1973).

[56] J. Rudnick, D. Jasnow, Phys. Rev.**B16**, 2032 (1977).

[57] D.J. Scalapino, S. White, S. Zhang, Phys. Rev. **B47**, 7995 (1993).

[58] T.Xiang, J.M. Wheatley, Phys. Rev. Lett. **77** 4632 (1996).

[59] R.J. Radtke, V.N. Kostur, Can. J. Phys. **75**, 363 (1997).

[60] D. E. Sheehy, T.P. David, M. Franz, Phys. Rev. **B.70**, 054510 (2004).

[61] D. M. Broun, W. A. Huttema, P. J. Turner, S. zcan, B. Morgan, Ruixing Liang, W. N. Hardy, and D. A. Bonn Phys. Rev. Lett. **99**, 237003 (2007).

[62] Ruixing Liang, D. A. Bonn, W. N. Hardy, and David Broun , Phys. Rev. Lett. **94**, 117001 (2005).

[63] A. Hosseini, S. Kamal, D.A. Bonn, R. Liang, W.N. Hardy, Phys. Rev. Lett. **81** 1298 (1998).

[64] P. J. Turner, R. Harris, Saeid Kamal, M. E. Hayden, D. M. Broun, D. C. Morgan, A. Hosseini, P. Dosanjh, G. K. Mullins, J. S. Preston, Ruixing Liang, D. A. Bonn, and W. N. Hardy Phys. Rev. Lett. 90, 237005 (2003)

[65] D. A. Bonn, S. Kamal, A. Bonakdarpour, Ruixing Liang, W. N. Hardy, C. C. Homes, D. N. Basov, and T. Timusk, Czech. J. Phys. **46**, 3195 (1996).

[66] M. Kennett, N. Komeilizadeh, K. Kaveh, P. Smith, Phys. Rev. **A83** 053636 (2011).

[67] K.S. Novoselov, A. K. Geim, S. V. Morozov, D. Jiang, Y. Zhang, S. V. Dubonos, I. V. Grigorieva, and A. A. Firsov, Science **306**, 666 (2004); K.S. Novoselov, A. K. Geim, S. V. Morozov, D. Jiang, M. I. Katsnelson, I. V. Grigorieva, S. V. Dubonos, and A. A. Firsov, Nature **438**, 197 (2005); G. W. Semenoff, Phys. Rev. Lett. **53**, 2449 (1984).

[68] C. L. Kane and E. J. Mele, Phys. Rev. Lett. **95**, 146802 (2005); D. Hsieh, D. Qian, L. Wray, Y. Xia, Y. S. Hor, R. J. Cava, and M. Z. Hasan, Nature **452**, 970 (2008).

[69] N. R. Cooper and N. K. Wilkin, Phys. Rev. B **60**, 16279 (1999); D. Jaksch and P. Zoller, New. J. Phys. **5**, 56 (2003); N. R. Cooper, Adv. Phys. **57**, 539 (2008); A. Klein and D. Jaksch, Europhys. Lett. **85**, 13001 (2009); M. Rosenkranz, A. Klein, and D. Jaksch, Phys. Rev. A **81**, 013607 (2010); L.-K. Lim, A. Hemmerich, and C. M. Smith, Phys. Rev. A **81**, 023404 (2010); F. Gerbier and J. Dalibard, New. J. Phys. **12**, 033007 (2010); A. Bermudez, L. Mazza, M. Rizzi, N. Goldman, M. Lewenstein, and M. A. Martin-Delgado, Phys. Rev. Lett. **105**, 190404 (2010); T.-L. Ho and S. Zhang, arXiv:1007.0650v1; D. Makogon, I. B. Spielman, and C. Morais Smith, arXiv:1007.0782v1; E. Kapit and E. J. Mueller, arXiv:1011.4021v1; N. R. Cooper, Phys. Rev. Lett. **106**, 175301 (2011).

[70] A. S. Sørensen, E. Demler, and M. D. Lukin, Phys. Rev. Lett. **94**, 086803 (2005).

[71] V. Schweikhard, I. Coddington, P. Engels, V. P. Mogendorff, and E. A. Cornell, Phys. Rev. Lett. **92**, 040404 (2004); Y.-J. Lin, R. L. Compton, K. Jiménez-García, J. V. Porto, and I. B. Spielman, Nature **462**, 628 (2009).

[72] D. R. Hofstadter, Phys. Rev.**B14**, 2239 (1976).

[73] A. Barelli, J. Bellissard, and R. Rammal, J. Phys. France **51**, 2167 (1990); M. C. Chang and Q. Niu, Phys. Rev.**B50**, 10843 (1994); G.-Y. Oh, Phys. Rev. **B60**, 1939 (1999); M. Ando, S. Ito, S. Katsumoto, and Y. Iye, J. Phys. Soc. Jpn. **68**, 3462 (1999); M.-C. Chang and M.-F. Yang, Phys. Rev. **B69**, 115108 (2004); Y. Iye, E. Kuramochi, M. Hara, A. Endo, and S. Katsumoto, Phys. Rev. **B70**, 144524 (2004); Y.-F. Wang and C.-D. Gong, Phys. Rev. **B74**, 193301 (2006).

[74] R. Shen, L. B. Shao, B. Wang, and D. Y. Xing, Phys. Rev.**B81**, 041410(R) (2010); D. Bercioux, D. F. Urban, H. Grabert, and W. Häusler, Phys. Rev. **A80**, 063603 (2009); V. Apaja, M. Hyrkäs, and M. Manninen, Phys. Rev. **A82**, 041402(R) (2010).

[75] H. Watanabe, Y. Hatsugai, and H. Aoki, arXiv:1009.1959v1.

[76] Z. Lan, N. Goldman, A. Bermudez, W. Lu, P. Ohberg, arXiv:1102.5283v1.

[77] D. J. Gross and A. Neveu, Phys. Rev. D **10**, 3235 (1974).

[78] B. Seradjeh, C. Weeks, and M. Franz, Phys. Rev. B **77**, 033104 (2008).

[79] D. Green, L. Santos, and C. Chamon, Phys. Rev. B **82**, 075104 (2010).

[80] K.Kim, D. Nelson, Phys. Rev. **B64**, 054508 (2001).

[81] I.F. Herbut, Phys. Rev. **B58**, 971 (1998).

[82] I.F. Herbut, Phys. Rev. Lett.**81**, 3916 (1998).

[83] Igor. F. Herbut, Int.J.Mod.Phys **14**, 575 (2000).

[84] P. W. Anderson, J. Phys. Chem. Solids **11**, 26 (1959).

[85] A. A. Abrikosov, L. P. Gorkov and I. E. Dzyaloshinski, *Methods of Quantum Field Theory in Statistical Physics* (Dover, New York, 1975).

[86] P. W. Anderson, J. Phys. Chem. Solids**11**, 26 (1959).

[87] M. P. A. Fisher, P. B. Weichman, G. Grinstein and D. S. Fisher, Phys. Rev. **B40**, 546 (1989).

[88] S.Maekawa and H.Fukuyama, J.Phys.Soc. Jpn**51**,1380 (1982).

[89] J.A. Chervenak, J.M.Valles, Phys. Rev.**B59**, 11209 (1999).

[90] Pollet et. al., Phys. rev. Lett **103**, 140402 (2009).

[91] Yuhai Tu and Peter B. Weichman, Phys. Rev. Lett.**73**, 6 (1994).

[92] M.Case, I.F. Herbut, J. Phys.**A34**, 7739 (2001).

[93] M.Ma and P.A.Lee, Phys. Rev. **B32**, 5658 (1985).

[94] M.Ma, B.I. Halperin and, P.A. Lee, Phys. Rev.**B34**, 3136 (1986).

[95] F. Pazmandi, G.Zimayi, R.Scalettar, Phys. Rev. Lett.**75**,1356 (1995).

[96] Ferenc Pazmandi and Gergely T. Zimnyi *Phys. Rev.* **B57**, 5044 (1998).

[97] S.Sachdev, *Quantum Phase Transitions*, ch.10, Cambridge University Press (2011).

[98] Sung Yong park, Ji-Woo Lee, Min-Chul Cha, M.Y. Choi, B.J. Kim and Doochul Kim Phys. Rev.**B59**, 8420 (1999).

[99] Ji Woo Lee, Min-Chul Cha and Jung Hoon Han, Phys Rev Lett **87**, 247006 (2001).

[100] R.T. Scalettar, G.G. Batrouni and G.T. Zimanyi, Phys. Rev. Lettt. **67**, 3144 (1991).